Behaviour of zirconium, niobium, yttrium and the rare earth elements in the Thor Lake rare-metal deposit, Northwest Territories, Canada

By

Emma Rebecca Sheard

A thesis submitted to the Faculty of Graduate Studies and Research in partial fulfillment of the requirements for the degree of Master of Science

Department of Earth and Planetary Sciences
McGill University, Montreal, QC, Canada
February 2010

ABSTRACT

The Thor Lake rare-metal (Zr, Nb, Y, REE, Ta, Be, Ga) deposit in the Northwest Territories of Canada represents one of the largest resources of zirconium, niobium, yttrium and the heavy rare earth elements in the world. Much of the potentially economic mineralization was concentrated by magmatic processes. However, there is also evidence of remobilization of Zr, Y and REE by hydrothermal fluids. Geologically, the deposit is situated at the southern edge of the Slave Province of the Canadian Shield, within the 2150 Ma alkaline to peralkaline Blachford Lake Complex (Davidson, 1978).

The rare metal mineralization occurs in two sub-horizontal tabular layers in the Nechalacho deposit, an upper and a lower zone, with Zr hosted primarily by zircon, Nb primarily by ferrocolumbite and fergusonite-(Y), and Y + HREE by fergusonite-(Y) and zircon. The LREE are hosted by monazite-(Ce), allanite-(Ce), bastnäsite-(Ce) and parisite-(Ce)/synchysite-(Ce).

A model is proposed in which REE and HFSE enriched layers were formed by injection of separate miaskitic and agpaitic magmas, to form an upper zone rich in zircon and a lower zone rich in eudialyte. Primary eudialyte was later altered to zircon-fergusonite-(Y)-bastnäsite-(Ce)-parisite-(Ce)/synchysite-(Ce)-allanite-(Ce)-albite-quartz-biotite-fluorite-kutnahorite-hematite-bearing pseudomorphs by an inferred fluorine-enriched magmatic hydrothermal fluid. Yttrium and REE were also mobilized from the cores of primary zircon crystals in the upper zone and locally precipitated as fergusonite-(Y) along micro-fractures. Hydrothermal fluids altered the distribution of REE, within the upper and lower mineralized zones, locally enriching and depleting them, and created a set of secondary minerals which will be the main target of future exploitation.

SOMMAIRE

Le gisement de terres rares (Zr, Nb, Y, REE, Ta, Be, Ga) de Thor Lake situé dans les Territoires du Nord-Ouest, Canada, représente l'une des plus grandes ressources de zircon, niobium, yttrium et des éléments du groupe des terres rares lourdes (REE) au monde. Une partie importante des minéralisations reconnues comme potentiellement économiques résulte de processus magmatiques. Il existe également des évidences d'une remobilisation du Zr, Y et REE par des fluides hydrothermaux. Le gisement se situe sur le versant méridional de la Province de l'Esclave dans le Bouclier canadien, dans les unités de roches alkalines à perakalines du Complexe du lac Blachford datées à 2150 Ma (Davidson, 1978).

La minéralisation de métal rare est associée à deux couches tabulaires sub-horizontales formant une zone supérieure et une zone inférieure. Le Zr est principalement associé au zircon; le Nb à la ferrocolumbite et la fergusonite-(Y); et Y + HREE à la fergusonite-(Y) et au zircon. Les LREE sont quant à eux associés à la monazite-(Ce), l'allanite-(Ce), la bastnäsite-(Ce) et la parisite(Ce)/synchysite-(Ce).

Nous proposons un modèle dans lequel les couches enrichies en REE et HFSE résultent d'injections indépendantes de magmas miaskitique et agpaitique pour former une zone supérieure riche en zircon et une zone inférieure riche en eudialyte. L'eudialyte primaire a été altérée par des fluides hydrothermaux d'origine magmatiques enrichis en fluor et se manifeste comme des pseudomorphes de zircon-fergusonite-(Y)-bastnäsite-(Ce)-parisite-(Ce)/synchysite-(Ce)-allanite-(Ce)-albite-quartz-biotite-fluorite-kutnahorite-hematite. L'yttrium et les REE ont été remobilisés dans des zircons primaires de la zone supérieure et précipités localement en fergusonite-(Y) dans des microfractures. Les fluides hydrothermaux ont affectés la distribution des REE dans les zones minéralisées supérieure et inférieure en les enrichissant et les appauvrissant localement et créant ainsi une suite de minéraux secondaires qui feront l'objet d'une future exploitation.

CONTRIBUTIONS OF AUTHORS

The journal manuscript included for submission in this thesis is co-authored by Emma R. Sheard, Anthony E. Williams-Jones, Martin Heiligmann, Chris Pederson and David L. Trueman. The manuscript is entitled *Behaviour of zirconium, niobium, yttrium and the rare earth elements in the Thor Lake rare-metal deposit, Northwest Territories, Canada*, and has been written in accordance with the regulations put forth by the Faculty of Graduate Studies and Research, McGill University. An introductory chapter, including a literature review and description of research objectives and methodology, a second chapter summarizing the regional and local geology, as well as a concluding chapter were included in addition to the manuscript in order to provide a comprehensive description of the research. Data was collected by Sheard in summer 2008 with the guidance and supervision of Williams-Jones, Heiligmann and Pederson. Williams-Jones, Heiligmann, Pederson and Trueman also provided valuable advice and scientific discussion during field investigations in Northwest Territories. Sample preparation, dataset analysis and interpretation was done primarily by Sheard with the guidance and collaboration of Williams-Jones and Heiligmann. Initial manuscript preparation was done by Sheard with supervision and subsequent revisions by Williams-Jones.

ACKNOWLEDGEMENTS

I would like to express my sincere gratitude to my supervisor, Professor A.E. Williams-Jones, for his guidance, support and enthusiasm. Not only has he served as my supervisor, but he has also encouraged and challenged me throughout my time at McGill and has been an incredible mentor. I am indebted to both him and Martin Heiligmann for the knowledge and inspiration they have given me. I could not have done this thesis without them.

I am also grateful to Avalon Rare Metals Inc. for providing access to the field area, drill core, geochemical data and internal reports, and the assistance of company geologists Chris Pederson, Dave Trueman and William Mercer and my co-worker Angela Martin. Lang Shi provided me with endless hours of assistance and expertise in the electron microprobe facility at McGill University, for which I am very grateful. Jim Clark, Vincent van Hinsberg, Artas Migdisov and Jeanne Paquette also provided helpful advice and discussion, which contributed greatly to this thesis.

The generous financial support provided to the author by NSERC, GEOTOP and through a McGill Principal's Graduate Fellowship is gratefully acknowledged.

Lastly, I would like to thank my family and friends for their endless support and encouragement. Special thanks are given to my fellow graduate students in EPS, for all the laughs, fun times and good memories, and most importantly to my partner Thomas Brosnan for his continued inspiration throughout the duration of my degree.

TABLE OF CONTENTS

LIST OF FIGURES

LIST OF TABLES

LIST OF APPENDICES

CHAPTER I

INTRODUCTION

GENERAL STATEMENT

Introduction

Recent technological advances, such as the development of environmentally friendly hybrid cars (new generations of batteries and catalytic converters) and the discovery of new superconducting and supermagnetic materials (with applications in computers, power generation and transportation) are creating a strong demand for yttrium and the heavy rare earth elements. These elements are currently supplied mainly as byproducts of the mining of LREE ores hosted by carbonatites in China (Bayan Obo, Maoniuping), Brazil (Araxa and Catalão), and Australia (Mt. Weld), in which the ratio of the LREE with respect to the HREE, as reflected in the ratio, La/Yb, is typically in excess of 100. Historically, the Mountain Pass deposit in California was the world's main producer of LREE but ceased production in 2002 (it is re-opening in 2010 due to the current demand for these elements). As a result, the supply of Y and the HREE, instead of being determined by the demand for these elements, is being determined by the demand for the LREE. It is therefore important that deposits be brought into production that are exploited primarily for the HREE.

Yttrium and the HREE are most commonly found in elevated concentrations in agpaitic intrusions. Agpaitic melts are defined by a molar $(Na_2O + K_2O)/Al_2O_3$ ratio > 1.2 (Ussing, 1912). It is well documented that these rocks, which are commonly silica under-saturated, are products of differentiation of partial melts from an undepleted, metasomatically enriched mantle (e.g., Marks et al., 2003; Halama et al., 2004). However, there is little agreement over why Y and REE concentrate in these intrusions, why HREE are enriched relative to LREE, and whether the deposits are purely magmatic or partly the product of hydrothermal processes (Boily and Williams-Jones, 1994; Schmitt et al., 2002; Marks et al., 2003; Salvi and Williams-Jones, 2005). One of the key questions to pose with reference to these types of intrusions is how the unusual enrichment of REE and HFSE were produced and whether hydrothermal or magmatic processes or both were responsible for the high concentrations of these economically important elements. Examples of such deposits enriched in Zr, Nb, Y and REE include Strange Lake in Québec-Labrador, Canada; Illimaussaq, Greenland; the Amis Complex, Namibia; the Pilanesberg Complex, South Africa; the Khaldzan-Buregtey Granitoid Complex, Mongolia; the Lovozero massif in Russia is the largest agpaitic intrusion in the world, but is preferentially enriched in LREEs.

Role of Magmatic Processes

The economic enrichment of REE and HFSEs at Illimaussaq and Lovozero are interpreted to have been produced by magmatic processes alone (Gerasimovsky, 1969; Kogarko, 1990). Both intrusions contain layered nepheline syenites with rhythmically repeated sequences grouped in three units. At Illimaussaq the lower black unit is rich in arfvedsonite and aegirine; the middle red unit is enriched in eudialyte $\{Na_{15}Ca_6(Fe^{2+},Mn^{2+})_3Zr_3(Si_{25}O_{73})(O,OH,H_2O)_3(OH,Cl)_2\}$, the principal HFSE mineral in the complex, and the upper white unit is enriched in alkali feldspar (Marks and Markl, 2001). At Lovozero, the three layer sequence is urtite-foyaite-lujavrite. Urtite is a rock with >90% nepheline and mafic minerals, usually pyroxene and also amphibole, titanite, apatite and melanite; foyaite is a variety of nepheline syenite with equal proportions of nepheline and potash feldspar and a subordinate mafic mineral e.g. aegirine; lujavrite is a textural variety of kakortokite (nepheline syenite containing red eudialyte and a sodic pyroxene, usually acmite) distinguished by slender plagioclase and acicular pyroxene. The layering was formed by differential settling of minerals and the repetition of these units by intermittent injection and crystallization of volatile rich peralkaline magma. In the case of Lovozero, cumulus loparite $\{(Ce,Na,Ca)_2(Ti,Nb)_2O_6\}$ is the main host to the REE and HFSE (Kogarko et al., 2002). Cumulus loparite is found at the bottom of urtite layers in the urtite-foyaite-lujavrite sequence, indicating that there is a strong association between the economic mineralization and magmatic layering. However, there is evidence that loparite was replaced by mosandrite, steenstrupine, lamprophyllite and phosphates of REE, Ca and Sr either during the later stages of magmatic crystallization, or during a subsequent hydrothermal event, and this could indicate the remobilization of REE after their initial concentration. Similar processes have been proposed to explain REE and HFSE enrichment in the layered arfvedsonite and aegirine lujavrites of the Illimaussaq intrusion. In both complexes, REE and HFSE enrichment was controlled primarily by saturation of minerals like eudialyte and loparite in the magma, crystallization and gravitational settling to form layers in which these minerals were dominant.

The importance of magmatic processes in producing extreme enrichments of these elements is apparent from studies of melt inclusions. For example, Kovalenko et al. (1995) reported concentrations of Zr, Nb, Y and REE several orders of magnitude higher than in most other types of magma (2.65, 0.58, 0.22 and 0.40 wt. % respectively) from the Khadlzan-Buregtey Agpaitic Granitoid Complex, Mongolia. Melt inclusion glasses from the Amis Complex, Namibia (Schmitt et al., 2002) also have high concentrations of incompatible trace elements including Nb (min 803 ppm), Zr (min 3,187 ppm) and Y and REE (min 1,271 ppm). Furthermore, Keppler (1993) experimentally investigated the solubility of zircon, rutile, manganocolumbite, manganotantalite and rare earth phosphate minerals in water-saturated halpogranitic melts at 800°C and 2kbar and showed that their solubilities increase with increasing content of F, which he interpreted to be due to the formation of fluoro-complexes or complexes between non-bridging oxygens and the HFSE. Experiments of Watson (1979) showed that in peralkaline melts, zircon solubility has a pronounced linear dependence on $(Na_2O + K_2O)/Al_2O_3$ and that the amount of Zr that can be dissolved in such melts ranges up to 3.9 wt. %. Linnen and Keppler (2002) published similar results, showing that at 800°C, 2kbar and water-saturated conditions, zircon solubility can range from 3 wt. % ZrO_2 for strongly peralkaline melts to approximately 500 ppm ZrO_2 for metaluminous compositions. These experimental studies show that the concentrations of Zr, Nb, Y and REE in agpaitic magmas are orders of magnitude higher than in most other types of magma. This is possible due to the high concentrations of alkalies and fluorine, which are known to increase the solubility of these elements.

Role of Hydrothermal Processes

Peralkaline magmas typically become saturated with aqueous fluids late in their crystallization history, when the melts are enriched in Zr, Nb, Y and REE. Hydrothermal fluids are potentially important in the dissolution, transportation and precipitation of these elements by forming stable aqueous complexes with them. However, these processes are poorly understood. We know little about the behaviour of Nb in hydrothermal solutions, a little about Zr and most about the REE. Recent work by Migdisov and Williams-Jones (2002; 2007) and Migdisov et al. (2009) on the speciation of the REE(III) in hydrothermal solutions has generated thermodynamic data suitable for modeling the solubility of these elements at elevated temperature (up to 300°C) and pressure.

These data now permit the mobility of all REE(III) in fluoride- and chloride-bearing hydrothermal systems to be reliably evaluated. Moreover, they show that $LREEF^{2+}$ species are more stable than $HREEF^{2+}$ species at elevated temperature, implying that the LREE will be mobilized in preference to the HREE. The behaviour of the chloride-bearing REE species is similar. Whether, fluoride or chloride REE species predominate in a given system depends on the relative activity of the two ligands. However, based on the modeling of their data for REE speciation with data for REE mineralization hosted by the Capitan Mountains alkali feldspar granitic pluton, New Mexico, Migdisov and Williams-Jones (2007) concluded that for this intrusion, at least, chloride complexes predominated. Overall, the implication of this work is that either chloride or fluoride complexes may be the dominant control of REE enrichment in magmatic-hydrothermal systems such as the one that operated at Thor Lake.

An example of an intrusive system in which hydrothermal processes played an important role in concentrating the REE and HFSE is provided by the Strange Lake peralkaline granite. Crystal fractionation dominated but formation of F or possibly Cl aqueous complexes in hydrothermal fluids was a significant process by which these metals were transported and enriched in this deposit. The principal Zr bearing mineral is gittinsite {$CaZrSi_2O_7$}; Y is hosted by kainosite {$Ca_2(Ce,Y,HREE)_2Si_4O_{12}CO_3.H_2O)$}, gagarinite {$Na(Y,Ca,Na,REE_{12}F_6)$} and gadolinite {$Y_2FeBe_2Si_2O_{10}$}; and the REE are hosted by bastnäsite {$(Ce,La,Y)F(CO_3)$}, monazite {$(Ce,La,Th)PO_4$} and pyrochlore {$(Ca,Na)_2(Nb,Ta,HREE)_2O_6(O,OH,F)$}. Geochemical data indicating that HFSE are concentrated in altered rocks in the deposit by up to 60% provides evidence for hydrothermal involvement in this enrichment (Salvi and Williams-Jones, 1996). Furthermore, bastnäsite was identified as a trapped phase in aqueous inclusions by Salvi and

Williams-Jones (1990). Two hydrothermal events were hypothesized, an initial event dominated by a F-, Cl- and Na-rich and Ca- free magmatic hydrothermal fluid and a later event involving a lower temperature, Ca-rich fluid interpreted to be an evolved groundwater of meteoric origin. The former was interpreted to be the ore fluid, and mixing of these fluids was inferred to be the mechanism by which the REE and HFSE were deposited. The model assumed transport of the REE and HFSE as fluoro-complexes and their deposition due to lowered fluoride activity as a result of the precipitation of fluorite. However, it is evident from the recent findings of Migdisov and Williams-Jones (2007) that the theoretical study on which this model was based (Wood, 1990) had overestimated the stability of fluoro-REE complexes and underestimated the stability of chloro-REE complexes. It is thus possible that chloride complexes may have played a much more important and perhaps dominant role in REE transport at Strange Lake; the putative ore fluid was a brine containing ~ 25 wt. % NaCl (Salvi and Williams-Jones, 1992). Reliable data on the fluoride and chloride activity will be required for the Strange Lake system, and other REE and HFSE depositing systems where hydrothermal processes are known to have been important, in order to satisfactorily model hydrothermal concentration of the REE and HFSE.

Concluding Statement

It is evident from the intrusions discussed above that in some cases magmatic processes alone are sufficient to produce such high concentrations of REE and HFSEs and in other cases where hydrothermal alteration is extensive, hydrothermal processes are important in terms of later remobilization of these elements. With these processes in mind, we have been able to develop a model that explains the genesis of the Zr, Nb, Y and REE mineralization in the Nechalacho rare-metal deposit.

PREVIOUS WORK

Mining and Exploration

Exploration of the Thor Lake rare-metal deposit was initiated by Highwood Resources Ltd. in 1976 after reports of radioactivity were made by prospectors in 1970 (Trueman et al., 1988). The deposit was shown to contain five zones of rare metal mineralization, namely the R-, S-, T-, F- and Lake Zones, recently renamed the Nechalacho deposit. However, after many years of intermittent exploration activity by several companies, the property was abandoned because of a combination of complex mineralogy and low metal prices. Avalon Rare Metals Inc. acquired mining leases to the area in 2005 with the aim of developing a mineable deposit of Y and HREE, and since then has completed a comprehensive evaluation of the historical drilling record in the two main mineralized zones, the Nechalacho deposit and North T-Zone, and drilled more than 140 holes (>27,000m) in the Nechalacho. As a result, an inferred resource in the lower mineralized zone of the Nechalacho deposit of 44.3 million tons grading 1.94 wt. % REE_2O_3 + Y_2O_3, 3.53 wt. % ZrO and 0.49 wt. % Nb_2O_5, and in the North T-Zone, a resource of 1.1 million tons grading 0.71 wt. % REE_2O_3 + Y_2O_3, 0.48 wt. % BeO and 0.53 wt. % Nb_2O_5, have been delineated. Definition drilling in the Nechalacho deposit is ongoing, with our research directly contributing to the current exploration model.

Research

Regional studies of the Blachford Lake Complex have been published by Davidson (1972; 1978; 1982), Hoffman et al. (1978), Cerny and Trueman (1985) and Bowring et al. (1984), who calculated U-Pb zircon ages, which have constrained the timing and development of the Athapuscow aulacogen in the eastern arm of Great Slave Lake.

Academic research at Thor Lake has been restricted to a few GAC and GSC reports (Pederson and Lecouteur, 1991; Birkett et al., 1992); a chapter published in a Mineralogical Society Series volume on the REE by Taylor and Pollard (1996) on fluid inclusions in the T-Zone; an overview paper on the Thor Lake rare-metal deposits by Trueman et al. (1988); and three Master's theses, two of which were published (Smith et al., 1991; Pinckston and Smith, 1995). In Pinckston's study, detailed descriptions of the geology and mineralogy of the Nechalacho deposit were made, including an overview of the silica under-saturated rocks encountered at depth beneath this deposit. Hudson (1987) reported the occurrence of gallium in the Nechalacho deposit, concluding that it is hosted by biotite and albite and occurs in association with Ta, Nb and REE mineralization. Finally de St. Jorre studied the geology and mineralogy of the North T-Zone and was a co-author on the Smith et al. (1991) paper on zonally metamict zircon from the North T-Zone. One of the key points of the earlier work was that Thor Lake differs from other deposits in that hydrothermal alteration obliterated most of the original igneous textures such that even the nature of the host rocks could not be properly discerned. As a result of the extensive drilling undertaken by Avalon Rare Metals Inc. since 2007, we have made considerable progress in our understanding of the deposit and are now able to partly decipher the pre-alteration history of the Nechalacho deposit.

PURPOSE AND METHODOLOGY

The main objective of this thesis is to develop a model that explains the genesis of Zr, Nb, Y and REE mineralization in the Nechalacho deposit, which is currently being explored by Avalon Rare Metals Inc. The project aims to investigate the role of magmatic and hydrothermal processes in Zr, Nb, Y and REE concentration in the deposit, determine the source of metals, and develop a genetic model for the deposit which could guide its further exploration. In order to develop such a model, it is necessary to: 1) build on previous work by establishing the distribution and paragenesis of the rare metal minerals in the Nechalacho, which has been subject to limited investigation; 2) evaluate the hydrothermal alteration and its relationship to rare metal mineralization; 3) assess the mineral chemistry of the zircon and other rare metal minerals; 4) use textural relationships and mineral chemical data to evaluate the roles of magmatic and hydrothermal processes in the crystallization of zircon and other rare metals minerals and determine the extent to which some or all of the REE and HFSE were remobilized.

The objectives of the research were pursued using a combination of:

1) A program of fieldwork at the Thor Lake rare-metal deposit, Northwest Territories, including drill core logging and sampling of rocks for petrographic and geochemical analyses.
2) Optical petrographic examination of polished thin sections to identify primary and secondary rock-forming, ore and alteration minerals, determine the textural relationships among them and relate this to an overall paragenetic sequence.
3) Compilation and analysis of the bulk-rock geochemical data acquired by Avalon Rare Metals Inc.

4) SEM microscopy, elemental X-ray maps and quantitative electron microprobe analyses to determine the chemical compositions of rock-forming, ore and alteration minerals; confirm optical identification of these minerals; assist in evaluating textural relationships used to establish the paragenetic sequence; and correlate chemical variations with changes in textural relationships. The data were obtained using a JEOL JXA-8900L electron microprobe equipped with 5 WDS spectrometers and a Si(Li) EDS detector at McGill University. Spot analyses using wavelength-dispersive spectrometry (WDS) performed on the zircon, fergusonite-(Y), eudialyte and ferrocolumbite were conducted at 20kV, with a 30nA beam current and a beam diameter of 3µm. A 10µm beam diameter was used for allanite-(Ce), monazite-(Ce) and bastnäsite-(Ce).
5) Cathodoluminescence responses of zircon and albite were analysed qualitatively using a Reliotron III luminoscope at McGill University. Analyses were performed using a voltage of around -5kV for zircon and 6kV for albite and a current of 0.5mA for both.

CHAPTER II

GEOLOGY

REGIONAL GEOLOGY

The Thor Lake rare-metal (Zr, Y, REE, Nb, Ta, Be, and Ga) deposit is located approximately 100 km southeast of Yellowknife, Northwest Territories and 5 km north of the Hearne Channel, Great Slave Lake. Geologically, it is situated at the southern edge of the Slave Province of the Canadian Shield, within the alkaline to peralkaline Blachford Lake Complex, which is thought to have been emplaced during development of the Authapuscow Aulacogen underlying the east arm of the Great Slave Lake (Davidson, 1978; Trueman et al., 1988; Sinclair et al., 1992). Approximately 2.1 billion years ago, the Slave Craton rested over two hot spots at Great Slave and Coronation Gulf (Hoffman, 1978). A series of rifts developed, some in the Wopmay Orogen (ca. 1900 Ma) and the others along the east arm of Great Slave Lake (the Athapuscow Aulacogen), which coincides with the Great Slave Fault Zone, a major strike slip shear zone with a postulated displacement of 500 kilometres (Davidson, 1978; Bowring et al., 1984). It is here, just prior to rifting, that a series of alkaline to peralkaline intrusive bodies and mafic dyke swarms were intruded to form the Blachford Lake Complex.

Davidson (1972; 1978) and Hoffman et al. (1980) subdivided the complex into two portions: a western, less alkaline series of gabbros, anorthosites, granites, and syenites, namely the Caribou Lake Gabbro, the Whiteman Lake Quartz Syenite, the Hearne Channel Granite and the Mad Lake Granite. In contrast, the rocks of the eastern portion: the Grace Lake Granite and Thor Lake Syenite are more alkaline in composition. Gravity modeling by Birkett et al. (1994) suggests that the eastern portion forms a thin tabular body with a maximum thickness of one kilometre. In contrast, the Caribou Lake Gabbro in the western portion is interpreted by them to be deeply rooted. The sequence of intrusive events has been established by cross-cutting relationships of dykes and major contacts and illustrates a progression towards increasingly alkaline to peralkaline rocks over time (Davidson, 1978). The youngest of these intrusive events gave rise to the Grace Lake Granite and Thor Lake Syenite, which have gradational contacts, and were therefore interpreted by Davidson (1982) to have been intruded contemporaneously with gradual inward crystallization of the Thor Lake Syenite, although subsequent U-Pb dating by Sinclair and Richardson (1994) showed the Grace Lake Granite to be slightly older than the Thor Lake Syenite (2176 ±1.3 Ma vs 2094 ±10 Ma). Air-photo interpretations have shown that circular ring-shaped fractures pervade the complex, indicating emplacement of a geometrically simple, anorogenic ring complex (Pinckston and Smith, 1994). A suite of intrusive rocks, which we interpret to represent a layered alkaline igneous complex comprising several types of nepheline syenite, has been intersected by drilling in the core of the Thor Lake Syenite and is the host to the bulk of the rare metal mineralization in the Nechalacho deposit.

All of the above rock units were intruded into Archean mica-schists of the Yellowknife Supergroup, which surround the Blachford Lake Complex and are present as rafts or xenoliths within. To the south are greywackes, shales and carbonates of the Great Slave Supergroup (Trueman et al., 1988), which are separated from the complex by a postulated faulted contact along the Hearne Channel of Great Slave Lake.

LOCAL GEOLOGY

Thor Lake Syenite

The Thor Lake Syenite occupies a roughly oval area of 30 km^2 in the centre of the Grace Lake Granite (Davidson, 1978), is medium- to coarse-grained, and consists of euhedral K-feldspar with interstitial amphibole, magnetite, and minor quartz (Trueman et al., 1988). Locally, the syenite can be pegmatitic with large (up to 15 cm) euhedra of amphibole and/or pyroxene, fine-grained albite or coarse-grained K-feldspar. The Thor Lake Syenite and other units within the Blachford Lake Complex are cut by narrow (less than 5 m wide) felsite dykes, of trachyte to quartz trachyte composition. They are generally vertical and strike northeasterly.

The Thor Lake-Nechalacho Layered Alkaline Complex

The complex comprises numerous sub-horizontal layers of sodalite syenite, possible eudialyte cumulate (the postulated eudialyte has been pseudomorphed by zircon, fergusonite-(Y) $\{(Ce,La,Nd,Y)NbO_4\}$, bastnäsite-(Ce) $\{(Ce,La,Y)F(CO_3)\}$, allanite-(Ce) $\{(Ce,Ca,Y)_2(Al,Fe^{3+})_3(SiO_4)_3(OH)\}$, parisite-(Ce) $\{Ca(Ce,La)_2(CO_3)_3F_2\}$/synchysite-(Ce) $\{Ca(Y,Ce,La,Nd,Gd)[F(CO_3)_2]\}$, albite, quartz, biotite, fluorite, kutnahorite $\{Ca(Mn,Mg,Fe)(CO_3)_2\}$ and minor hematite), and lujavrite but is dominated by aegirine nepheline syenite. Sharp sub-horizontal intrusive contacts can be observed between the different layers, which range in thickness from tens of centimetres to several tens of metres.

The aegirine nepheline syenite is a medium- to coarse-grained rock, which is heterogeneous in texture and grain size; pegmatitic lenses are common. Aegirine and nepheline form phenocrysts in a matrix consisting dominantly of albite with minor accessory phases and secondary alteration minerals. The nepheline phenocrysts are subhedral, up to 1cm in diameter and typically display a poikilitic texture produced by lath-shaped inclusions of orthoclase and albite, and anhedral inclusions of chlorite and zircon. Minor aegirine anhedra have also been identified within nepheline. Aegirine phenocrysts display a range of shapes and sizes. They range from <1mm up to 8mm in length and can be both unzoned and rimmed by an inclusion-free overgrowth. Most aegirine crystals are fractured along cleavage planes and infilled by biotite, albite, magnetite/hematite and minor fluorite, which also locally replace aegirine. They also host a number of inclusions, namely of allanite, zircon, a Ca-Zr silicate (possibly gittinsite or vlasovite) and an unknown REE bearing phase which could be melanocerite-(Ce) $\{(Ce,Ca)_5(Si,B)_3O_{12}(OH,F).nH_2O\}$, as Ce, Ca, Si and B were identified as peaks in energy dispersive spectra (EDS). Interstitial bladed albite is common in the groundmass between nepheline and aegirine crystals and locally replaced both, suggesting that it crystallized slightly later. Small pockets of rare metal mineralization occur throughout, and are dominated by zircon with minor allanite-(Ce), britholite-(Ce) $\{Ca_2[(Y,Ce)Ca]_3[(OH,F)(SiO_4,PO_4)_3]\}$ and thorite. Many of these pockets, particularly in the lower mineralized zone, have regular geometric shapes with planar elements reminiscent of crystal faces, suggesting that they represent pseudomorphs of an earlier mineral. Fresh eudialyte intergrown with analcime $\{NaAl(Si_2O_6).(H_2O)\}$ and oneillite $\{Na_{15}Ca_3Mn_3Fe^{2+}{}_3Zr_3Nb(Si_{25}O_{73})(O,OH,H_2O)_3(OH,Cl)_2\}$ was found in one of these pockets at a depth of 349 metres. Thus it is probable that these mineralized pockets represent former eudialyte.

The lujavrite is a fine-grained rock, characterized by a sub-horizontal alignment of albite and aegirine crystals. Albite and orthoclase are interstitial to nepheline and elongated primary bladed albite crystals can be observed clearly wrapping around nepheline phenocrysts and displaying a pronounced sub-horizontal lamination. Nepheline phenocrysts, 2-3mm in diameter, are commonly observed with a rim of analcime and are poikilitic with abundant inclusions of fragmented aegirine, orthoclase and zircon. Fragments and platy crystals of aegirine are fine-grained, intensely fractured but also oriented with their longest direction in the plane of lamination. Aegirine crystals are commonly associated closely with or contain inclusions of zircon. Both nepheline and aegirine were locally replaced by bladed albite, which crystallized slightly later.

Sodalite syenite is a highly altered, medium-grained intrusive rock, which has been pervasively hematized and sericitized. Primary sodalite was completely altered to hematite, sericite and chlorite in most samples examined. Sodalite crystals display a distinctive orange fluorescence under UV illumination, which allows them to be easily identified in drill core despite their extensive alteration and replacement. In less altered samples, it is evident that crystals of altered sodalite are enclosed in coarse anhedra of orthoclase and an unknown altered dark green mineral, which could be aegirine. Orthoclase and albite are the interstitial minerals, and are commonly intergrown and display a perthitic exsolution texture.

Nechalacho Mineralization

Five discrete zones of mineralization have been identified, namely the R-, S-, T-, F- and Lake Zones, renamed the Nechalacho deposit. The T-Zone, hosted in the north by the Grace Lake

Granite and in the south by the Thor Lake Syenite, measures roughly 150 to 300 metres in diameter and extends discontinuously southeast for approximately 900 metres. A total of 15 lithological units have been recognized in the T-Zone, and have been grouped into four spatially distinguishable zones (wall-, lower intermediate-, upper intermediate-, quartz-zones). The lower intermediate unit has elevated concentrations of Be (phenakite), Nb (columbite), Y and REE, mainly as xenotime and to a lesser extent as fergusonite-(Y), yttrialite, and thorite, whereas the upper intermediate unit hosts LREE-fluorocarbonates comprising bastnäsite-(Ce), parisite-(Ce), röntgenite-(Ce) and synchysite-(Ce).

The largest of the mineralized zones is the Nechalacho deposit, which is the focus of this research and has been the focus of recent exploration by Avalon Rare Metals Inc. for Zr, Y, REE, Nb and Ta. Based on the exploration that has been conducted to date, the Nechalacho comprises two mineralized zones, a 15 to 30 metre thick upper zone and a more homogeneous 15 to 60 metre thick lower zone. In some drill holes, two distinct zones separated by unmineralized rocks are present, whereas, in other holes, the upper zone grades directly into the lower zone. Plots of REE abundance with depth indicate that the heavy REE are concentrated in the lower mineralized zone, that intermediate REE (e.g., Gd) show no real preference for upper or lower mineralized zones and that the light REE are concentrated in the upper mineralized zone.

The ore mineralogy in each zone is broadly similar. Zirconium is hosted mainly by zircon, niobium by ferrocolumbite and fergusonite-(Y), yttrium and the HREE by fergusonite-(Y) and zircon and the LREE by monazite-(Ce), allanite-(Ce), bastnäsite-(Ce) and parisite-(Ce)/synchysite-(Ce). Zircon and bastnäsite-(Ce) are the only two minerals visible macroscopically in drill core. In the upper zone, bastnäsite-(Ce) is brick red in colour and is spatially associated with fluorite and albite. Zircon is finely disseminated and commonly occurs in undulating laminations. It is also present in veins and wrapped around brecciated k-feldspar fragments. In the lower mineralized zone, zircon occurs as a secondary phase in pseudomorphs after probable eudialyte.

Alteration

The rocks in the upper part of the layered alkaline complex have been intensely altered by hydrothermal fluids, leaving only relicts of the primary mineralogy. Magnetite and biotite are the two dominant alteration minerals in the Nechalacho deposit and are temporally and spatially associated with fergusonite-(Y), ferrocolumbite, allanite-(Ce), monazite-(Ce) and bastnäsite-(Ce) in the upper mineralized zone. Magnetite remains important in the lower zone but is accompanied by hematite, and biotite is less important. Both magnetite and biotite replaced earlier minerals such as aegirine and zircon and infill veins and fractures in primary K-feldspar, with biotite locally replacing magnetite. Hematite is a late alteration mineral, which locally replaced magnetite-biotite-quartz-zircon, pseudomorphs after eudialyte and is more prevalent beneath the lower zone.

Alteration of the rocks to magnetite and/or hematite and biotite was followed by albitization, primarily as a replacement of primary K-feldspar by albite. However, in many cases, albitization also removed magnetite, biotite and REE mineralization including zircon-bearing pseudomorphs after eudialyte. Albitization is encountered at irregular intervals to the maximum depth of drilling (~ 200 m) but is most common in the upper 50 metres or so of the complex where a vuggy and typically brecciated, pegmatitic unit is intersected. The latter is composed almost entirely of blades of albite ('cleavelandite'). Albitites at greater depth have also commonly formed by alteration of pegmatite. Remnant, partially altered K-feldspar megacrysts are observed where albitization is less pervasive. Vugs produced by albitization were variably open to infilling by later carbonates, clays, fluorite and minor pyrite.

Late stage silicification (quartz), illitization and sericitization also occur in the deposit, but appear to have been of limited importance in concentrating or redistributing Y and HREE. However, carbonatization (calcite, ankerite, siderite) may have been associated with REE fluoro-carbonate precipitation, as calcite, fluorite and bastnäsite-(Ce) are intimately associated within the albitites. Carbonatization was the latest alteration event, and accompanied calcite veins that cross-cut all lithologies in the Nechalacho deposit.

CHAPTER III

JOURNAL MANUSCRIPT

Behaviour of zirconium, niobium, yttrium and the rare earth elements in the Thor Lake rare-metal deposit, Northwest Territories, Canada

Emma R. Sheard, Anthony E. Williams-Jones, Martin Heiligmann, Chris Pederson and David L. Trueman

Emma R. Sheard, Anthony E. Williams-Jones and Martin Heiligmann
Earth and Planetary Sciences, McGill University
3450 University Street, Montreal, QC
Canada H3A 2A7

Chris Pederson and David L. Trueman
Avalon Rare Metals Inc.
130 Adelaide Street West, Suite 1901, Toronto, ON.
Canada M5H 3P5

Submitted to: Economic Geology

ABSTRACT

The Thor Lake rare-metal (Zr, Nb, Y, REE, Ta, Be, Ga) deposit in the Northwest Territories of Canada represents one of the largest resources of zirconium, niobium, yttrium and the heavy rare earth elements in the world. Much of the potentially economic mineralization was concentrated by magmatic processes. However, there is also evidence of remobilization of Zr, Y and REE by hydrothermal fluids. Geologically, the deposit is situated at the southern edge of the Slave Province of the Canadian Shield, within the 2150 Ma alkaline to peralkaline Blachford Lake Complex (Davidson, 1978). A layered alkaline intrusion dominated by aegirine nepheline syenite occurs in the centre of this suite of rocks and is considered to represent the youngest phase of the complex.

Much of the rare metal mineralization occurs in two sub-horizontal tabular layers, an upper and a lower zone of the Nechalacho deposit (formerly the Lake Zone), with Zr hosted primarily by zircon, Nb primarily by ferrocolumbite and fergusonite-(Y), and Y + HREE by fergusonite-(Y) and zircon. The LREE are present mainly in monazite-(Ce), allanite-(Ce), bastnäsite-(Ce) and parisite-(Ce)/synchysite-(Ce). Much of the HREE mineralization in the lower mineralized zone occurs in secondary zircon, which forms small (10-30 μm) anhedral grains in pseudomorphs after probable eudialyte. In the upper zone, zircon is a magmatic cumulate mineral, which locally was replaced by secondary REE-bearing minerals. Element-distribution maps of zircon crystals in the upper zone indicate that Y and REE were mobilized from the cores and locally precipitated as fergusonite-(Y) along micro-fractures. The LREE were also mobilized locally from both primary zircon and inferred primary eudialyte. The occurrence of zircon in fractures,

wrapped around brecciated K-feldspar fragments and as a secondary phase in pseudomorphs are evidence of its hydrothermal origin and/or remobilization of primary zirconium.

A model is proposed in which injection of separate pulses of miaskitic and agpaitic magma resulted in the crystallization of an upper zone rich in zircon and a lower zone rich in eudialyte. Primary eudialyte was later altered to zircon-fergusonite-(Y)-bastnäsite-(Ce)-parisite-(Ce)/synchysite-(Ce)-allanite-(Ce)-albite-quartz-biotite-fluorite-kutnahorite-hematite-bearing pseudomorphs by an inferred fluorine-enriched magmatic hydrothermal fluid. Zirconium, niobium, yttrium and REE in both the upper and lower zones were subsequently mobilized during multiple hydrothermal alteration events, which, for the most part, served to further enrich the primary layers in REE (albitization generally dispersed REE and HFSE) and create new secondary REE-bearing phases.

INTRODUCTION

Zirconium is an incompatible trace element and occurs in most igneous rocks at ppm concentrations as the accessory mineral, zircon. However, in peralkaline systems (e.g., Ilimaussaq: Gerasimovsky, 1969; Lovozero: Kogarko, 1990; Strange Lake: Miller, 1986; and Thor Lake, Trueman, 1988), it is locally present in percentage level concentrations and may be accompanied by concentrations and quantities of yttrium and the heavy rare earth elements (HREE) sufficient to form a potentially exploitable resource. In most of these systems, the zirconium occurs mainly as complex zirconosilicate minerals such as elpidite {$Na_2ZrSi_6O_{15}.3H_2O$}, catapleiite {$Na_2ZrSi_3O_9.2H_2O$}, wadeite {$K_2ZrSi_3O_9$}, eudialyte

$\{Na_{15}Ca_6(Fe^{2+},Mn^{2+})_3Zr_3(Si_{25}O_{73})(O,OH,H_2O)_3(OH,Cl)_2\}$, vlasovite $\{Na_2ZrSi_4O_{11}\}$ and gittinsite. $\{CaZrSi_2O_7\}$, but at Thor Lake, the principal zirconium mineral is zircon.

There is a broad consensus that peralkaline igneous rocks are products of differentiation of partial melts from an undepleted, metasomatically enriched mantle (e.g., Marks et al., 2003; Halama et al., 2004). However, there is little agreement over why Y and REE concentrate in these intrusions, why HREE are enriched relative to LREE, and whether the deposits are purely magmatic or partly the product of hydrothermal processes (Boily and Williams-Jones, 1994; Schmitt et al., 2002; Marks et al., 2003; Salvi and Williams-Jones, 2005). Although the reasons for the very high concentrations of Zr, Nb, Y and HREE in peralkaline igneous systems are still poorly understood, experiments by Watson (1979) and Linnen and Keppler (2002) have shown that zircon solubility in magmas increases with increasing concentration of alkalis, and in peralkaline melts can exceed 3 wt. % ZrO_2. Studies of melt inclusions have yielded similar results, showing that agpaitic magmas can have concentrations of Zr, Nb, Y and REE, that in some cases are orders of magnitude higher than those in other types of magma. For example, Kovalenko et al. (1995), reported concentrations of Zr, Nb, Y and REE from the Khadlzan-Buregtey Granitoid complex of 2.65, 0.58, 0.22 and 0.40 wt. %, respectively.

In several peralkaline complexes, fractional crystallization has served to further increase concentrations of the above elements over those originally present in the melt. For example, at both Ilimaussaq and Lovozero, REE and HFSE were enriched locally by saturation of minerals like eudialyte and loparite $\{(Ce,Na,Ca)_2(Ti,Nb)_2O_6\}$ in the magma, and their gravitational settling to form layers in which these minerals are dominant. There is also evidence that in some of these complexes hydrothermal processes have further concentrated these elements. For example, REE and the HFSE in the Tamazeght Complex, Morocco, are hosted in secondary phases such as calcic catapleiite $\{(Ca,Na)ZrSi_{13}O_9.2H_2O\}$ and rinkite $\{(Ca,Ce)_4Na(Na,Ca)_2Ti(Si_{12}O_7)_2F_2(O,F)_2\}$, which replaced primary zircon and eudialyte (Salvi et al., 2000). In the most evolved lujavrites at Ilimaussaq (Sorensen, 1997), there are hydrothermal veins of steenstrupine $\{Na_{14}Ce_6Mn^{++}Mn^{+++}Fe^{++}{}_2(Zr,Th)(Si_6O_{18})_2(PO_4)_7.3(H_2O)\}$ and at Strange Lake, Quebec/Labrador, bulk rock chemical analyses of fresh and altered rocks point to hydrothermal enrichment of the HFSE by as much as 25% (Salvi and Williams-Jones, 1996).

The Thor Lake deposit is an ideal setting in which to investigate the relative importance of magmatic and hydrothermal processes involved in producing unusual enrichments of Zr, Nb, Y and REE. The bulk of the rare-metal mineralization is hosted in zircon, which contains the highest concentrations of REE ever reported in the literature. There are cumulate textures involving both zircon and inferred eudialyte, there is extensive hydrothermal alteration and there is strong evidence for the remobilization of these elements from primary zircon and eudialyte.

Exploration of the Thor Lake deposit began in 1976, and after years of intermittent exploration activity, five zones of rare metal mineralization were delineated, namely the R-, S-, T-, Fluorite and Lake Zones (Trueman et al., 1988). By far the largest of these is the Lake Zone, recently renamed the Nechalacho deposit, which has been shown through drilling to be present in the subsurface over an area of at least $2km^2$. This zone has been the focus of recent exploration by Avalon Rare Metals Inc. for Zr, Nb, Y and REE mineralization, and is the subject of the present study. Provisional estimates of the concentrations of these elements are shown in Table 3.1.

Only a limited number of papers have been published on the Thor Lake deposit (Davidson, 1981; Cerny and Trueman, 1985; Trueman et al., 1988; Smith et al., 1991; Pinckston and Smith, 1995). However, an important conclusion of all of these studies is that Thor Lake differs from other deposits in that hydrothermal alteration obliterated most of the original igneous textures such that even the nature of the host rocks could not be properly discerned. As a result of recent drilling by Avalon Rare Metals Inc., we are now able to partly decipher the pre-alteration history of the deposit. The purpose of our study was to use the textural relationships and composition of zircon and other rare metal minerals in the Nechalacho deposit to investigate the role of magmatic and hydrothermal processes in their crystallization and determine the extent to which some or all of the REE and HFSE were remobilized. This paper describes an important example of a newly recognized large REE and HFSE enriched layered alkaline complex and proposes a model that explains the genesis of the Nechalacho deposit, and perhaps similar deposits elsewhere.

Table 3.1 Provisional concentrations of Y, REE, Ta, Nb, Zr, Ga and Hf oxides for the Nechalacho deposit (Avalon Rare Metals Inc. Resource Estimate, updated August 2009). Cut-off grades for TREO (%) are 1.6.

		Upper zone *(inferred)*	Lower zone *(inferred)*	Lower zone *(indicated)*
TREO (wt.%)		2.01	1.94	1.97
Tonnes		19,896,817	44,257,886	4,400,189
Oxide (ppm)	Y	689	2,165	2,662
	La	3,643	3,094	2,998
	Ce	9,416	7,091	6,737
	Pr	1,001	883	851
	Nd	3,776	3,521	3,362
	Sm	664	718	752
	Eu	70	89	98
	Gd	465	663	754
	Tb	47	98	119
	Dy	173	501	628
	Ho	23	88	116
	Er	53	216	300
	Tm	7	30	41
	Yb	47	176	243
	Lu	7	24	33
	Ta	208	462	497
	Nb	3,716	4,947	4,698
	Zr	24,348	35,329	36,006
	Ga	168	135	132
	Hf	460	726	763

GEOLOGICAL SETTING

Regional Geology

The Thor Lake rare-metal (Zr, Nb, Y, REE, Ta, Be, and Ga) deposit is located approximately 100 km southeast of Yellowknife, Northwest Territories (Figure 3.1) at the southern edge of the Slave Province of the Canadian Shield in alkaline to peralkaline rocks of the Blachford Lake Complex (Davidson, 1978; Trueman et al., 1988; Sinclair et al., 1992). According to Hoffman (1978), the Slave Craton rested over two hot spots at Great Slave and Coronation Gulf at ~ 2.1 billion Ga (Figure 3.2). A series of rifts developed, some in the Wopmay Orogen (ca. 1900 Ma) and the others along the east arm of Great Slave Lake (the Athapuscow Aulacogen), which coincides with the Great Slave Fault Zone, a major strike-slip shear zone with a postulated displacement of 500 kilometres (Davidson, 1978; Bowring et al., 1984). It is here, just prior to rifting, that a series of alkaline to peralkaline plutons were intruded to form the Blachford Lake Complex.

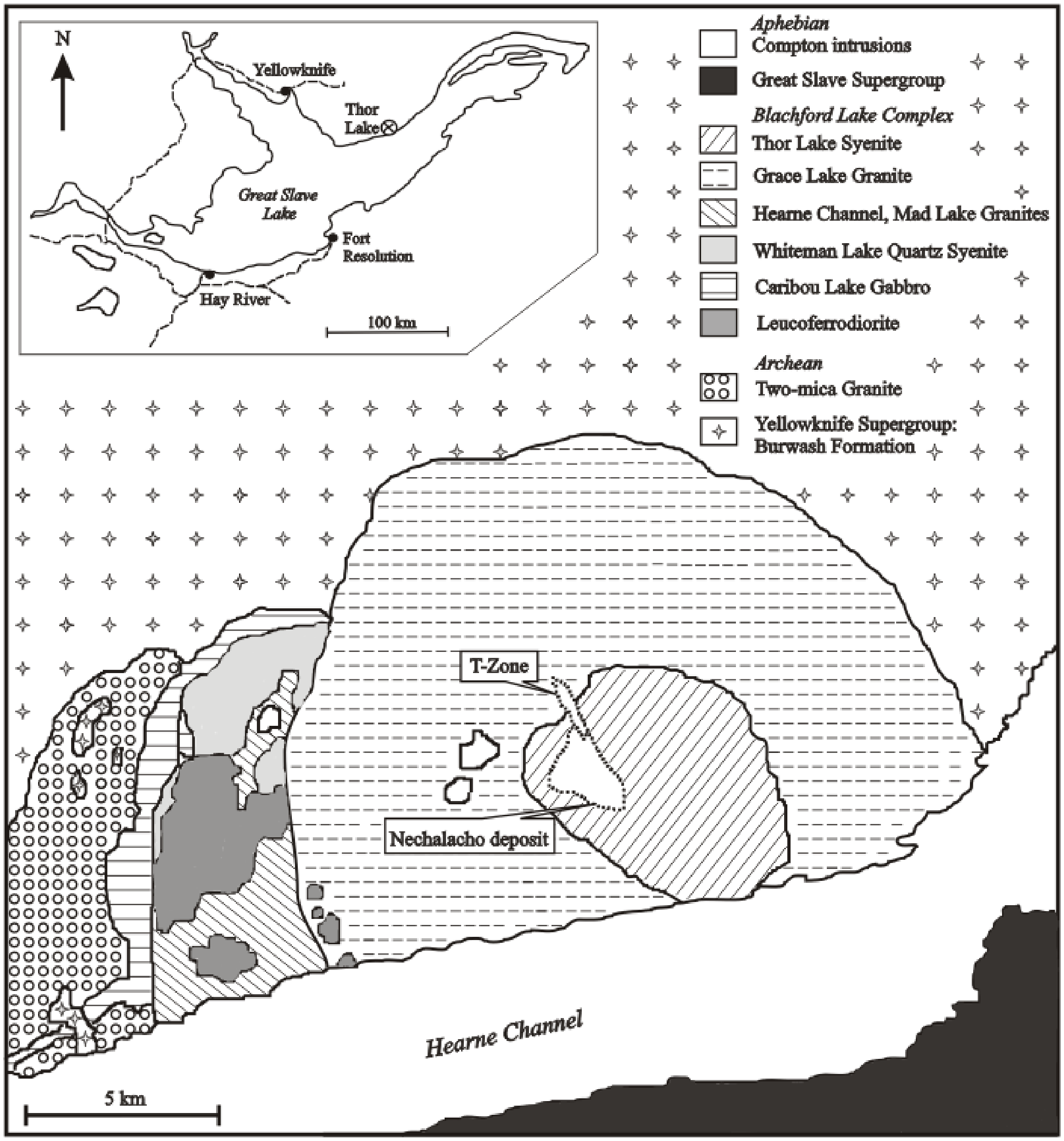

Figure 3.1 Geological map of the Blachford Lake complex showing the location of the mineralized Nechalacho deposit and T-Zone within the Thor Lake rare-metal deposit. (modified after Davidson, 1982).

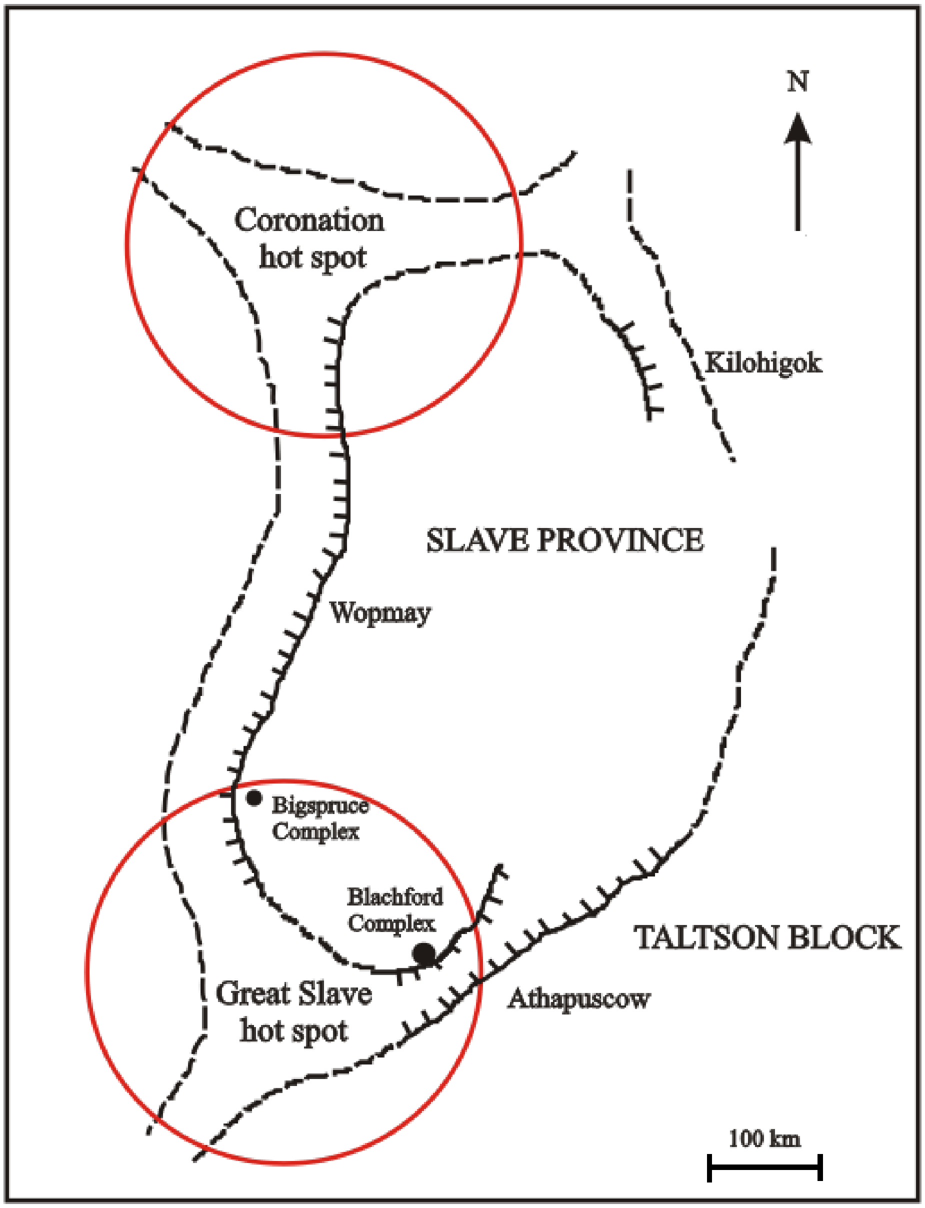

Figure 3.2 Schematic map showing the location of the Great Slave and Coronation hot spots in relation to the Slave Province. The Blachford Lake complex is marked with a black dot (modified after Hoffman, 1978).

Davidson (1972; 1978) and Hoffman et al. (1980) subdivided the Blachford Lake Complex into six units representing five distinct intrusive events, namely the Caribou Lake Gabbro, the Whiteman Lake quartz Syenite, the Hearne Channel Granite, the Mad Lake Granite, the Grace Lake Granite and the Thor Lake Syenite (Figure 3.1). The youngest of these events gave rise to the Grace Lake Granite and Thor Lake Syenite, which have gradational contacts, and were therefore interpreted by Davidson (1982) to have been intruded contemporaneously, although subsequent U-Pb dating by Sinclair and Richardson (1994) showed the Grace Lake Granite to be slightly older than the Thor Lake Syenite (2176 ±1.3 Ma vs 2094 ±10 Ma). A suite of intrusive rocks, which we interpret to represent a layered alkaline igneous complex has been intersected by drilling in the core of the Thor Lake Syenite and is the host to the bulk of the rare metal mineralization in the Nechalacho deposit.

All of the above rock units were intruded into Archean mica-schists of the Yellowknife Supergroup, which surround the Blachford Lake Complex. To the south are greywackes, shales and carbonates of the Great Slave Supergroup (Trueman et al., 1988), which are separated from the complex by a postulated faulted contact along the Hearne Channel of Great Slave Lake.

The Thor Lake-Nechalacho Layered Alkaline Complex

The complex comprises numerous sub-horizontal layers of sodalite syenite, inferred eudialyte cumulate (the inferred eudialyte has been pseudomorphed by zircon, fergusonite-(Y) {$(Ce,La,Nd,Y)NbO_4$}, bastnäsite-(Ce) {$(Ce,La,Y)F(CO_3)$}, allanite-(Ce) {$(Ce,Ca,Y)_2(Al,Fe^{3+})_3(SiO_4)_3(OH)$}, parisite-(Ce) {$Ca(Ce,La)_2(CO_3)_3F_2$}/synchysite-(Ce) {$Ca(Y,Ce,La,Nd,Gd)[F(CO_3)_2]$}, albite, quartz, biotite, fluorite, kutnahorite

$\{Ca(Mn,Mg,Fe)(CO_3)_2\}$ and minor hematite) and lujavrite but is dominated by aegirine nepheline syenite. Sharp sub-horizontal intrusive contacts can be observed between these different layers, which range in thickness from tens of centimetres to several tens of metres.

The aegirine nepheline syenite is a medium- to coarse-grained rock, which is heterogeneous in texture and grain size, with common pegmatitic lenses. Its composition is fairly consistent and similar to that of other HFSE-enriched alkaline intrusions such as Pilanesberg, South Africa (Olivo and Williams-Jones, 1999). Aegirine and nepheline form phenocrysts in a matrix consisting dominantly of albite with minor accessory phases and secondary alteration minerals (Figure 3.3A). The nepheline phenocrysts are subhedral, up to 1cm in diameter and typically display a poikilitic texture produced by lath-shaped inclusions of aegirine and albite, and anhedral inclusions of chlorite and zircon (Figure 3.3B). Small numbers of anhedral aegirine inclusions have also been observed. Aegirine phenocrysts display a range of shapes and sizes. They vary in length from <1mm up to 8mm, and can be both unzoned and rimmed by an inclusion-free overgrowth (Figure 3.3C). Most aegirine crystals are fractured along cleavage planes and infilled by biotite, albite, magnetite/hematite and minor fluorite, which also locally replaced the aegirine. They also host inclusions of allanite, zircon, a Ca-Zr silicate (possibly gittinsite or vlasovite) and an unknown REE bearing phase which, based on peaks for Ce, Ca, Si and B in EDS spectra, could be melanocerite-(Ce) $\{(Ce,Ca)_5(Si,B)_3O_{12}(OH,F).nH_2O\}$. Interstitial bladed albite is common in the groundmass between nepheline and aegirine crystals (Figure 3.3D) and locally replaced both, suggesting that it crystallized later. Sporadic patches of rare metal mineralization occur throughout, and are dominated by zircon but also contain minor allanite-(Ce), britholite-(Ce) $\{Ca_2[(Y,Ce)Ca]_3[(OH,F)(SiO_4,PO_4)_3]\}$ and thorite. Many of these patches, particularly in the lower mineralized zone (see below), have regular geometric shapes with planar elements reminiscent of crystal faces, suggesting that they represent pseudomorphs of an earlier mineral, possibly eudialyte. This interpretation is supported by the occurrence of fresh eudialyte intergrown with analcime {$NaAl(Si_2O_6).(H_2O)$} and oneillite {$Na_{15}Ca_3Mn_3Fe^{2+}{}_3Zr_3Nb(Si_{25}O_{73})(O,OH,H_2O)_3(OH,Cl)_2$} in core from a single drill hole (85-L6) at a depth of 349 metres.

The lujavrite is a fine-grained intrusive unit, characterized by a sub-horizontal alignment of albite and aegirine crystals. Albite and orthoclase are interstitial to nepheline, and crystals of bladed primary albite can be observed wrapped around nepheline phenocrysts, imparting a pronounced sub-horizontal lamination to the rock. Nepheline phenocrysts, 2-3mm in diameter, are commonly observed with a rim of analcime, and are poikilitic with abundant inclusions of fragmented aegirine, orthoclase and zircon (Figure 3.3E). Fragments and platy crystals of aegirine are fine-grained, intensely fractured but also oriented with their longest direction in the plane of lamination. Aegirine crystals are commonly associated closely with zircon or contain inclusions of zircon. Both nepheline and aegirine were replaced locally by bladed albite.

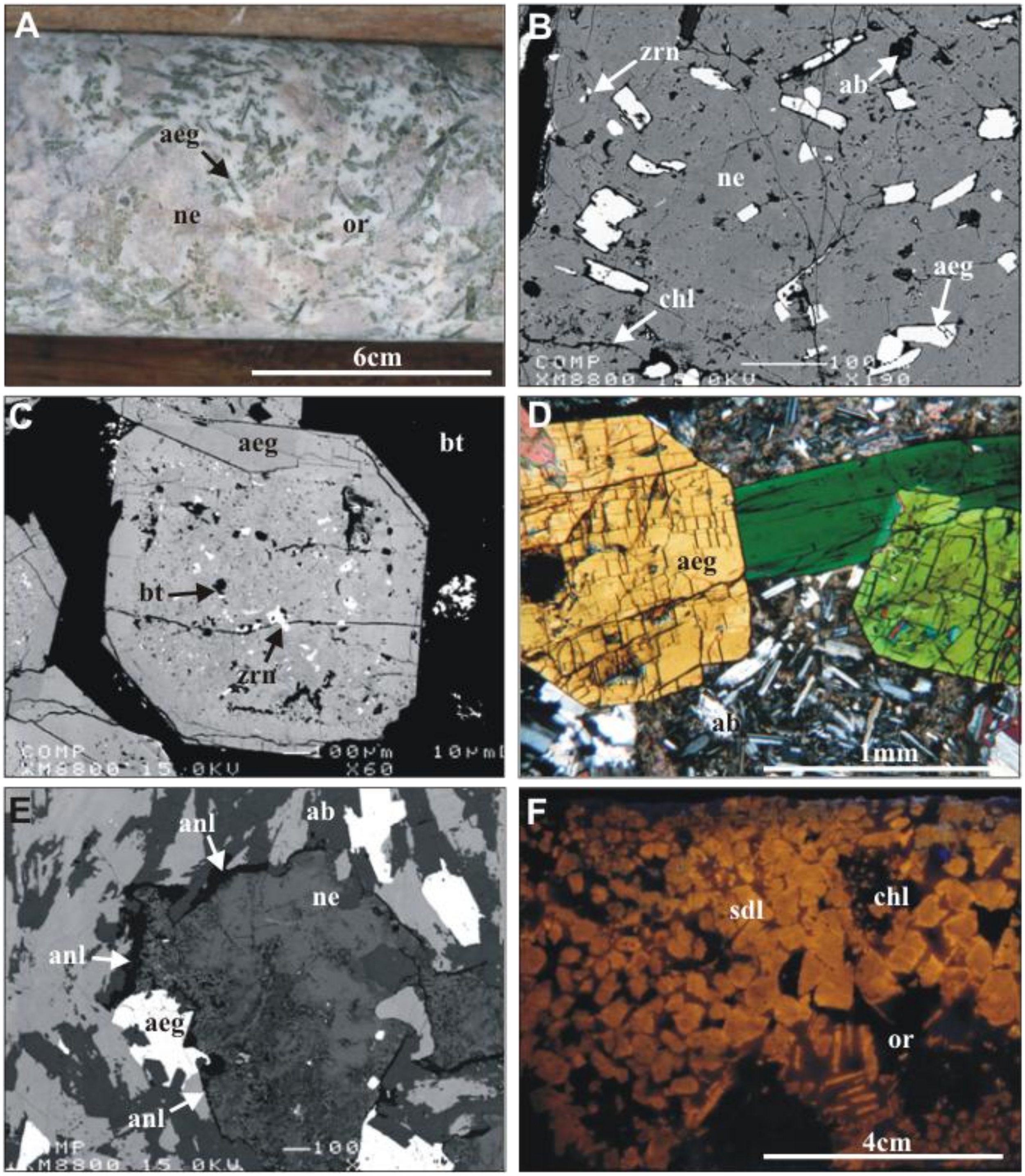
A
aeg
ne
or
6cm
B
zrn
ab
ne
aeg
chl
COMP
C
aeg
bt
bt
zrn
COMP
XM8800 15.0KV
X60
D
aeg
ab
1mm
E
anl
ab
ne
anl
aeg
anl
F
sdl
chl
or
4cm

Figure 3.3 A. Photograph of aegirine-nepheline syenite in drill core showing aegirine and nepheline phenocrysts in a matrix of orthoclase; B. BSE image of a nepheline phenocryst containing inclusions of aegirine, albite, chlorite and zircon; C. BSE image of an aegirine phenocryst with an inclusion-free rim; D. Photomicrograph in crossed polars of aegirine phenocrysts surrounded by laths of albite; E. BSE image of a nepheline phenocryst rimmed by analcime; F. Photograph of sodalite syenite in drill core under UV illumination showing a distinctive orange fluorescence.

Sodalite syenite is a highly altered, medium-grained intrusive rock, which has been pervasively hematized and sericitized. Primary sodalite was completely altered to hematite, sericite and chlorite in most samples examined. Sodalite crystals display a distinctive orange fluorescence under UV illumination (Figure 3.3F), which allows them to be easily identified in drill core despite their extensive alteration and replacement. In less altered samples, it is evident that crystals of altered sodalite are enclosed in coarse anhedra of orthoclase and an unknown altered dark green mineral, which could be aegirine or nepheline. Orthoclase and albite are the interstitial minerals, and are commonly intergrown and display a perthitic exsolution texture.

Nechalacho Mineralization

Based on the exploration that has been conducted to date, the Nechalacho deposit comprises two mineralized zones, a 15 to 30 metre thick upper zone and 15 to 60 metre thick lower zone. In some drill holes, two distinct zones separated by unmineralized rocks are present, whereas, in other holes, the upper zone grades directly into the lower zone. The primary host rock in both zones is the aegirine nepheline syenite described above. However, this identification is tentative because of pervasive hydrothermal alteration (described below). Plots of REE abundance with depth (Figure 3.4) indicate that the heavy REE are concentrated in the lower mineralized zone, that intermediate REE (e.g., Gd, Dy) show no real preference for upper or lower mineralized zones and that the light REE are concentrated in the upper mineralized zone.

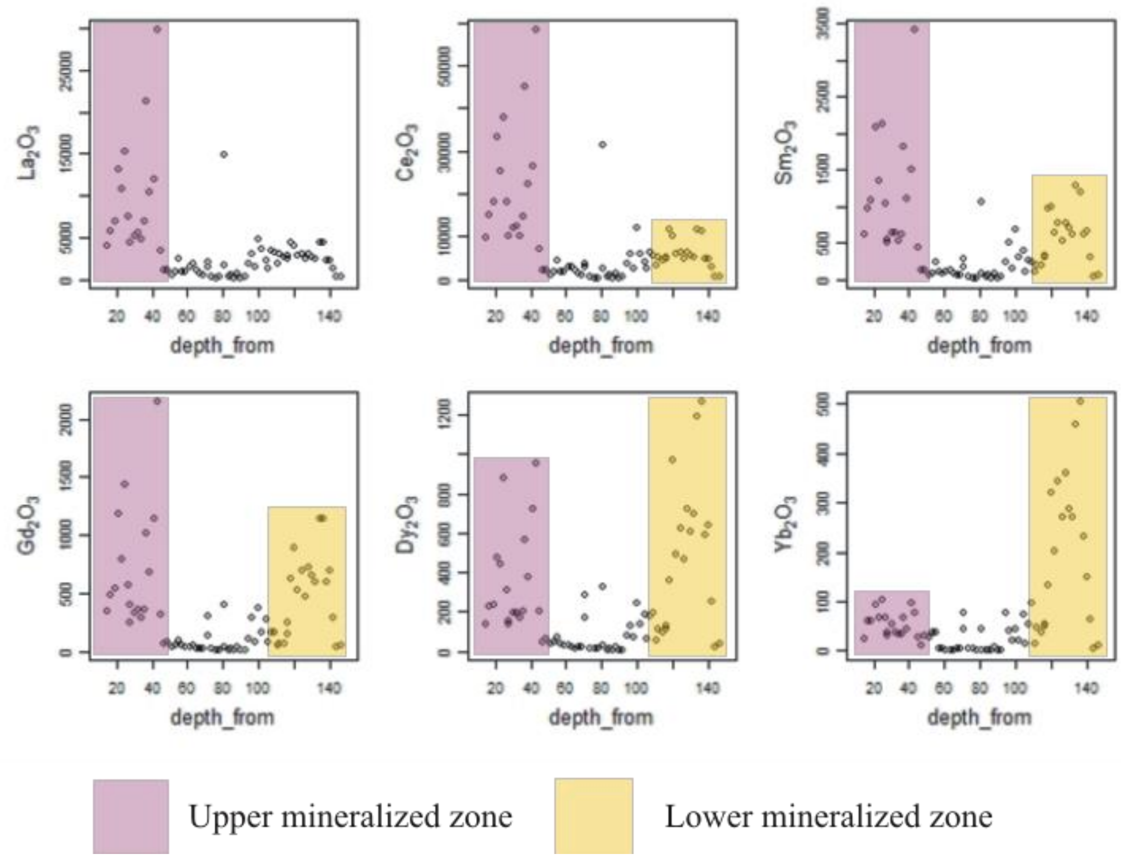

Figure 3.4 Plots of REE abundance (ppm) with depth (metres) illustrating differences in the distribution of the REE content in the upper and lower mineralized zones in drill hole L07-55.

The ore mineralogy in each zone is broadly similar. Zirconium is hosted mainly by zircon, niobium by ferrocolumbite and fergusonite-(Y), yttrium and the HREE by fergusonite-(Y) and zircon and the LREE by monazite-(Ce), allanite-(Ce), bastnäsite-(Ce) and parisite-(Ce)/synchysite-(Ce). Table 3.2 lists the names and compositions of ore minerals identified in the deposit. Zircon and bastnäsite-(Ce) are the only two minerals visible macroscopically in drill core. In the upper zone, bastnäsite-(Ce) is brick red in colour and is spatially associated with fluorite and albite. Zircon is finely disseminated and commonly occurs in undulating laminations (Figures 3.5A and B). It is also present in veins and wrapped around brecciated K-feldspar fragments. In the lower mineralized zone, zircon occurs as a secondary phase in pseudomorphs.

Table 3.2 Names and compositions of minerals found in the Nechalacho deposit.

Name	Formula	Name	Formula
Silicates		**Halides**	
Aegirine	$NaFe^{3+}(Si_2O_6)$	Fluorite	CaF_2
Aenigmatite	$Na_2Fe^{2+}_5TiSi_6O_{20}$		
Albite	$Na(AlSi_3O_8)$	**Phosphates**	
Allanite	$Ca(La,Y,Ce)(Al_2Fe^{2+})Si_3O_{12}$	Apatite	$Ca_5(PO_4)_3(OH,F,Cl)$
Analcime	$NaAl(Si_2O_6).(H_2O)$	Monazite	$(Ce,La,Th)PO_4$
Annite	$KFe^{2+}_3AlSi_3O_{10}(OH)_{1.5}F_{0.5}$		
Barkevikite	$Ca_2(Fe,Mg,Al)_{.5}(Si,Al)_8O_{22}(OH)_2$	**Carbonates**	
Biotite	$K_2(Mg,Fe^{2+})_{6-4}(Fe^{3+},Al,Ti)_{0-2}[Si_{6-5}Al_{2-3}O_{20}](OH,F)_4$	Ankerite	$Ca(Mg,Fe^{2+},Mn)(CO_3)_2$
Britholite	$Ca_2[(Y,Ce)Ca]_3[(OH,F)(SiO_4,PO_4)_3]$	Bastnäsite	$(Ce,La,Y)F(CO_3)$
Catapleiite	$Na_2Zr(Si_3O_9).2H_2O$	Calcite	$CaCO_3$
Cerianite	$(Ce^{4+},Th)O_2$	Dolomite	$CaMg(CO_3)_2$
Chamosite	$(Fe^{2+},Mg)_5Al[(OH)_8AlSi_3O_{10}]$	Kutnahorite	$Ca(Mn,Mg,Fe)(CO_3)_2$
Chlorite	$(Mg,Fe^{2+},Fe^{3+},Mn,Al)_{12}[(Si,Al)_8O_{20}](OH)_{16}$	Lanthanite	$(Ce,La,Nd)_2(CO_3)_3 8H_2O$
Eudialyte	$Na_{15}Ca_6(Fe^{2+},Mn^{2+})_3Zr_3(Si_{25}O_{73})(O,OH,H_2O)_3(OH,Cl)_2$	Parisite	$Ca(Ce,La)_2(CO_3)_3F_2$
Ferro-bustamite	$Ca(Fe^{2+},Ca,Mn^{2+})Si_2O_6$	Siderite	$FeCO_3$
		Synchysite	$Ca(Y,Ce,La,Nd,Gd)[F(CO_3)_2]$
Ferroricherite	$Na[Ca,Na][Fe^{2+}_5][(OH)_2Si_8O_{22}]$	**Oxides**	
Gittinsite	$CaZrSi_2O_7$	Aeschynite	$(Ce,Nd,Y,Ca,Fe,Th)(Ti,Nb)_2(O,OH)_6$
Lepidolite	$K(Li,Al)_3(Si,Al)_4O_{10}(OH,F)_2$	Ashanite	$(Nb,Ta,U,Fe,Mn)_4O_8$
Mesolite	$Na_2Ca_2(Al_2Si_2O_{10})3.8H_2O$	Betafite	$(Ca,U)_2(Ti,Nb)_2O_6(OH)$
Natrolite	$Na_2(Al_2Si_3O_{10}).2H_2O$	Cassiterite	SnO_2
Oneillite	$Na_{15}Ca_3Mn_3Fe^{2+}_3Zr_3Nb(Si_{25}O_{73})(O,OH,H_2O)_3(OH,Cl)_2$	Ceriopyrochlore	$(Ce,Ca,Y)_2(Nb,Ta)_2O_6(OH,F)$
Orthoclase	$K(AlSi_3O_8)$	Columbite	$(Fe,Mn)(Nb,Ta)_2O_6$
Pectolite	$NaCa_2(HSi_3O_9)$	Columbo-tantalite	$(Fe,Mn)(Nb,Ta)_2O_6$
Quartz	SiO_2	Fergusonite	$(Ce,La,Nd,Y)NbO_4$
Scapolite	$Na_4[Cl(AlSi_3O_8)_3] – Ca_4[CO_3(Al_2Si_2O_8)_3]$		
Sericite	$K_2Al_4(Si6Al_2O_{20})(OH,F)_4$	Ferrocolumbite	$Fe^{++}Nb_2O_6$
Sodalite	$Na_8(Al_6Si_6O_{24})Cl_2$	Hematite	Fe_2O_3
Thorite	$(Th,U)SiO_4$	Ilmenite	$Fe^{2+}TiO_3$
Topaz	$Al_2SiO_4(OH,F)_2$	Ixiolite	$(Ta,Nb,Sn,Fe,Mn)_4O_8$
Uranothorite	$(Th,U)SiO_4$	Limonite	$FeO.OH.nH_2O$
Willemite	$ZnSiO_4$	Magnetite	$Fe^{2+}Fe_2^{3+}O_4$
Wollastonite	$CaSiO_3$	Nioboaeschynite	$(Y,Ca,Ce,Nd,Th)(Nb,Ta,Ta)_2(O,OH)_6$
Zinnwaldite	$K(Li,Fe,Al)_3(Si,Al)_4O_{10}(OH)F$ $ZrSiO_4$	Polycrase	$(Y,Ca,Ce,U,Th)(Ti,Nb,Ta)_2O_6$
Zircon	$ZrSiO_4$	Samarskite	$(Y,Ce,U,Fe,Nb)(Nb,Ta,Ti)O_4$
		Specularite	Fe_2O_3
Sulfides		Titanomagnetite	$Fe(Fe,Ti)_2O_4$
Barite	$BaSO_4$	Uraninite	UO_2
Chalcopyrite	$CuFeS_2$	Yttrocolumbite	$(Y,U,Fe^{++})(Nb,Ta)O_4$
Molybdenite	MoS_2		
Pyrite	FeS_2		
Pyrrhotite	Fe_7S_8		
Sphalerite	ZnS		

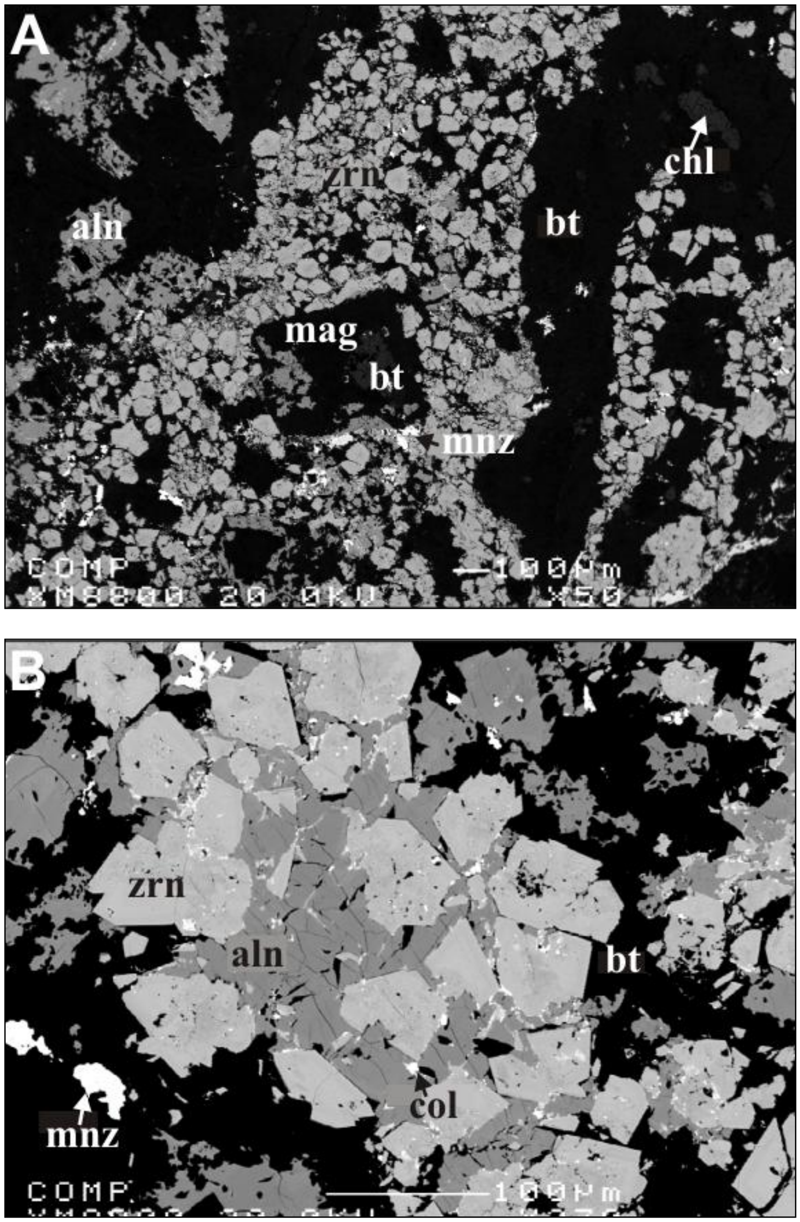

Figure 3.5 A. BSE image of Type 1a zircon in undulating laminations wrapping around pseudomorphs of precursor aegirine now filled by magnetite and biotite; B. Within the laminations, zircon crystals are broken and locally replaced by allanite-(Ce) (darker grey) and monazite-(Ce) (white). Biotite and magnetite are the darker grey/black phases surrounding zircon-rich layers.

HYDROTHERMAL ALTERATION

The rocks in the upper part of the layered complex have been intensely altered by hydrothermal fluids, leaving only relicts of their primary mineralogy. The principal alteration minerals are magnetite, hematite, biotite, chlorite, illite, muscovite, calcite, quartz, fluorite and bladed albite (‘cleavelandite’). Minor alteration minerals are ankerite, siderite, kutnahorite, scapolite, pyrite and sphalerite.

Magnetite and biotite are the dominant alteration minerals in the upper mineralized zone and were temporally and spatially associated with the deposition of fergusonite-(Y), ferrocolumbite, allanite-(Ce), monazite-(Ce) and bastnäsite-(Ce) These minerals replaced earlier minerals such as aegirine and zircon, and infilled fractures in primary K-feldspar. Locally, biotite replaced magnetite. Magnetite is also the dominant alteration mineral in the lower mineralized zone, but biotite is much less abundant than in the upper mineralized zone. Magnetite replaced the secondary minerals in pseudomorphs after eudialyte and is the dominant mineral in the fine-grained groundmass surrounding the pseudomorphs, where it is accompanied by minor biotite and albite. Below the lower mineralized zone, magnetite decreases sharply in abundance and hematite, which is observed throughout the deposit, becomes prevalent, forming rims around feldspar phenocrysts and locally magnetite, commonly replacing these minerals completely.

Albitization is widespread, but is most pervasive in the upper 50 metres of the complex where a brecciated pegmatite unit was replaced almost entirely by blades of albite (‘cleavelandite’) displaying intense red luminescence (triggered by Fe^{3+} activators). Albite having these characteristics is a common product of the fenitization of alkaline igneous rocks (Rae and Chambers, 1988; McLemore and Modreski, 1990). Pegmatites lower down in the complex have also been albitized and, where the albitization is less intense, remnant, partially altered K-feldspar megacrysts are observed. Vugs are common in all the albitized pegmatites suggesting that this alteration was accompanied by a significant loss of volume; the vugs have been variably filled by late carbonates, clays, fluorite and minor pyrite. In addition to affecting the pegmatites, albitization also locally overprinted magnetite- and biotite-altered aegirine nepheline syenite and where these rocks were mineralized, destroyed zircon and the associated Y and REE-bearing minerals.

Late stage silicification (quartz), illitization and carbonatization also affected the deposit. These alteration types, which overprint all the earlier alteration types including albitization, were only developed locally and except, for carbonatization, do not appear to have been accompanied by any redistribution of Y and HREE. However, carbonatization (calcite, ankerite, siderite) may have been associated with REE fluoro-carbonate precipitation, as calcite, fluorite and bastnäsite-(Ce) commonly occur together.

DISTRIBUTION AND PARAGENESIS OF RARE METAL MINERALS

HREE-Bearing Minerals

Zircon and fergusonite-(Y) are the two main hosts of the heavy rare earth elements in the deposit; minor amounts of HREE are also present in ferrocolumbite. Three varieties of zircon are distinguishable microscopically:

Type 1 zircon is a tan-coloured variety that occurs almost exclusively in the upper mineralized zone and consists of euhedral, bipyramidal, zoned crystals (30-60 μm and locally 100 μm in diameter), which have distinct cores and rims. In most crystals, the cores are a dark brown colour due to alteration by very fine-grained chlorite, quartz, samarskite-(Y), monazite-(Ce), and uranothorite. The cores are also the focus for fractures, which radiate outwards and transect the translucent rims. Locally, this type of zircon is fragmented and unzoned. Type 1 zircon occurs either as isolated crystals or is concentrated in sub-horizontal undulating laminations, which wrap around pseudomorphs (now filled mainly by magnetite and biotite), interpreted to represent aegirine phenocrysts (Figure 3.5A). The laminations are parallel to the igneous layering and locally form zones up to 30 cm thick, containing >30 vol. % zircon. In thin section and particularly in backscattered SEM images, the zircon in these laminations is observed to have been extensively replaced by allanite-(Ce) and to a much lesser extent by monazite-(Ce) and ferrocolumbite (Figure 3.5B).

A second tan-coloured variety, which like Type 1 zircon is also restricted to the upper ore zone, forms clots and irregular streaks, occurs in veinlets (Figure 3.6A) and wraps around brecciated feldspar crystals (Figure 3.6B). The crystals are typically broken and form fragments in a cement of biotite and magnetite. For this reason and its chemical similarity to Type 1 zircon (discussed later), this variety is interpreted to represent mechanically remobilized Type 1 zircon. In order to distinguish this zircon from that described in the previous paragraph, it will be referred to henceforth as Type 1b zircon and that of the previous paragraph as Type 1a zircon.

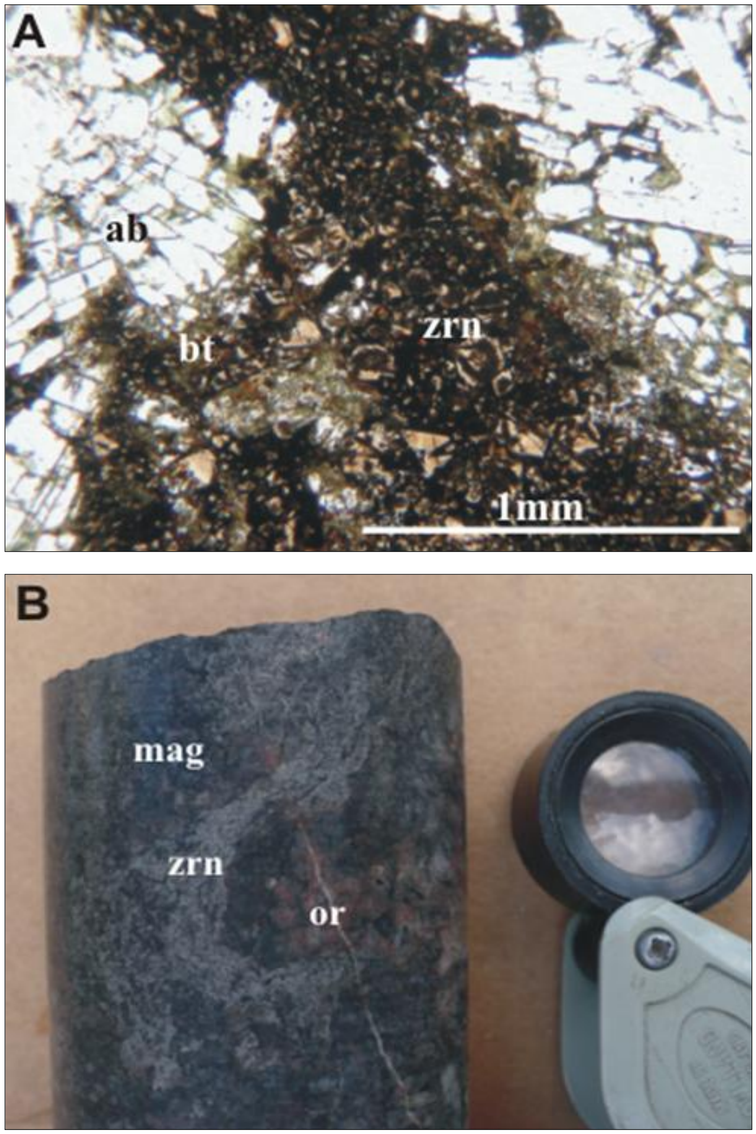

Figure 3.6 A. Photomicrograph in plane-polarized light of broken Type 1b zircon crystals in a biotite-cemented vein through brecciated albite; B. Fine-grained tan coloured zircon wrapped around brecciated K-feldspar fragments in drill core.

The bulk of the zircon in the lower mineralized zone (Type 2) forms small (10-30 µm) anhedral grains that occur as a secondary phase in pseudomorphs (Figure 3.7A). The latter have two distinctive morphologies, and are present in layers interpreted to represent cumulates of former phenocrysts. These layers vary from tens of centimetres to several metres in thickness. The pseudomorphs range in diameter from several millimetres up to one centimetre and contain no relicts of their precursor mineral(s). However, one of these pseudomorph types (the overwhelmingly predominant type) has a habit very similar to that of eudialyte. These pseudomorphs typically have sub-rounded shapes and contain the following mineral assemblage: zircon + fergusonite-(Y) + bastnäsite-(Ce) + parisite-(Ce)/synchysite-(Ce) + allanite-(Ce) + albite + quartz + biotite + fluorite + kutnahorite ± minor hematite and rare sphalerite (Figure 3.7B). The zircon within these pseudomorphs forms anhedral grains or larger clusters of grains (Figure 3.7C), some of which are rimmed by an overgrowth of later zircon. Pseudomorph cores are commonly replaced entirely by hematite and more rarely magnetite, leaving a rim of zircon inside the original outline of the pseudomorph (Figure 3.7D). Over several metres, the mineralized pseudomorphs are partially to completely destroyed by magnetite/hematite, indicating that the mineralized zone may have extended much further prior to alteration. Some pseudomorphs contain spherical patches of quartz with radiating zircon vermicelli which are reminiscent of symplectic intergrowths (Figure 3.7E). These pseudomorphs contain the same mineral assemblage reported for Figure 3.7B and thus represent a variant of the original alteration of eudialyte.

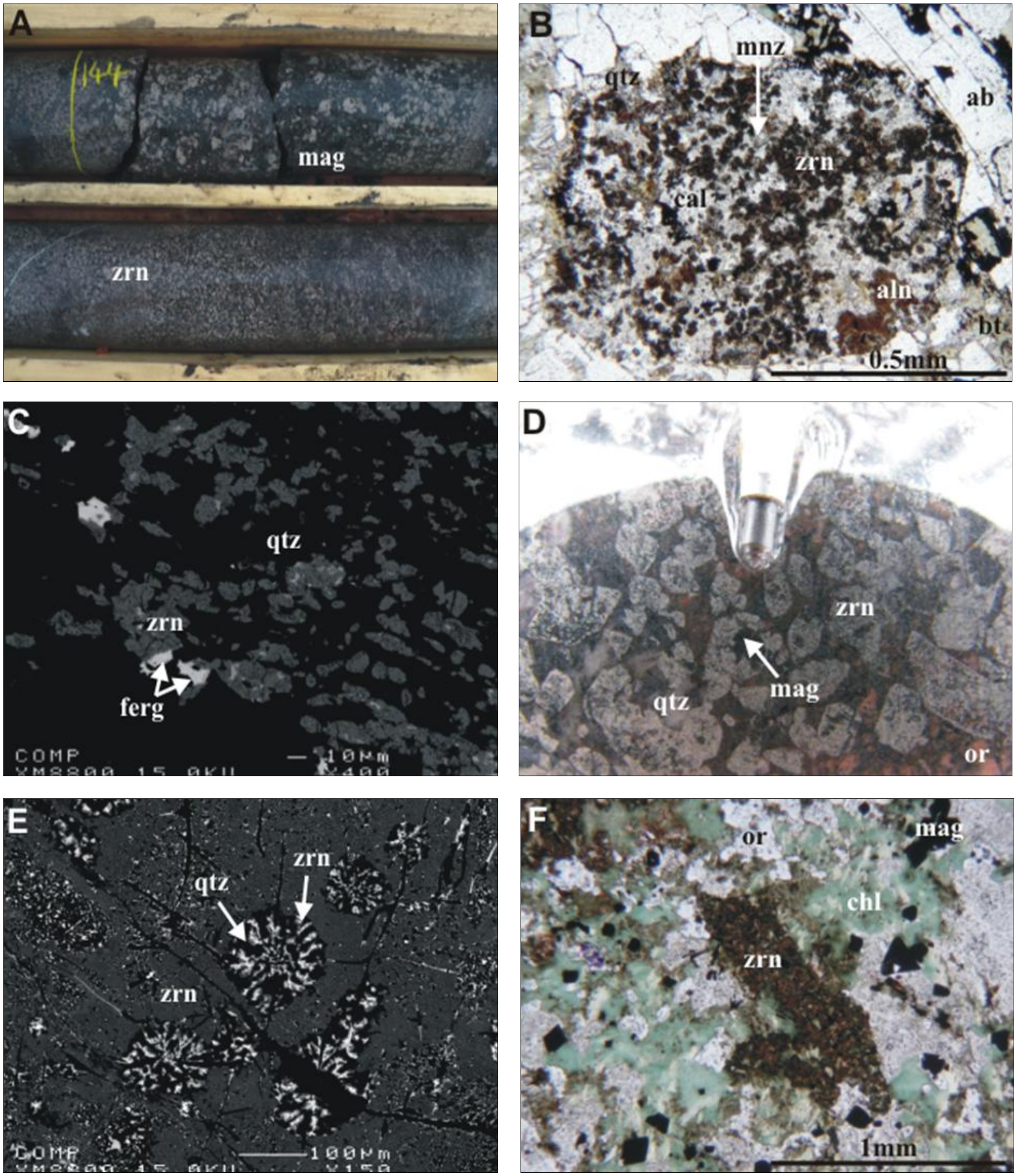
A
mag
zrn
B
mnz
qtz
ab
zrn
cal
aln
bt
0.5mm
C
qtz
zrn
ferg
COMP
10μm
D
zrn
mag
qtz
or
E
qtz
zrn
zrn
COMP
100μm
F
or
mag
chl
zrn
1mm

Figure 3.7 A. Photograph of core typical of the lower mineralized zone containing abundant zircon-filled pseudomorphs after probable eudialyte; B. Photomicrograph in plane polarized light of a single pseudomorph replaced by zircon + fergusonite-(Y) + bastnäsite-(Ce) + allanite-(Ce) + parisite-(Ce)/synchysite-(Ce) + albite + quartz + biotite + fluorite + kutnahorite; C. BSE image of anhedral to sub-rounded grains of zircon within a pseudomorph (white is fergusonite-(Y)); D. Photograph of pseudomorphs in drill core with their cores preferentially replaced by magnetite; E. BSE image illustrating several pseudomorphs containing radially-distributed vermicelli of zircon (pale grey) and interstitial quartz (black); F. Photomicrograph of a zircon pseudomorph after probable elpidite.

The second variety of pseudomorph, which is far less common, has the shape of a doubly-terminated prism and has been replaced predominantly by zircon (Figure 3.7F). This shape is similar to that of elpidite, a common primary magmatic mineral in the Strange Lake pluton, Quebec/Labrador (Salvi and Williams-Jones, 1995). The proportion of zircon in these pseudomorphs is approximately 80 vol. %, which is much higher than would be expected for elpidite, suggesting that, if our interpretation of their precursors is correct, Na, silica and H_2O were removed during alteration.

The third type of zircon is relatively uncommon, occurs in irregular patches and in zones of brecciation, mainly in the upper mineralized zone, and is locally replaced by secondary albite. The rims on this zircon are narrow and characterized by unusually high birefringence, oscillatory zoning and colloform textures (Figure 3.8A). This type of zircon can be further distinguished by its response to UV illumination. Whereas, Type 1 and 2 zircons do not fluoresce or luminesce, Type 3 zircon exhibits a blue to greenish-yellow fluorescence. Cathodoluminescence images reveal bright greenish-yellow fluorescing patches within crystals and pale blue zoned rims (Figure 3.8B). This oscillatory growth zoning is also evident in backscattered SEM images. The greenish-yellow emission is most likely related to Sm^{3+} or Dy^{3+} activation, as these REE are known to produce a green emission. Similar luminescence has been reported for zircon from the Nb-Zr-REE deposits, Khaldzan Buregte and Tsakhir, in the Mongolian Altai (Kempe et al., 1999), for which it was clearly demonstrated that the emission was caused by Dy^{3+} activators.

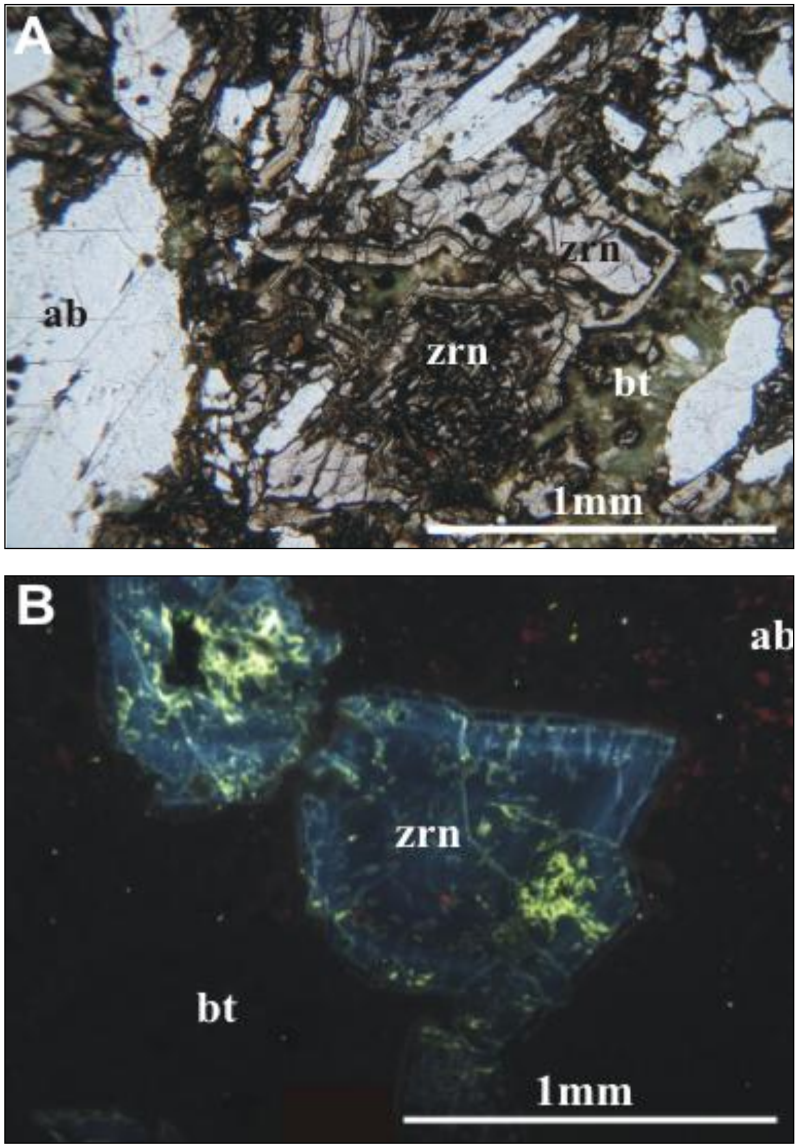

Figure 3.8 A. Photomicrograph in plane polarized light of Type 3 zircon with colloform zoned rims, locally replaced by albite and biotite; B. Cathodoluminescence image of the same zircon showing oscillatory zoning (blue fluorescence) and bright green-yellow fluorescent patches.

Fergusonite-(Y) is present in both the upper and lower mineralized zones, but is much more abundant in the latter, typically comprising one to five volume percent of the rock, and is the dominant HREE-bearing mineral along with zircon. In the upper mineralized zone, fergusonite-(Y) occurs as small (<1mm) anhedral grains adjacent to primary zircon, whereas in the lower mineralized zone, it forms small (<1 mm) anhedral grains and more densely packed aggregates within the pseudomorphs after eudialyte, where it is intimately associated with zircon, which it also locally replaced (Figure 3.9A). Some fergusonite-(Y) is present beyond the confines of pseudomorphs as a replacement product of columbite-(Mn).

Ferrocolumbite occurs as pinwheels with rounded black centres and radiating spines up to 0.1 mm in diameter (Figure 3.9B). It also locally replaced both zircon and fergusonite-(Y), in both the upper and lower mineralized zones. Columbite-(Mn) forms small, isolated anhedral crystals and larger clusters of these crystals (up to 50 µm in diameter) adjacent to Type 1 zircon and eudialyte pseudomorphs (it also occurs within some pseudomorphs) and as inclusions within biotite, chlorite, magnetite and albite. Commonly these crystals have been replaced by both fergusonite-(Y) (Figure 3.9C) and bastnäsite-(Ce). The relationship of columbite-(Mn) to ferrocolumbite is unclear as these minerals are not observed together. However, the fact that fergusonite-(Y) replaced columbite-(Mn) and was in turn replaced by ferrocolumbite indicates that ferrocolumbite formation post-dated that of columbite-(Mn). Finally, samarskite-(Y) is present as anhedral inclusions in the cores of zircon crystals in the upper mineralized zone and also as larger grains (up to 30 µm diameter) in biotite.

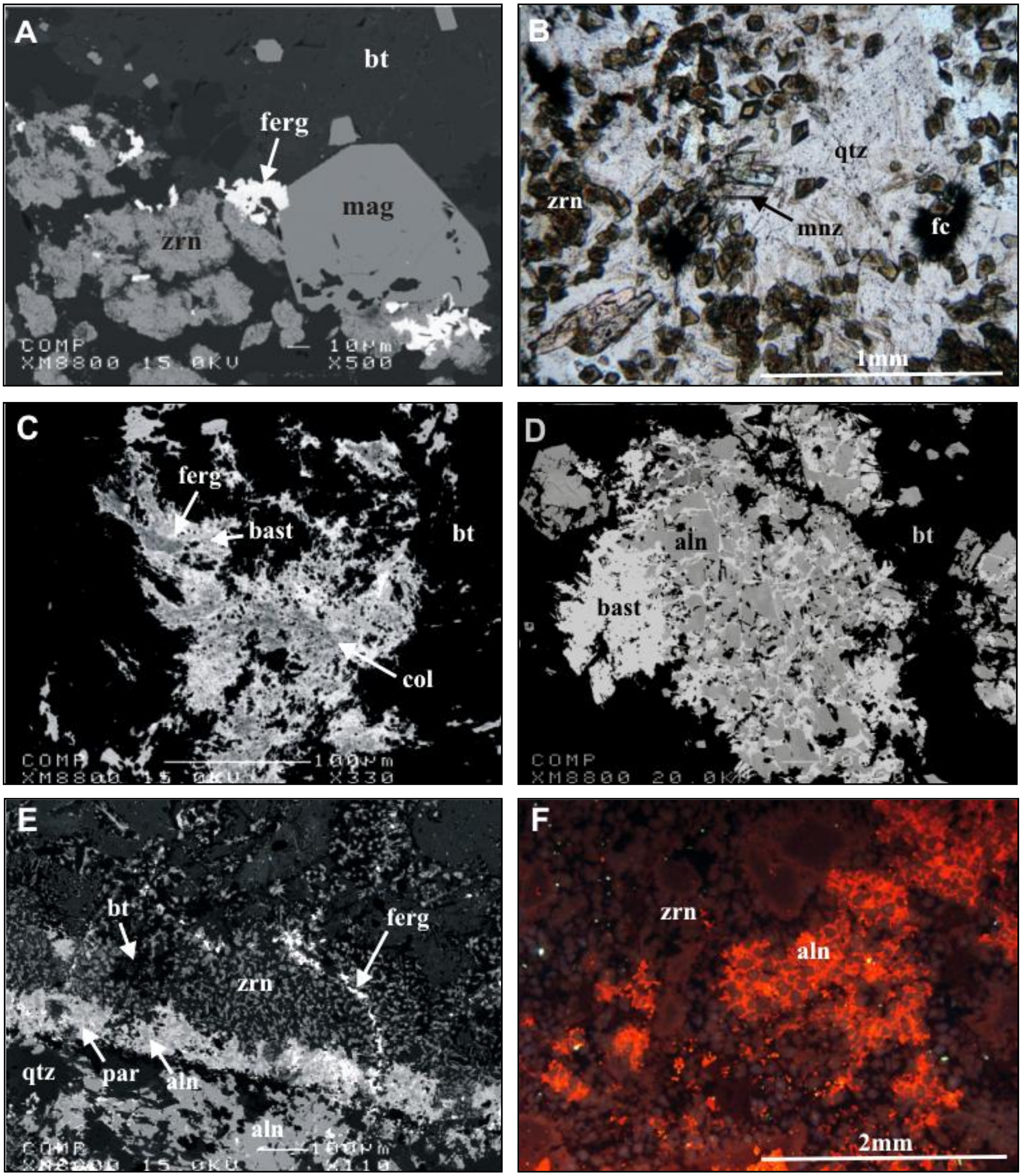
A
bt
ferg
mag
zrn
COMP
XM8800 15.0KV
10μm
X500
B
zrn
qtz
mnz
fc
1mm
C
ferg
bast
bt
col
COMP
100μm
X330
D
aln
bt
bast
COMP
XM8800 20.0KV
E
bt
ferg
zrn
qtz
par
aln
aln
COMP
100μm
F
zrn
aln
2mm

Figure 3.9 A. BSE image illustrating fergusonite-(Y) (white) locally replacing zircon; B. Photomicrograph in plane polarized light of zircon, monazite-(Ce) and ferrocolumbite (pinwheels with black rounded centres and radiating spines) surrounded by quartz. Ferrocolumbite can be seen replacing zircon on the right-hand size of the photograph; C. BSE image illustrating columbite-(Mn) being replaced by fergusonite-(Y) and bastnäsite-(Ce); D. BSE image illustrating bastnäsite-(Ce) after allanite-(Ce); E. BSE image of allanite-(Ce) intergrown with parisite-(Ce) on the rim of a pseudomorph after probable eudialyte in the lower mineralized zone; F. Cathodoluminescence image of fiery orange allanite-(Ce) between zircon crystals.

LREE-Bearing Minerals

REE fluoro-carbonate minerals, predominantly bastnäsite-(Ce) with minor parisite-(Ce) and synchysite-(Ce), are most common metres above the intervals containing the highest concentrations of HREE in the upper mineralized zone where they are associated with fluorite and calcite, and are important hosts of the light rare earth elements. Macroscopically, bastnäsite-(Ce) is brown-red to brick red in colour as a result of alteration by hematite. It occurs with the other fluoro-carbonate minerals as fine-grained disseminations in interstices between earlier-formed minerals, e.g., biotite, magnetite and zircon, rarely forms rims around zircon crystals and replaced allanite-(Ce), occurring as streaks and irregular patches within this mineral (Figure 3.9D). Parisite-(Ce) and synchysite-(Ce) are rare but can be intimately intergrown with both bastnäsite-(Ce) and allanite-(Ce) (Figure 3.9E).

Allanite-(Ce) forms anhedral grains up to 1.5 mm in diameter and more massive agglomerations or clusters, which are commonly interstitial to zircon and probable eudialyte pseudomorphs. It occurs in both the upper and lower mineralized zones but is much more abundant in the upper zone. Typically red in colour, it displays a fiery orange fluorescence under cathodoluminescence (Figure 3.9F). Monazite-(Ce), which is found mainly in the upper zone proximal to zones of HREE mineralization, occurs as elongate needles/rods or as tiny crystals in zircon, K-feldspar, quartz and biotite, replacing the interiors of these minerals. Locally, monazite-(Ce) also replaced both bastnäsite-(Ce) and allanite-(Ce).

In the lower mineralized zone, the LREE occur predominantly in bastnäsite group minerals and allanite-(Ce), and are found both within and beyond the confines of the pseudomorphs after probable eudialyte. There are a number of intimate intergrowths of these minerals and other HREE-bearing minerals within the pseudomorphs, namely between bastnäsite-(Ce)-parisite-(Ce)/synchysite-(Ce)-allanite(Ce) and fergusonite-(Y)-bastnäsite-(Ce)-gittinsite. The textures suggest that these minerals were most likely coeval.

Fluorite, Sulphides, Thorite and Apatite

Dark purple fluorite is common throughout the deposit and occurs in many forms: infilling vugs in albitized pegmatites, together with bastnäsite-(Ce) and other LREE-rich minerals; as a local replacement of magnetite and biotite; in fractures in primary K-feldspar; intergrown with illite in massive patches from tens of centimetres to several metres in thickness; and intergrown with zircon and other REE-bearing minerals in zones of brecciation. Pyrite, chalcopyrite, sphalerite and molybdenite are locally abundant in the upper parts of the deposit. In particular, pyrite occurs in calcite veins and commonly as disseminations in magnetite-rich horizons, where it locally replaced magnetite. Thorite and other minor accessory minerals occur as small (1-3µm) anhedral grains in the cores of Type 1 zircon crystals. Minor apatite, surrounded by albite is associated with monazite-(Ce).

Summary

In summary, all the rare earth element minerals described above locally replaced zircon, an observation that is significant and will be discussed later. The simplified paragenesis of rare metal minerals and major alteration minerals in the upper mineralized zone is represented by the sequence: zircon $\rightarrow$ magnetite-biotite-zircon-REE minerals $\rightarrow$ albite $\rightarrow$ fluorite-calcite-quartz-chlorite-hematite. A more detailed paragenesis is given in Figure 3.10. In the lower zone, all the REE minerals formed synchronously by replacement of eudialyte to create pseudomorphs.

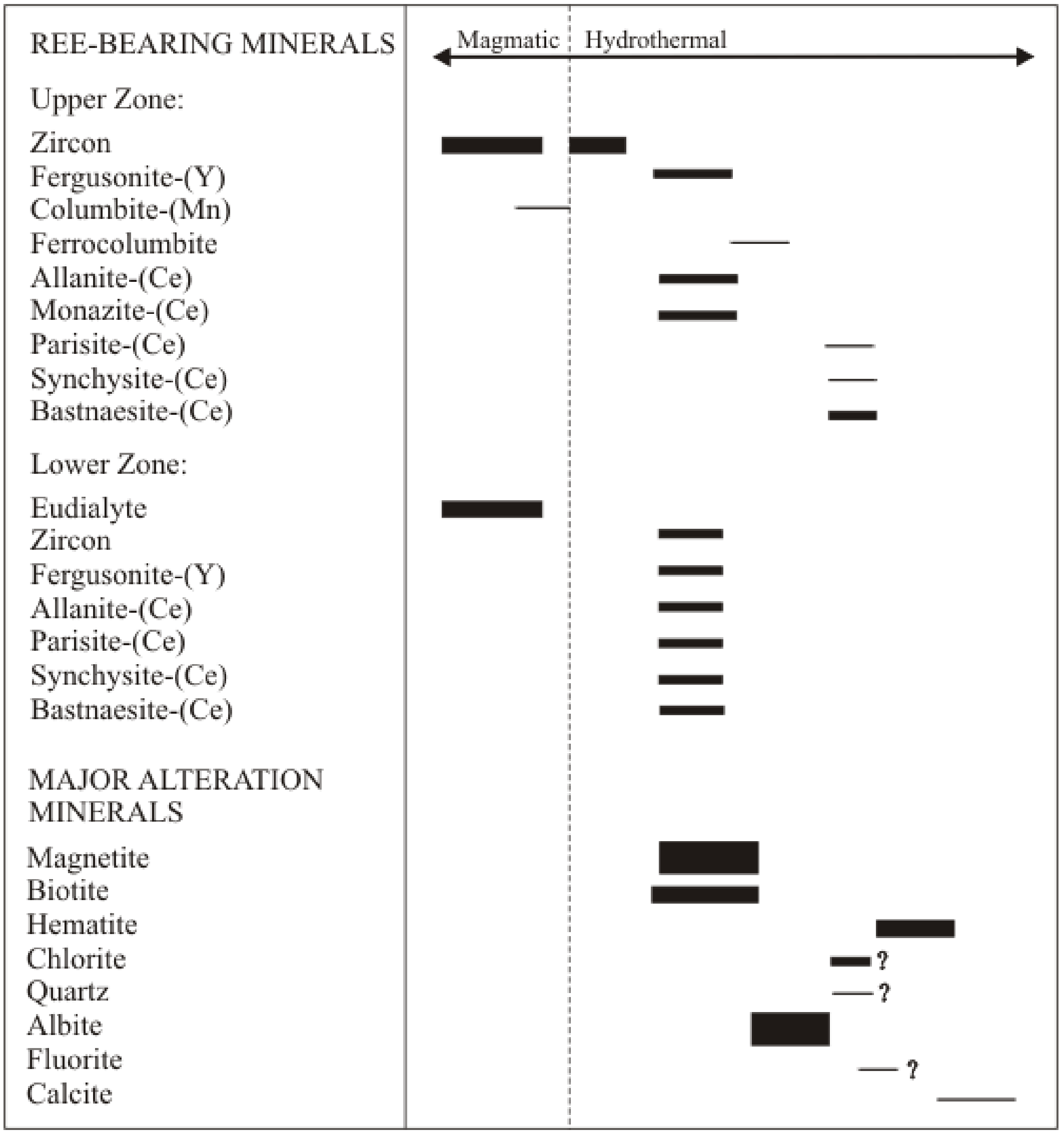

Figure 3.10 Paragenetic sequence for the major REE-bearing and alteration minerals in the Nechalacho deposit. Line widths indicate relative abundances of phases. Uncertainty in the precise placement of a phase within the paragenesis due to a lack of textural evidence is indicated by '?'.

MINERAL CHEMISTRY

The compositions of the REE-bearing minerals were determined using a JEOL JXA-8900L electron microprobe with a focused beam and an acceleration voltage of 20kV, a 30nA beam current, a beam diameter of 3µm for zircon, fergusonite-(Y), ferrocolumbite and eudialyte; and a 10µm beam diameter for allanite-(Ce), monazite-(Ce) and bastnäsite-(Ce). Counting times and standards used for each element analysed are provided in Table 3.3. Data reduction was performed using the ZAF correction method. Results of these analyses are presented in Appendices C to I.

Table 3.3 Counting times and standards used for each element analysed in electron microprobe analyses of REE-bearing mineral phases.

Element	Counting time (secs.)	Standard
La	150	MAC-La
Y	50	MAC-Y
Nb	100	$Na_2Nb_2O_6$
Eu	150	MAC-Eu
Ce	60	MAC-Ce
F	100	CaF_2
Hf	40	Zircon
Dy	60	MAC-Dy
Er	60	MAC-Er
Si	20	Zircon
U	100	UO_2
Ca	20	Diopside
Gd	60	MAC-Gd
Fe	20	gar1
Al	20	gar1
Pr	60	MAC-Pr
Th	100	ThO_2
Sm	60	MAC-Sm
Nd	60	MAC-Nd
Zr	20	Zircon
Yb	70	MAC-Yb
Na	20	$Na_2Nb_2O_6$
Tb	60	MAC-Tb
Ti	20	TiO_2
Mg	20	Spinel
Mn	20	Spessartine
P	20	Ba-Feld
K	20	Orthoclase
Ta	60	MAC-Nd

REE Mineral Chemistry

The REE are present in significant concentrations in zircon, fergusonite-(Y), ferrocolumbite, allanite-(Ce), monazite-(Ce) and bastnäsite-(Ce). The concentration of total REE plus yttrium (as REE_2O_3 and Y_2O_3) in Type 1 zircon crystals is highly variable, ranging from <1 to 11 wt. %, and the distribution varies from rim to core with significant zoning apparent in backscattered electron images. Electron microprobe element maps were produced in order to observe the chemical nature of the zonation and changes in the distribution of Zr, Nb, Y, Ce, Nd, Gd, Hf, Th, Si, Fe, Mg, K and Ca within the structure of the four types of zircon and within the pseudomorphs. These images were acquired by scanning the beam across the sample in a grid. The signals collected at each point in the grid were plotted with pixel brightness as a function of signal intensity (i.e., higher intensities were plotted as brighter colours). The above elements were selected as they are the major elements in zircon, markers for the light, middle and heavy REE or help identify alteration minerals present in the altered cores.

All the Type 1a and b zircon crystals that were mapped display a central Y (up to 7 wt. % Y_2O_3) and Gd-rich, Nd and Hf-poor core and an outer Y-poor, Nd and Hf-rich rim, with sharp boundaries between the core and rim. This suggests that the rims were overgrown on the cores. Light REE, represented by La_2O_3 and Ce_2O_3, occur in concentrations up to 0.05 and 0.50 wt. % in the rims, but only 0.02 and 0.35 wt. % in the cores, respectively. The corresponding concentrations of middle REE, represented by Sm_2O_3, Gd_2O_3 and Dy_2O_3, are up to 0.98, 0.88 and 0.55 wt. % in the rims, and 1.18, 1.14 and 1.04 wt. % in the cores, respectively. Heavy REE, represented by Yb_2O_3, occur in concentrations up to 0.43 wt. % in the rims, and 0.72 wt. % in the cores. In general, it is therefore the MREE, namely Sm, Gd and Dy which are most enriched in

Type 1 zircon. An important feature of these crystals is that the cores have been preferentially altered and yttrium was mobilized from the cores along radiating fractures to the rims and beyond (Figures 3.11 and 3.12). This alteration likely represents an atoll texture, in which the core of the crystal was less stable than the rim and therefore more susceptible to alteration. The occurrence of rare crystals of monazite-(Ce), samarskite-(Y) and thorite in some zircon cores can be explained by calling upon the radiating fractures to act as pathways for hydrothermal fluids into the grains. Transects from rim to rim across individual crystals show that concentrations of thorium are elevated in the altered cores (Figure 3.13), suggesting that metamictization may have played an important role in promoting core alteration.

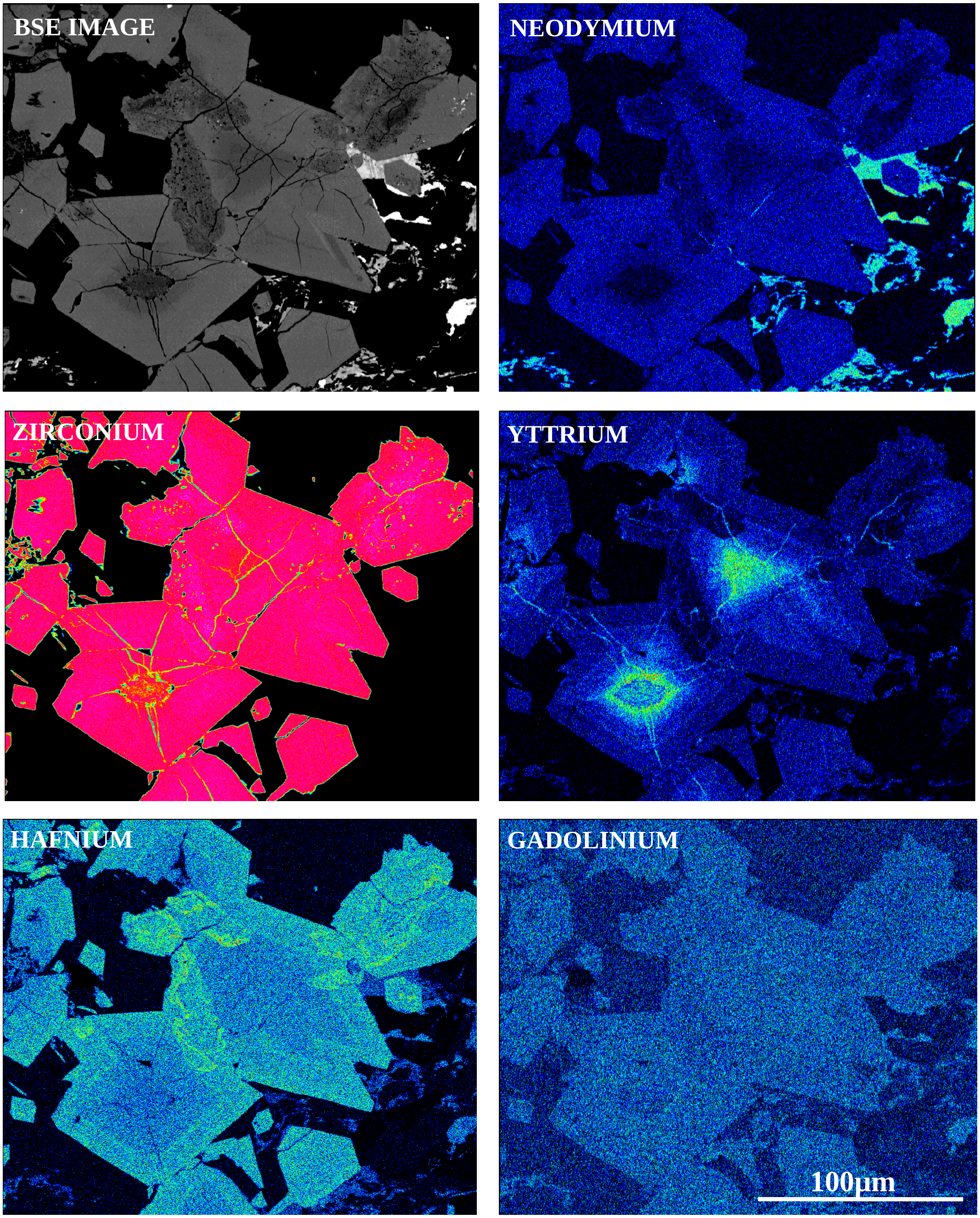
BSE IMAGE
NEODYMIUM
ZIRCONIUM
YTTRIUM
HAFNIUM
GADOLINIUM
100μm

Figure 3.11 Electron microprobe element maps of Type 1a zircon crystals showing the distribution of neodymium, zirconium, yttrium, hafnium and gadolinium. The key features to note are the preferential enrichment of Nd, Zr, Hf and Gd in the rims and Y in the cores. Yttrium is also observed along fractures penetrating the rims.

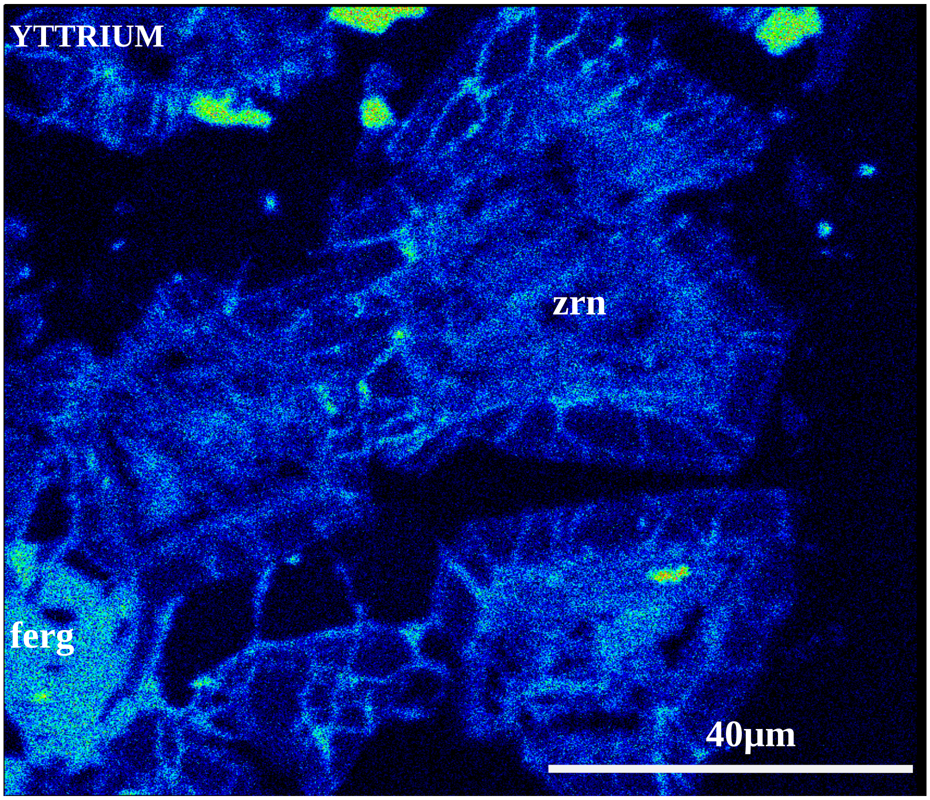

Figure 3.12 Electron microprobe map for yttrium illustrating fractures along which yttrium moved from zircon cores to form adjacent fergusonite-(Y).

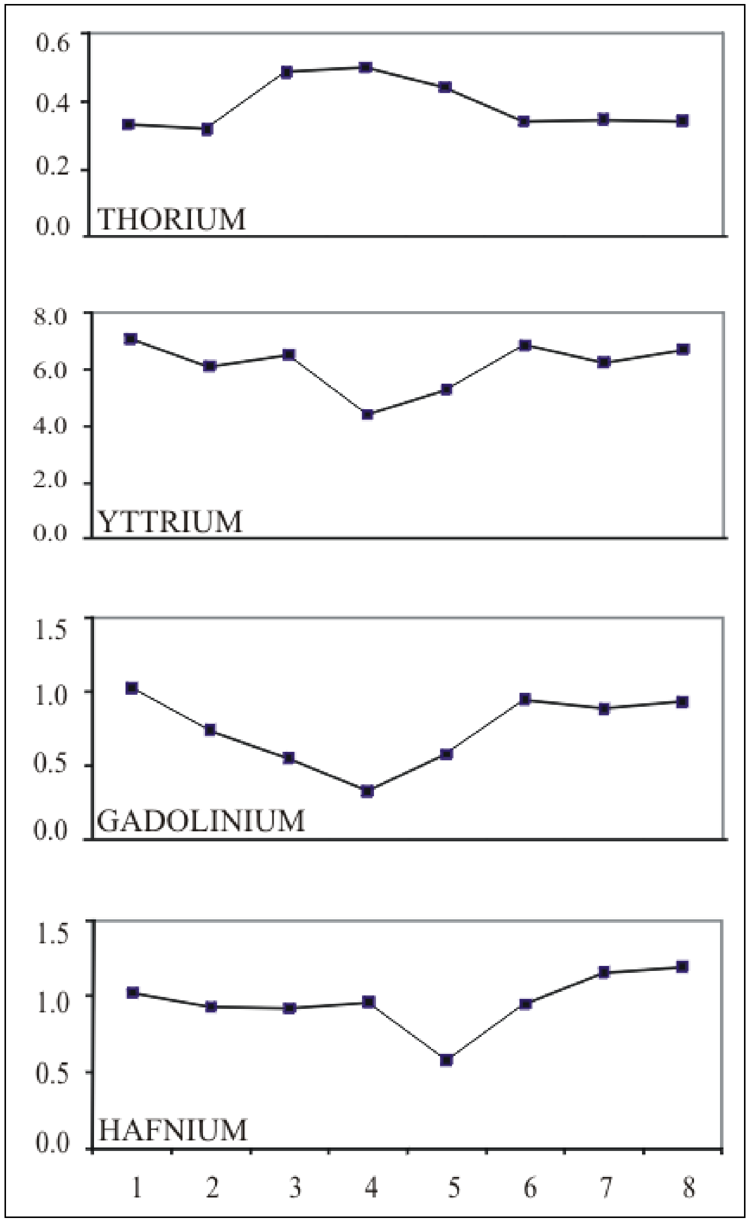

Figure 3.13 Transects from rim to rim across a single zircon crystal, illustrating differences in the distribution of Th, Y, Gd and Hf between the core (3-5) and rims (1-2 and 6-8). The Y-axis is in wt. %.

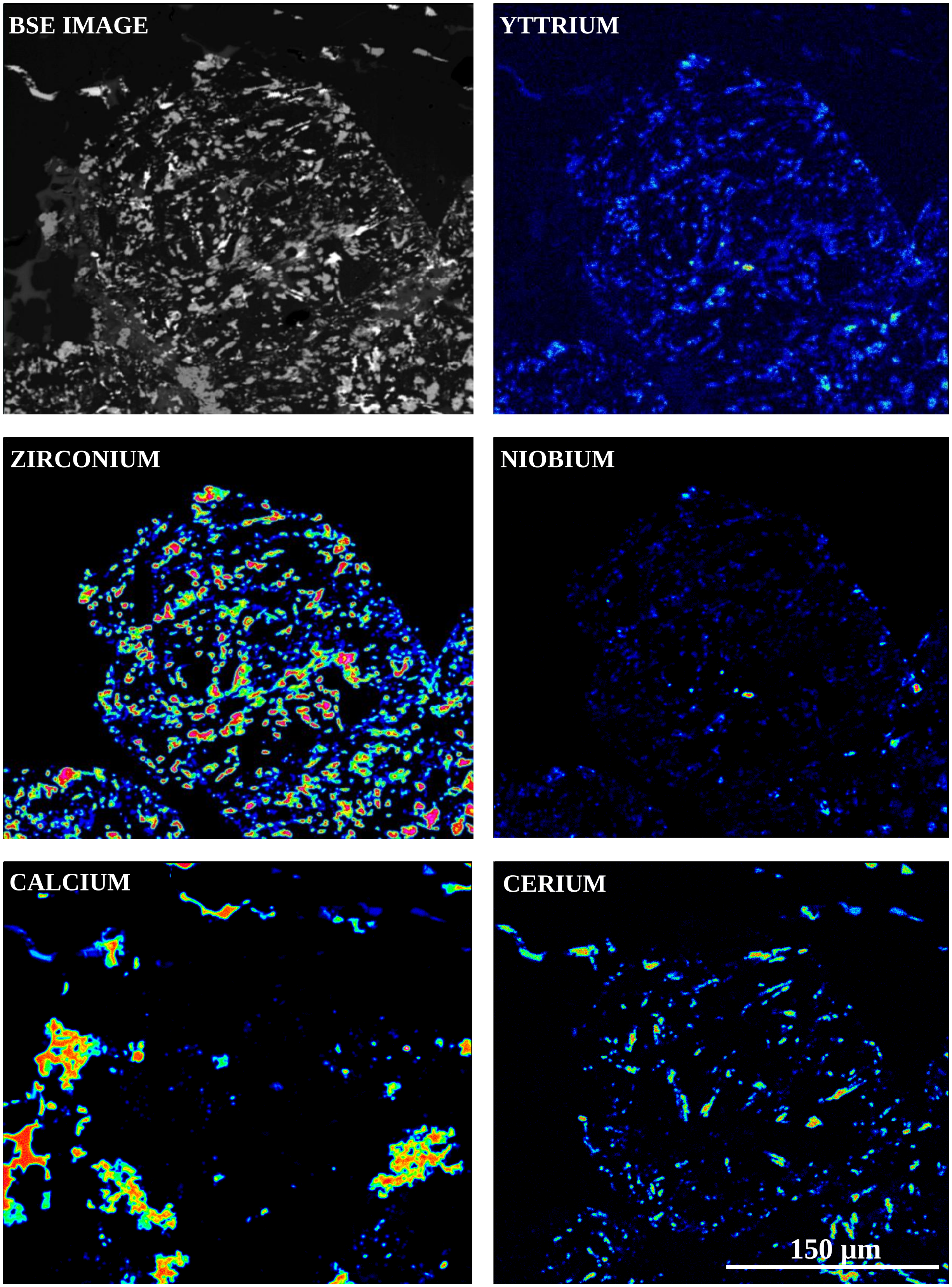
BSE IMAGE
YTTRIUM
ZIRCONIUM
NIOBIUM
CALCIUM
CERIUM
150 µm

Figure 3.14 Electron microprobe element maps of a pseudomorph of inferred eudialyte illustrating the intensities of yttrium, zirconium, niobium, calcium and cerium. The relative proportions of each of these elements within the outline of the original crystal are approximately equal to that of the primary eudialyte.

Electron microprobe element maps of the pseudomorphs after eudialyte (Figure 3.14) show that Zr, Y and Nb are confined within the crystal boundaries, suggesting that these elements were only remobilized on a scale of tens of microns. By contrast, Ca and light REE such as Ce are observed beyond the crystal boundaries and were thus remobilized on a larger scale.

Table 3.4 reports the compositions of the different zircon types. Overall, the compositions of Type 1a and b zircon crystals are fairly similar (Figures 3.15A and 3.15B). The rims, in particular, have very similar compositions, but their cores differ somewhat in that the cores of Type 1b zircon are slightly more enriched in Y and REE than those of Type 1a. Type 2 zircon has a distinctive chondrite-normalized REE profile characterized by a strong depletion in the LREE and enrichment in the HREE (Figure 3.15C) relative to Type 1 zircon. For example, the average concentration of Y_2O_3 in Type 2 zircon is 4.11 wt. %, two or three times the concentration in Type 1 zircon. The HREE, namely Yb_2O_3 and Er_2O_3 behave similarly to Y_2O_3. Type 3 zircon is enriched in Y + HREE in the narrow oscillatory zoned rims and is depleted in all REE in the cores (Figure 3.15D). The compositions of the rims are similar to those of Type 1a and b zircon.

Table 3.4 Average compositions of rims and cores of the different zircon types analysed using the electron microprobe.

	Type 1a core (n=18)	Type 1a rim (n=18)	Type 1b core (n=24)	Type 1b rim (n=36)	Type 2 core (n=49)	Type 2 rim (n=9)	Type 3 core (n=7)	Type 3 rim (n=7)
ZrO_2	60.478	60.694	59.012	60.604	55.147	57.977	64.756	60.808
SiO_2	29.457	29.249	27.112	28.357	32.074	28.008	30.899	28.998
HfO_2	1.384	1.093	1.159	1.208	1.216	1.056	1.560	1.285
FeO	1.011	0.569	0.720	0.325	1.903	0.612	0.419	0.523
Al_2O_3	0.246	0.078	0.156	0.100	0.364	0.152	0.101	0.210
UO_2	b.d.	b.d.	b.d.	b.d.	0.042	b.d.	b.d.	b.d.
ThO_2	0.050	0.185	0.098	0.065	0.167	0.201	b.d.	0.045
CaO	0.318	0.125	0.208	0.247	0.191	0.139	0.284	0.247
F	0.658	0.695	0.668	0.622	0.145	0.994	0.156	0.688
Na_2O	0.201	0.075	0.055	b.d.	0.212	0.190	0.057	0.306
Y_2O_3	0.810	0.660	1.698	0.363	2.706	3.632	0.032	0.629
Nb_2O_5	1.159	2.617	1.321	3.305	0.706	2.070	0.444	1.751
Ce_2O_3	0.213	0.282	0.152	0.371	0.058	0.123	0.033	0.299
Pr_2O_3	b.d.	0.163	b.d.	0.175	b.d.	b.d.	b.d.	b.d.
Nd_2O_3	0.534	1.174	0.443	1.178	0.067	0.424	0.029	0.924
Sm_2O_3	0.441	0.518	0.459	0.515	0.044	0.307	0.012	0.285
Eu_2O_3	0.107	0.102	0.103	b.d.	b.d.	b.d.	b.d.	b.d.
Gd_2O_3	0.563	0.413	0.841	0.361	0.271	0.697	0.019	0.287
Dy_2O_3	0.280	0.192	0.457	0.108	0.351	0.791	0.006	0.285
Er_2O_3	0.071	0.085	0.147	0.034	0.279	0.303	0.038	0.084
Yb_2O_3	0.025	0.102	0.105	0.043	0.230	0.146	0.036	0.015
Total	98.146	99.119	95.026	98.071	96.279	97.974	98.955	97.958

*b.d. = below detection limit

Table 3.5 reports the compositions of the other major REE-bearing minerals in the Nechalacho deposit. Fergusonite-(Y) is preferentially enriched in the middle and heavy REE, up to 7.5 wt. % Dy_2O_3 and Gd_2O_3 (Figure 3.15E), and is the main host of yttrium in the deposit (it contains ~25 wt. % Y_2O_3). It also hosts significant concentrations of Ta_2O_5 (up to 6 wt. %; avg. ~2.7 wt. %), which has its highest bulk rock concentration in the lower parts of the lower mineralized zone (up to 0.12 wt. %; avg. ~0.06 wt. %) where fergusonite-(Y) is most abundant. The average stoichiometry of fergusonite-(Y) is $(Y_{0.51}Gd_{0.10}Dy_{0.08}Nd_{0.04}Sm_{0.04}Ta_{0.04})Nb_{1.00}O_4$. Ferrocolumbite has an average composition of $(Fe^{2+}_{0.92}Mn_{0.14})Ta_{0.11}Nb_{1.80}O_6$ and a Nb:Ta ratio that is very similar to that of fergusonite-(Y) (16.4 vs. 25), consistent with the observation that ferrocolumbite replaced fergusonite-(Y). Ferrocolumbite hosts up to 7.95 wt. % Ta_2O_5, 0.68 wt. % Y_2O_3 and an average of ~68.5 wt. % Nb_2O_5. Columbite-(Mn) is similar in composition to ferrocolumbite but hosts higher concentrations of Ta_2O_5 and MnO (up to 21.85 and 6.04 wt. % respectively) and lower concentrations of Nb_2O_5 and FeO (36.54 and 9.11 wt. % respectively).

The unaltered eudialyte in drill core from hole 85-L6 has an average composition of $(Na_{11.96}Ca_{1.32}K_{0.33})(Ca_{4.19}REE_{1.08}Y_{0.65}Mn_{0.08})_{\Sigma 6}(Mn^{2+}_{2.98}Fe^{2+}_{0.02})_{\Sigma 3}Zr_{2.94}Nb_{0.98}(Si_{26.09}O_{72})$ $(O,OH,H_2O)_3(OH,Cl_{0.38}F_{0.45})_{\Sigma 2}$, calculated using the method proposed by Johnsen et al. (2003). This is close to the composition of the end member, kentbrooksite, in terms of Mn-REE-Nb-F, but in terms of Ca-Fe-Si-Cl is intermediate between kentbrooksite and eudialyte. In view of this, the mineral is referred to as eudialyte in this paper. This phase hosts up to 4.08 wt. % Nb_2O_5, 2.97 wt. % Y_2O_3 and 5.97 wt. % total REE as oxides.

Table 3.5 Average compositions of fergusonite-(Y), ferrocolumbite, eudialyte, monazite-(Ce), allanite-(Ce) and bastnäsite-(Ce) analysed using the electron microprobe.

	Fergusonite-(Y) (n=36)	**Ferrocolumbite (n=12)**	**Eudialyte (n=21)**	**Monazite-(Ce) (n=47)**	**Allanite-(Ce) (n=33)**	**Bastnäsite-(Ce) (n=26)**
ZrO_2	-	-	10.730	-	-	-
SiO_2	-	-	46.680	-	31.730	-
HfO_2	0.200	-	0.310	-	-	-
TiO_2	-	1.960	-	-	-	-
FeO	0.560	19.010	b.d.	0.090	13.890	b.d.
Al_2O_3	-	-	-	-	16.400	-
MgO	-	0.220	-	-	0.370	-
MnO	-	2.650	6.420	-	0.630	-
P_2O_5	-	-	-	29.800	-	-
UO_2	-	0.050	-	-	-	-
ThO_2	0.440	b.d.	-	1.510	-	-
CaO	0.280	0.060	9.160	0.230	9.010	0.140
F	-	-	0.210	0.480	-	7.760
Na_2O	-	-	10.990	-	-	-
K_2O	-	-	0.460	-	-	-
Y_2O_3	24.530	0.300	2.180	0.660	0.130	0.310
Nb_2O_5	45.880	70.640	3.870	-	-	-
Ta_2O_5	2.570	4.230	-	-	-	-
SnO_2	-	0.180	-	-	-	-
La_2O_3	-	-	1.340	14.420	6.530	16.670
Ce_2O_3	0.470	-	1.860	31.990	12.680	35.310
Pr_2O_3	0.210	-	0.200	3.990	1.480	4.220
Nd_2O_3	2.560	-	0.750	14.260	4.500	15.240
Sm_2O_3	2.800	b.d.	0.150	1.620	0.340	1.380
Eu_2O_3	0.880	-	-	0.170	0.160	0.330
Gd_2O_3	6.760	-	0.400	0.950	0.250	0.870
Dy_2O_3	5.910	-	0.370	0.180	-	0.100
Er_2O_3	2.060	b.d.	0.200	-	-	-
Yb_2O_3	0.760	-	0.120	-	-	-
CO_2	-	-	-	-	-	20.740
Total	96.870	99.300	96.400	100.350	98.100	103.070

*b.d. = below detection limit

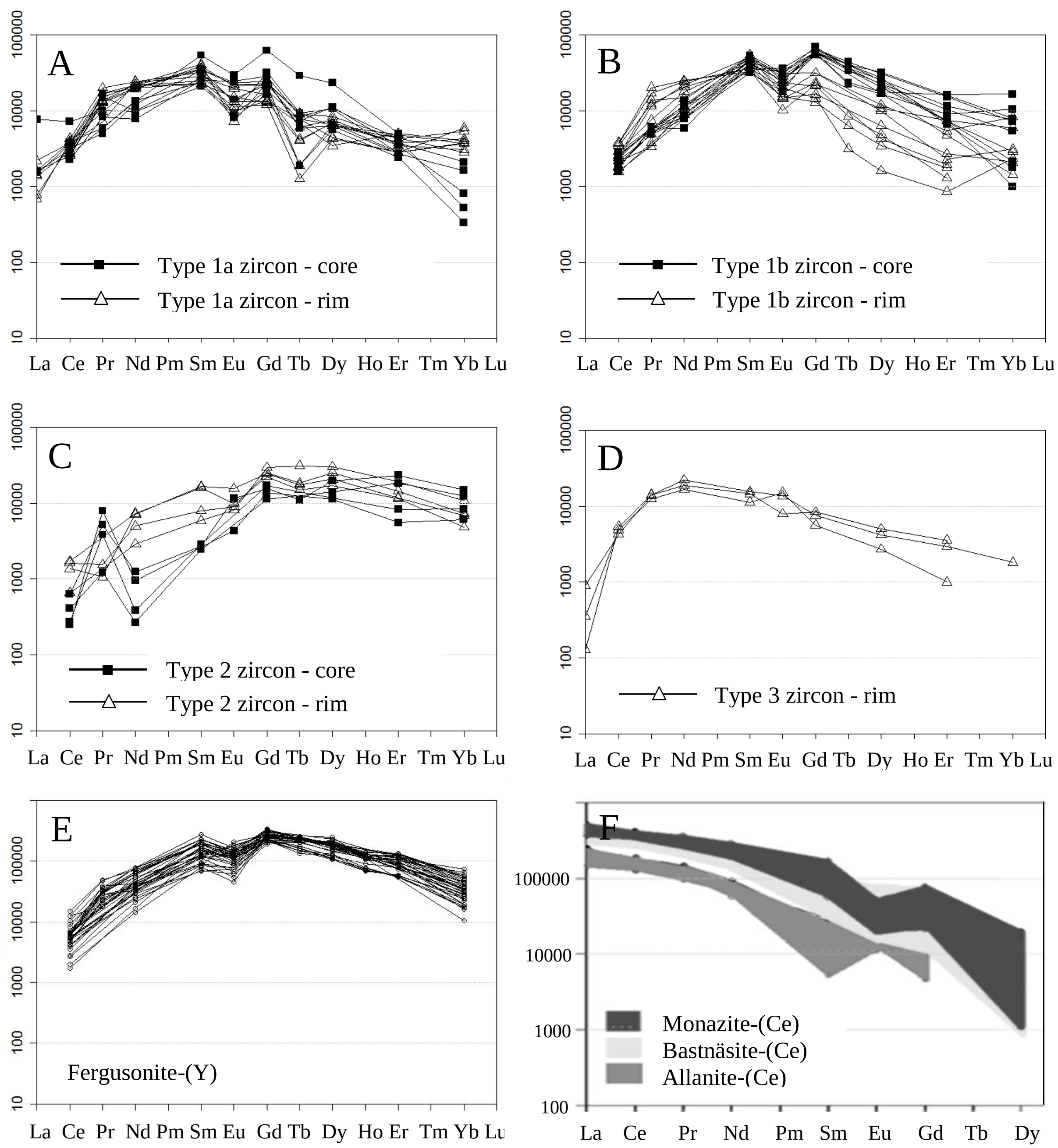

Figure 3.15 Chondrite-normalized REE profiles (Boynton, 1984) for zircon, fergusonite-(Y), monazite-(Ce), bastnäsite-(Ce) and allanite-(Ce). The Y-axis in all graphs represents sample/REE chondrite.

Monazite-(Ce), allanite-(Ce) and bastnäsite-(Ce) all display similar chondrite normalized REE profiles, being preferentially enriched in the LREE with a concave trend from La to Sm (Figure 3.15F). The average compositions of these minerals are $(Ce_{0.47}Nd_{0.22}La_{0.19}Pr_{0.06})P_{0.99}O_4$, $(Ca_{0.89}Ce_{0.45}La_{0.22}Nd_{0.15}Pr_{0.05})(Al_{1.78}Fe_{1.12})Si_{2.93}O_{12}$ and $(Ce_{0.38}Nd_{0.19}La_{0.17}Pr_{0.05})F_{0.66}C_{0.87}O_3$, respectively. The HREE concentrations are generally below the limit of detection of the electron microprobe. Monazite-(Ce) contains the highest concentrations of Ce_2O_3 (35 wt. %) and Nd_2O_3 (15 wt. %) of any of the REE-bearing minerals and rare zoned crystals have rims that are preferentially enriched in MREE and thorium. By contrast, allanite-(Ce) contains, on average, 7 wt. % La_2O_3, 13 wt. % Ce_2O_3 and 4.5 wt. % Nd_2O_3.

DISCUSSION

Origin of the Zircon

Although zirconium is widely believed to be immobile during fluid-rock interaction and zircon is regarded by many as a strictly igneous mineral, there have been a number of reports in the literature of textures involving zircon consistent with its formation by hydrothermal processes (e.g., Rubin et al., 1993; Schaltegger, 2007; Anderson et al., 2008; Lichtervelde et al., 2009). For example, Rubin et al. (1989) reported Hf-enriched hydrothermal overgrowths on magmatic zircon from the Sierra Blanca Peaks, Texas and similar overgrowths have since been reported for the Boggy Plain zoned pluton, Australia (Hoskin, 2005) and the Mole Granite, Australia (Pettke et al., 2005). Kerrich and King (1993) also documented hydrothermal zircon with a "spongy texture" containing abundant inclusions of Au and fluid.

In the Nechalacho deposit, there is evidence for the occurrence of both magmatic and hydrothermal zircon. Based on the nature of its distribution in undulating laminations, which parallel igneous layering and lithological contacts, Type 1 zircon (the main variety of zircon in the upper mineralized zone) is interpreted to be a magmatic cumulate mineral. It is, however, likely that the rims of Type 1 zircon crystals represent overgrowths on primary cores which acted as nuclei for crystallization of later zircon and, it is thus possible that this later zircon deposited from a hydrothermal fluid. It is also possible that the overgrowths simply represent a second stage of magmatic crystallization. Irrespective of which interpretation is correct, an important finding of our study is that the zircon of the upper mineralized zone is dominantly of magmatic origin and therefore substantial proportions of the Y and REE (particularly the HREE) were concentrated magmatically as a result of their incorporation in zircon; the cores of Type 1 zircon are elevated in Y and the middle to heavy REE.

In contrast to Type 1 zircon, Type 2 zircon (the main variety of zircon in the lower mineralized zone) is clearly hydrothermal in origin. It formed in pseudomorphs of a mineral that we interpret to be eudialyte and, we consider it likely that it obtained its zirconium from the residues of the dissolution of that mineral. There are several lines of evidence that support this interpretation. Firstly, the relative volume proportions of each of the secondary minerals (zircon + fergusonite-(Y) + bastnäsite-(Ce) + parisite-(Ce)/synchysite-(Ce) + allanite-(Ce) + albite + quartz + biotite + fluorite + kutnahorite ± minor hematite) are roughly consistent from one pseudomorph to another, suggesting that one or more elements (e.g., Zr, Y, Ce, Mn, Fe) was conserved. Secondly, the homogeneous distribution of zircon in the pseudomorphs (Figure 3.14) suggests strongly that Zr was conserved, and thirdly, the volume proportion of zircon (~ 15%), is consistent with the proportion of Zr that would be made available by dissolution of eudialyte (eudialyte contains ~11 mole percent zirconium silicate). Finally, we note that the LREE:HREE ratio of the bulk rocks in the lower mineralized zone is approximately 3:1, which is comparable to the ratio of these elements in eudialyte from Ilimaussaq (Sorensen et al., 2006) and the North Qôroq Centre, South Greenland (Coulson, 1997).

The colloform nature of Type 3 zircon (Figure 3.8A) provides strong evidence that this variety of zircon is also hydrothermal in origin but that in contrast to Type 2 zircon, both Zr and Si were supplied by the fluid. If this interpretation is correct, then it follows that the rims of Type 1 zircon are also hydrothermal in origin as the distribution of the REE in them is very similar to that of Type 3 zircon.

In summary, our observations of the Nechalacho deposit suggest that zircon in the upper mineralized zone was dominantly magmatic and that zircon in the lower mineralized zone formed by a replacement of eudialyte but without hydrothermal mobilization of Zr on a scale of more than tens of microns. However, there was more substantial mobilization of Zr in the upper mineralized zone and this produced colloform hydrothermal Type 3 zircon and overgrowths on Type 1 zircon.

Magmatic Concentration of Zr, Nb, Y and REE

Zr, Nb, Y and REE mineralization in the Nechalacho deposit is confined to cumulate layers of zircon in the upper zone, with associated columbite-(Mn) and to layers of pseudomorphs after cumulate eudialyte in the lower zone. The layers in both zones typically contain > 60,000 ppm

ZrO_2, up to 8000 ppm Nb_2O_5 and 5000 ppm Y_2O_3 and >3 wt. % TREO, achieved by a combination of crystal settling and compaction of discrete zircon and eudialyte crystals and later alteration, remobilization and concentration by magmatic hydrothermal fluids.

Most authors agree that peralkaline melts are products of low degrees of partial melting in an undepleted, metasomatically enriched mantle (Marks et al., 2003; Halama et al., 2004) and that silica-undersaturated rocks originate from differentiation of these magmas under relatively dry and low fO_2 conditions. A key characteristic of such magmas is their ability to evolve to high Cl and F contents before exsolving an aqueous fluid phase (Kogarko, 1974; Markl et al., 2001), allowing for extreme fractionation to low temperature. It is known that elevated concentrations of alkalis and F in these magmas increase the solubility of the REE and HFSE by promoting formation of alkali-silicate or alkali-fluoride complexes with them (Keppler, 1993; Peiffert et al., 1996; Linnen, 1998; Marr et al., 1998; Baker et al., 2002), thereby providing a mechanism for transporting these elements. Keppler (1993) examined the effect of fluorine on zircon solubility in felsic melts and demonstrated a strong positive correlation between solubility and fluorine content in melts containing 0 to 6 wt. % F. Concentrations of Zr, Nb, Y and REE can reach several thousands of ppm in natural systems. For example, Olivo and Williams-Jones (1999) reported concentrations of Zr, Nb, Y and REE in nepheline syenite from the Pilanesberg Complex, South Africa of 1.81, 0.21, 0.05 and 0.66 wt. %, respectively. In many cases, the REE and HFSE are further concentrated by saturation of the magma with minerals like eudialyte and settling under gravity to form cumulate layers in which these minerals are dominant (Sorensen et al., 2006). However, to our knowledge, there have been no reports in the literature of cumulate zircon.

The presence of both simple and complex zirconosilicates, namely primary zircon and eudialyte in the same system is rare but has been reported, for example, from the Tamazeght Complex, Morocco (Salvi et al., 2000; Marks et al., 2008). In this complex eudialyte is the principal Zr-bearing mineral in agpaitic nepheline syentites and forms cumulates, whereas zircon is the main Zr-bearing mineral in miaskitic nepheline syenites but is a comparatively minor phase and does not form cumulates. Another example of the same phenomenon is provided by the McGerrigle Mountains, Quebec, where zircon is concentrated in miaskitic rocks (2.2 modal % in one sample) and eudialyte is restricted to agpaitic rocks (Wallace et al., 1990).

The primary zirconium mineralogy is a function of the alkalinity of the rocks, where zircon is dominant in miaskitic rocks, eudialyte in agpaitic rocks and both zircon and eudialyte occur in rocks of intermediate composition. Indeed, the term agpaitic, which was originally introduced to refer to syenites with a molar (Na_2O +K_2O)/Al_2O_3 ratio > 1.2 (alkalinity index; Ussing, 1912), now has the added restriction that Zr and Ti minerals should be in the form of complex minerals such as eudialyte and rinkite rather than zircon or ilmenite (Sorensen, 1997). The term miaskitic is reserved for nepheline syenites in which Zr is in the form of zircon and for which the alkalinity index is generally but not exclusively less than unity.

We propose that the upper mineralized zone of the Nechalacho deposit at Thor Lake, which contains zircon cumulates, represents less evolved miaskitic rocks, and that the eudialyte cumulate-bearing lower mineralized zone represents more evolved agpaitic rocks. This interpretation is supported by large numbers of bulk rock analyses of 1 - 2 m long intervals of drill core (Figure 3.16) which show that rocks from the upper mineralized zone generally have alkalinity indices < 1 (mean of 169 samples = 0.89), whereas those from the lower mineralized zone generally have alkalinity indices >1 (mean of 38 samples = 1.20). However, it needs to be recalled that both zones were intensely altered and it is therefore likely that there was considerable mobilization of the alkalis.

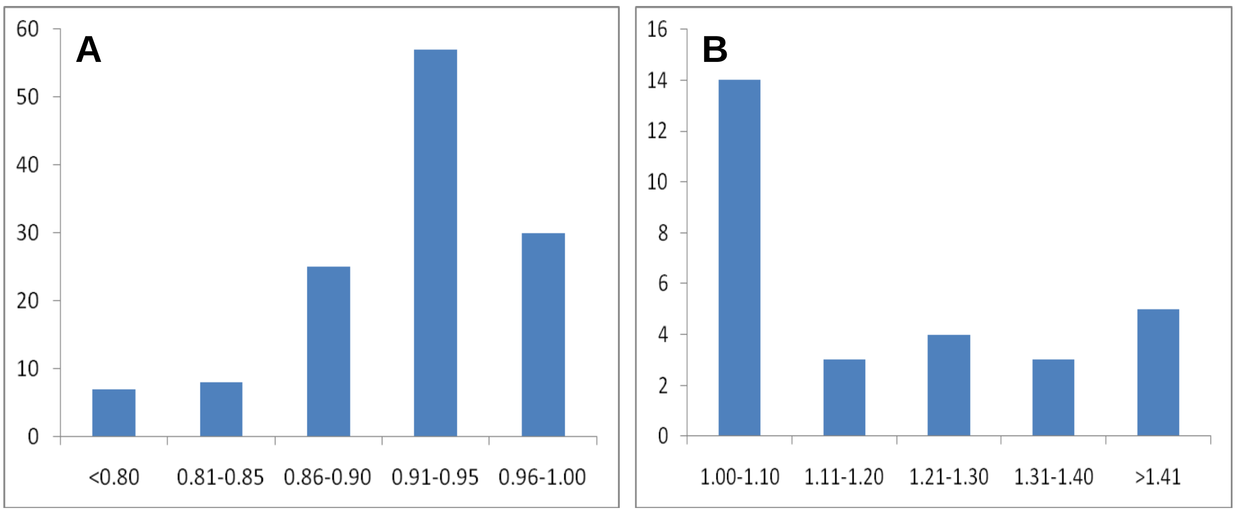

Figure 3.16 Histograms of bulk rock alkalinity indices ($(Na_2O + K_2O)/Al_2O_3$) of 1 - 2 m long intervals of drill core: A. Upper mineralized zone; B. Lower mineralized zone. These show that rocks from the upper mineralized zone generally have alkalinity indices < 1, whereas those from the lower mineralized zone generally have alkalinity indices > 1.

The factors determining whether a magma crystallizes zircon or more complex zirconosilicates are not well understood. Clearly and not surprisingly the formation of complex zirconosilicate minerals is favoured by high alkalinity as shown by field observations that zircon occurrence seems to be restricted to miaskitic rocks. However, silica activity may also play a role as suggested by the results of experiments by Marr et al. (1998) with peralkaline melts, which showed that zircon was the melt-saturated phase for SiO_2 contents above 55 wt. %, whereas for lower SiO_2 contents wadeite, a potassium zirconosilicate, was the melt-saturated phase. In the Nechalacho deposit, it may therefore not be coincidence that rocks in the zircon-rich upper mineralized zone have a higher content of SiO_2 than in the lower zone, where Zr is interpreted to have been present dominantly as eudialyte (Figure 3.17). Finally, there is evidence from field studies that temperature may play a role. For example, at Strange Lake, zircon was the earliest mineral to crystallize, followed by the sodium zirconosilicates, vlasovite and elpidite (Birkett et al., 1992).

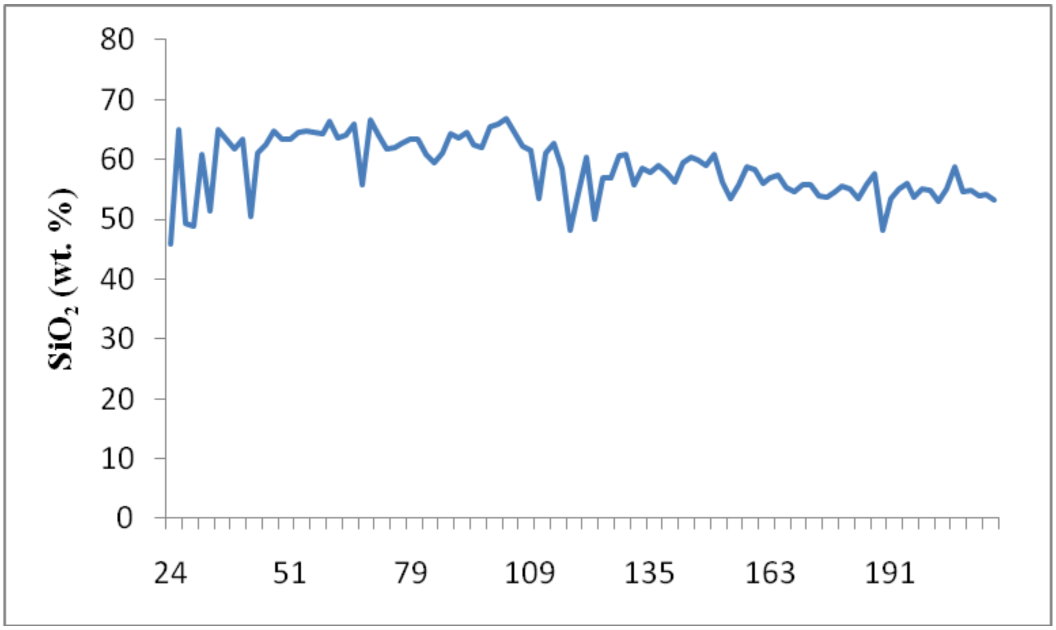

Figure 3.17 Bulk-rock silica content (wt. %) as a function of depth in drill hole L09-162. Samples represent analyses of 1 – 2 m long intervals of drill core.

Another important HREE-bearing primary magmatic mineral is columbite-(Mn), which, because of its relatively high density, accumulated with zircon in the upper mineralized zone, where it is most abundant, and with eudialyte in the lower mineralized zone. This interpretation is based on its close spatial association with primary zircon and eudialyte, textural evidence of selective replacement of columbite-(Mn) by fergusonite-(Y) and the occurrence of columbite-(Mn) as inclusions in alteration minerals such as biotite, chlorite, magnetite and albite. However, columbite-(Mn) can also be secondary as indicated by its presence in some pseudomorphs after eudialyte.

Hydrothermal Zr, Nb, Y and REE Mobilization

In most igneous systems, Zr, Nb, Y and REE are immobile during fluid-rock interaction, and for this reason are widely used as petrogenetic indicators (Pupin, 1980; Hoskin and Schaltegger, 2003; Schaltegger et al., 2005). However, there is increasing evidence in the literature that these elements can be transported by hydrothermal fluids under the restrictive sets of conditions that commonly prevail in alkaline igneous settings. It has also been shown that the hydrothermal durability of many minerals enriched in HFSE is compromised by alpha-decay-induced damage (Pidgeon et al. 1966, Sinha et al. 1992, Geisler et al. 2001, Lumpkin 2001). Our study has provided evidence of metamict processes, which resulted in preferential alteration of the cores of Type 1 zircon crystals and mobilization of Y and HREE from these crystals to form minerals such as fergusonite-(Y), which only occurs adjacent to zircon. Similar alteration has been documented by Anderson et al. (2008) for zircon from the Georgeville granite, Nova Scotia. In this latter study, Anderson et al. (2008) showed that Y and REE in metamict zircon were redistributed during alteration by diffusion and dissolution and re-precipitation along micro-fractures on a scale of tens of micrometres.

The current study has provided evidence of some remobilization of Zr, Y and HREE by hydrothermal fluids. In the upper mineralized zone, minor zircon (Type 3) forms colloform lamellae and overgrowths, and much of the yttrium and HREE were mobilized out of the cores of Type 1 zircon to form crystals of fergusonite-(Y) by replacement of nearby grains of primary magmatic columbite-(Mn). The latter is also true to a lesser extent in the lower mineralized zone, where columbite-(Mn) adjacent to eudialyte pseudomorphs was replaced by fergusonite-(Y). In contrast to this limited mobility of Zr, Y and the HREE, the LREE appear to have been mobilized on scales ranging from micrometres to metres. They are concentrated in the minerals allanite-(Ce) and monazite-(Ce), which typically form interstitially to magmatic zircon and eudialyte, and as bastnäsite-(Ce), parisite-(Ce) and synchysite-(Ce), which commonly show no spatial association with primary zircon and eudialyte pseudomorphs; in the upper mineralized zone these minerals are most abundant metres above the intervals containing the highest concentrations of HREE.

As a result of recent experimental studies, we now have some insights into the behaviour of Zr in hydrothermal fluids (Migdisov and Williams-Jones, 2009) and a relatively good understanding of the behaviour of the REE in these fluids (Migdisov and Williams-Jones; 2002; 2007 and Migdisov et al. 2009). The study of Zr shows that it forms its strongest complexes with fluoride and that fluids with HF concentrations on the order of 0.1 m can dissolve tens of ppm of zircon at 200 °C. Significantly higher concentrations of REE can be dissolved by fluids with such HF concentrations. Furthermore, the LREE form considerably stronger complexes with fluoride than the HREE and are therefore more easily mobilized. The REE also form relatively strong complexes with chloride and as for fluoride, the strongest complexes are with the LREE. These studies satisfactorily explain the relatively limited mobility of Zr, Y (although there are no experimental data for Y, it is expected to behave like a HREE) and the HREE, and the much greater mobility of the LREE in the Nechalacho deposit.

In light of the above discussion and the abundance of fluorite in the deposit, it seems plausible that Y and REE were leached from primary minerals, namely zircon and eudialyte, by forming fluoride complexes, and then re-deposited as fergusonite-(Y), allanite-(Ce), monazite-(Ce), bastnäsite-(Ce), parisite-(Ce) and synchysite-(Ce). In the case of fergusonite-(Y), allanite-(Ce) and monazite-(Ce), the mobilization, for the most part, was on the scale of millimetres, and for fergusonite-(Y) was controlled by the occurrence of proximal columbite-(Mn). However, as noted above, the REE concentrated in the bastnäsite-(Ce), parisite-(Ce) and synchysite-(Ce) of the upper mineralized zone were mobilized on a scale of metres. By analogy with the model proposed for the deposition of these minerals in the Strange Lake pluton, Québec-Labrador (Salvi and Williams-Jones, 1990), and noting their association with fluorite and calcite, we propose that the LREE were transported as fluoride complexes in magmatic hydrothermal fluids, which subsequently mixed with external calcium- and carbonate-bearing fluids near the top of the layered complex. This mixing caused immediate deposition of fluorite, which is relatively insoluble in the presence of Ca, and consequent destabilization of the REE-fluoride complexes, making the REE available for deposition as fluoro-carbonate minerals.

Genetic Model

The proposed geological model for the Zr, Nb, Y and REE mineralization in the Nechalacho deposit involves intrusion of an alkaline, volatile-rich, aegirine nepheline syenite into the Thor Lake Syenite, at the centre of the Blachford Lake Complex. The alkaline nature of the rocks and their high concentration of incompatible elements, in particular the HREE, suggests a small degree of partial melting of deep crust or shallow mantle, possibly at depths of 60-100 km (Sorensen, 1997; Martin, 2006). Repeated injections of magma, fractional crystallization and convective overturn produced a layered igneous body. As the convecting magma went through cycles of saturation and under-saturation in a phase (i.e., aegirine, nepheline, K-feldspar, sodalite, zircon or eudialyte) because of changes in pressure associated with convective overturn and mixing of different pulses of magma, layers were formed (Figure 3.18). This mixing likely caused monomineralic crystallization of zircon or eudialyte by displacing the system from a cotectic to a field in which only a zirconosilicate mineral was stable. The result was a lower mineralized zone comprising multiple eudialyte cumulate layers and an upper zone comprising multiple zircon cumulate layers. We propose that the difference between these two zones was the result of the alkali content of the magmas that formed them, i.e., miaskitic in the case of the upper mineralized zone and agpaitic in the case of the lower mineralized zone.

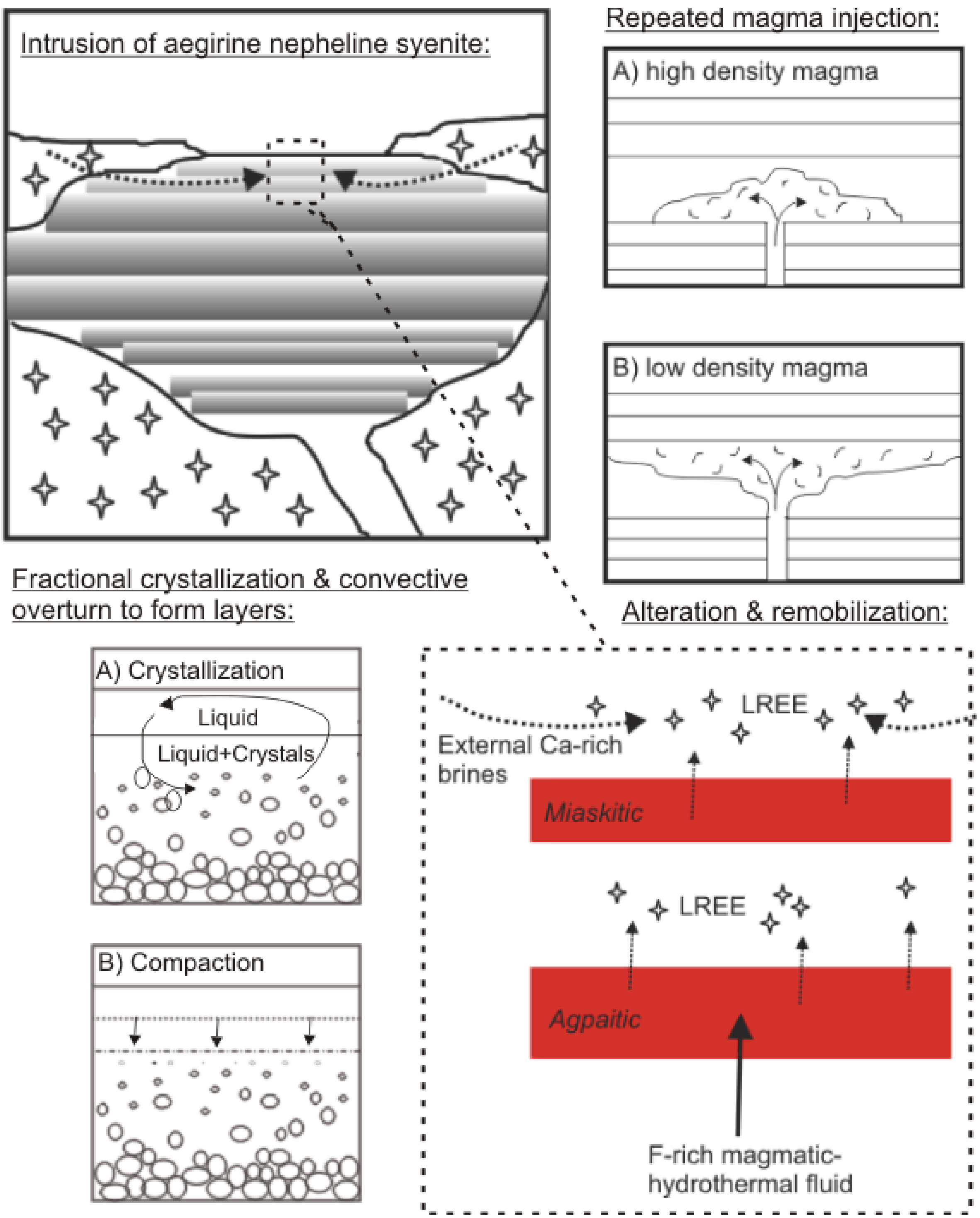
Intrusion of aegirine nepheline syenite:
Repeated magma injection:
A) high density magma
B) low density magma
Fractional crystallization & convective overturn to form layers:
A) Crystallization
Liquid
Liquid+Crystals
B) Compaction
Alteration & remobilization:
LREE
External Ca-rich brines
Miaskitic
LREE
Agpaitic
F-rich magmatic-hydrothermal fluid

Figure 3.18 Cartoon illustrating the intrusion of aegirine nepheline syenite into the Thor Lake Syenite. Repeated injections of magma, bottom upwards crystallization due to decreasing pressure and convective overturn due to decreasing temperature produce a layered igneous body. Hydrothermal alteration of the upper and lower mineralized zones leads to remobilization of certain elements, including the LREE.

Fluids of possible magmatic origin expelled from the intrusion of the aegirine nepheline syenite at depth were responsible for alteration of the primary eudialyte and zircon. These fluids also caused biotitization, K-feldspathization, and replacement of primary minerals (mainly aegirine) by magnetite or hematite. The eudialyte crystals were dissolved and completely replaced by secondary phases within the original crystal boundaries. Some elements, e.g., Zr, Nb and the HREE, were only remobilized on a scale of microns or tens of microns, i.e., they remained largely within the boundaries of the pseudomorphs, whereas other elements, e.g., Na, Ca, Cl, H_2O and LREE, were removed by the fluids. Zirconium, Y and REE were mobilized from Type 1a and b metamict zircon cores in the upper mineralized zone along fractures to form secondary zircon, fergusonite-(Y), allanite-(Ce) and monazite-(Ce). The LREE were mobilized from both eudialyte and zircon as fluoride complexes and deposited distal to their hosts. In the upper parts of the complex this occurred as a result of mixing with external Ca-bearing fluids, which destabilized the complexes by precipitating fluorite. Later Na-rich fluids overprinted and locally replaced the bulk of the primary mineralogy, including zircon and eudialyte, with albite (cleavelandite), mainly, but not exclusively, in the upper parts of the deposit.

Comparison to Other Deposits

A small number of other HREE-enriched deposits occur in other parts of the world. The Ilimaussaq layered alkaline complex in Southern Greenland (Marks et al., 2004) is similar in many respects to the Nechalacho deposit, in geological setting, size and the preferential enrichment of the HREE. At Ilimaussaq, the HREE are concentrated in lujavrites, which comprise cumulates of aegirine, arfvedsonite and eudialyte (Larsen and Sorensen, 1987), whereas in the Nechalacho deposit there are also cumulates of zircon and eudialyte has been pseudomorphed by a zircon-bearing mineral assemblage. To our knowledge, Nechalacho is the only HREE deposit in which zircon cumulates have been recognized. However, both zircon and eudialyte occur in the Tamazeght alkaline complex in Morocco (Salvi et al., 2000) and although zircon is not a cumulate mineral and is present in relatively small proportions, it is hosted by miaskitic rocks as has been proposed for the Nechalacho deposit. There is also abundant evidence of hydrothermal mobilization of high field strength elements at Tamazeght, with secondary phases which are richer in F and Ca, such as cancrinite, calcic catapleiite and rinkite, partly or completely replacing primary phases, namely zircon and eudialyte. Although many similarities can be drawn between Ilimaussaq, Tamazeght and the Nechalacho deposit, the Nechalacho deposit is unusual in its REE mineralogy and in hosting a potentially economic resource of the HREE.

CONCLUSIONS

The Nechalacho deposit at Thor Lake contains extraordinarily high concentrations of Zr, Nb, Y and REE as zircon, fergusonite-(Y) and ferrocolumbite, bastnäsite-(Ce), allanite-(Ce) and monazite-(Ce). Upper and lower mineralized zones have been defined, with the latter representing multiple cumulate eudialyte layers and the former representing discontinuous, heterogeneous zircon-rich cumulate layers. Primary eudialyte has been completely replaced by secondary phases, namely zircon, fergusonite-(Y), bastnäsite-(Ce), parisite-(Ce)/synchysite-(Ce), allanite-(Ce), albite, quartz, biotite, fluorite, kutnahorite and minor hematite, which pseudomorph the precursor eudialyte, and primary zircon has been leached of REE. The model proposed to explain the origin of the mineralization in the Nechalacho deposit calls on both magmatic and hydrothermal processes. The eudialyte and zircon cumulate layers can be explained by injection of separate agpaitic and miaskitic magmas. Hydrothermal fluids altered the distribution of REE, within the upper and lower mineralized zones, locally enriching and depleting them, and created a set of secondary minerals, which will be the main target of future exploitation.

ACKNOWLEDGEMENTS

E. Sheard gratefully acknowledges the support of a Natural Sciences and Engineering Research Council (NSERC) Alexander Graham Bell post-graduate scholarship, a GEOTOP (Quebec inter-university network for advanced studies and research in geoscience) post-graduate scholarship and a McGill Principal’s Graduate Fellowship. Financial support for the research was provided by a grant from Avalon Rare Metals Inc. and a matching grant from the NSERC-CRD program to AEW-J. Avalon Rare Metals Inc. also provided access to the field area, drill core, geochemical data and internal reports. We thank V.J. van Hinsberg, J.R. Clark and A. Migdisov for helpful discussions and L. Shi for assistance during SEM analyses.

CHAPTER IV

CONCLUSIONS AND CONTRIBUTIONS TO KNOWLEDGE

CONCLUSIONS

Academic research at Thor Lake has been restricted to a few Geological Association of Canada abstracts and Geological Survey of Canada reports, a chapter published in a Mineralogical Society Series volume on the REE by Taylor and Pollard (1996) on fluid inclusions in the T-Zone; an overview paper on the Thor Lake rare-metal deposits by Trueman et al. (1988); and three Master's theses, two of which were published. This study has built upon previous work and with the assistance of the extensive drilling undertaken by Avalon Rare Metals Inc. since 2007, has considerably enhanced our understanding of the genesis of the deposit. The Thor Lake-Nechalacho complex is a layered intrusion comprising numerous sub-horizontal layers of aegirine nepheline syenite, sodalite syenite, eudialyte and zircon cumulates and lujavrite with variations in grain size from fine-grained to pegmatitic. Evidence of cumulate and adcumulus textures and rhythmic layering of mafic and felsic units on scales ranging from tens of centimetres to several metres indicate a complex history of pulsed injection of magma and magmatic differentiation.

The Nechalacho deposit at Thor Lake contains extraordinarily high concentrations of Zr, Nb, Y and REE as zircon, fergusonite-(Y) and ferrocolumbite, bastnäsite-(Ce), allanite-(Ce) and monazite-(Ce). Upper and lower mineralized zones have been defined, with the latter representing multiple cumulate eudialyte layers and the former representing discontinuous, heterogeneous zircon-rich cumulate layers. Primary eudialyte has been altered and completely replaced by secondary phases, namely zircon, fergusonite-(Y), bastnäsite-(Ce), parisite-(Ce)/synchysite-(Ce), allanite-(Ce), albite, quartz, biotite, fluorite, kutnahorite and minor hematite, which pseudomorph the precursor eudialyte. In the upper zone, zircon is a magmatic cumulate mineral, which locally was replaced by secondary REE-bearing minerals. Element-distribution maps of zircon crystals in the upper zone indicate that Y and REE were mobilized from the cores and locally precipitated as fergusonite-(Y) along micro-fractures. The LREE were also mobilized locally from both primary zircon and inferred primary eudialyte. The occurrence of zircon in fractures, wrapped around brecciated K-feldspar fragments and as a secondary phase in pseudomorphs are evidence of its hydrothermal origin and/or remobilization of primary Zr.

The model proposed to explain the origin of the mineralization in the Nechalacho deposit calls on both magmatic and hydrothermal processes. The eudialyte and zircon cumulate layers can be explained by injection of separate agpaitic and miaskitic magmas. Hydrothermal fluids altered the distribution of REE, within the upper and lower mineralized zones, locally enriching and depleting them, and created a set of secondary minerals which will be the main target of future exploitation.

In conclusion, the Nechalacho deposit is the only HREE deposit in which zircon cumulates have been recognized. Many similarities can be drawn between Ilimaussaq, Tamazeght and the Nechalacho deposit; however, the Nechalacho deposit is unusual in its REE mineralogy and in hosting a potentially economic resource of the HREE.

CONTRIBUTIONS TO KNOWLEDGE

This study provides the first comprehensive investigation of the nature and distribution of the Zr, Nb, Y and REE mineralization in the Nechalacho deposit and, contrary to earlier interpretations, has demonstrated that concentration of the rare metals was controlled dominantly by magmatic processes. Earlier studies had concluded that the rare metal mineralization was dominantly hydrothermal and concentrated near the top of the host intrusion. Demonstration that the mineralization is largely magmatic in origin is influencing exploration strategy and has already played an important role in the discovery of new mineralization.

An important contribution of the study which has more global importance is that much of the mineralization in the upper part of the Nechalacho deposit is hosted by magmatic zircon cumulates that form layers tens of centimetres in thickness. To our knowledge, this represents the first report of the occurrence of macroscopically evident zircon cumulates anywhere.

A further important contribution to knowledge is the demonstration that the alkali/alumina ratio controlled the nature of the magmatic zirconium phase. In rocks with an alkalinity index less than unity, the main zirconium mineral is zircon, whereas in rocks with higher alkalinity indices it was eudialyte. Although, this contrasting primary zirconium mineralogy of miaskitic and agpaitic rocks in the same intrusive complex has been recognized previously, the present study is the first to report magmatic zircon in potentially economic concentrations in miaskitic rocks.

Finally, this study has also provided evidence of the differential mobilization of LREE and HREE predicted by the experimental study of Migdisov et al. (2009) and hydrothermal mobilization of zirconium, an element which is generally believed to be immobile but was shown experimentally (Migdisov and Williams-Jones, 2009) to be relatively mobile in fluoride-bearing hydrothermal fluids.

Overall, the research has made a number of important contributions to knowledge of both local and global importance. Moreover, in reconstructing the genesis of a rare metal mineral deposit of a type that has received limited previous scientific investigation, it has contributed new understanding that will be essential to successful future exploration for commodities that will be in great demand due to the emergence of new technologies.

REFERENCES

Anderson, A.J. 2008. The alteration of metamict zircon and its role in the remobilization of high-field-strength elements in the Georgeville Granite, Nova Scotia. *The Canadian Mineralogist*, v. 46, pp. 1-18.

Baker, D.R., Conte, A.M., Freda, C. and Ottolini, L. 2002. The effect of halogens on Zr diffusion and zircon dissolution in hydrous metaluminous granitic melts. *Contributions to Mineralogy and Petrology*, v. 142, pp. 666-678.

Banks, D.A., Yardlet, B.W.D., Campbell, A.R. and Jarvis, K.E. 1994. REE composition of an aqueous magmatic fluid: A fluid inclusion study from Capitan Pluton, New Mexico, U.S.A. *Chemical Geology*, v. 113, pp. 259-272.

Birkett, T.C., Miller, R.R., Roberts, A.C. and Mariano, A.N. 1992. Zirconium-bearing minerals of the Strange Lake Intrusive Complex, Québec-Labrador. *The Canadian Mineralogist*, v. 30, pp. 191-205.

Birkett, T.C., Richardson, D.G. and Sinclair, W.D. 1994. Gravity modeling of the Blachford Lake Intrusive Suite, Northwest Territories. *In* Studies of rare-metal deposits in the Northwest Territories. *Edited by* W.D. Sinclair and D.G. Richardson. Geological Survey of Canada, Bulletin 475.

Birkett, T.C., Sinclair, W.D. and Richardson, D.G. 1992. Geochemical, isotopic and gravity studies of the Thor Lake deposits and associated host rocks of the Blachford Lake intrusive complex (*in* Project summaries; Canada-Northwest Territories Mineral Development Subsidiary Agreement 1987-1991). Open-File Report – Geological Survey of Canada, pp. 127-128.

Boily, M. and Williams-Jones, A.E. 1994. The role of magmatic and hydrothermal processes in the chemical evolution of the Strange Lake plutonic complex, Québec-Labrador. *Contributions to Mineralogy and Petrology*, v. 118, pp. 33-47.

Bollingberg, H.J., Ure, A.M., Sørensen, I. and Leonardsen, E.S. 1983. Geochemistry of some eudialyte-eucolite specimens and a co-existing catapleiite from Langesund, Norway. *Tschermaks Min. Petr. Mitt.*, v. 32, pp. 153-169.

Bowring, S.A., Van Schmus, W.R. and Hoffman, P.F. 1984. U-Pb zircon ages from Athapuscow aulacogen, East Arm of Great Slave Lake, N.W.T., Canada. *Canadian Journal of Earth Science*, v. 21, pp. 1315-1324.

Cerny, P. and Trueman, D.L. 1985. Polylithionite from the rare-metal deposits of the Blachford Lake alkaline complex, N.W.T., Canada. *American Mineralogist*, v. 70, pp. 1127-1134.

Coulson, I. 1997. Post-magmatic alteration in eudialyte from the North Qôroq centre, South Greenland. *Mineralogical Magazine*, v. 61, pp. 99-109.

Davidson, A. 1972. Granite studies in the Slave Province; *in* Report of Field Activities, Part A, Geological Survey of Canada, Paper 72-1A, pp. 109-115.

Davidson, A. 1978. The Blachford Lake Intrusive Suite: an Aphebian Alkaline Plutonic Complex in the Slave Province, Northwest Territories; *in* Current Research, Part A, Geological Survey of Canada, Paper 78-1A, pp. 119-127.

Davidson, A. 1981. Petrochemistry of the Blatchford Lake Complex, District of Mackenzie, Geological Survey of Canada Open File 764.

Davidson, A. 1982. Petrochemistry of the Blachford Lake Complex Near Yellowknife, Northwest Territories; in Uranium in Granites (ed. Y.T. Maurice) Geological Survey of Canada Paper 81-23, p.71-79.

De St. Jorre, L. 1986. Economic mineralogy of the T zone, Thor Lake, N.W.T. M.Sc. thesis, University of Alberta, Edmonton.

Geisler, T., Ulonska, M., Schleicher, H., Pidgeon, R.T. and van Bronswijk, W. 2001. Leaching and differential recrystallization of metamict zircon under experimental hydrothermal conditions. *Contributions to Mineralogy and Petrology*, v. 141, pp. 53-65.

Gerasimovsky, V.I. 1969. Geochemistry of the Ilimaussaq Alkaline Massif (South-West Greenland), 174 p. Nauka Moskow (in Russian) (not seen; extracted from *Lithos*, v. 26, p. 167, 1990).

Hamala, R., Marks, M., Bruegmann, G., Siebel, W., Wenzel, T. and Markl, G. 2004. Crustal contamination of mafic magmas; evidence from a petrological, geochemical and Sr-Nd-Os-O isotopic study of the Proterozoic Isortoq dike swarm, South Greenland. *Lithos*, v. 74(3-4), pp. 199-232.

Harris, C. and Rickard, R.S. 1987. Rare-earth-rich eudialyte and dalyite from a peralkaline granite dyke at Straumsvola, Dronning Maud Land, Antarctica. *The Canadian Mineralogist*, v. 25, pp. 755-762.

Haas, J.R., Shock, E.L. and Sassani, D.C. 1995. Rare earth elements in hydrothermal systems: estimates of standard partial molal thermodynamic properties of aqueous complexes of the rare earth elements at high pressure and temperatures. *Geochimica et cosmochimica acta*, v. 59(21), pp. 4329-4350.

Hoffman, P.F. 1978. Tectonic history of Athapuscow Aulacogen (middle Precambrian), Great Slave Lake, Northwest Territories. *AAPG Bulletin*, v. 62(3), pp. 522-523.

Hoffmn, P.F. 1980. Wopmay Orogen: a Wilson cycle of early Proterozoic age in the Northwest of the Canadian Sheild. *In* The continental crust and its mineral deposits. *Edited by* D.W. Strangway. Geological Association of Canada, Special Paper 20, pp. 523-549.

Hoskin, P.W.O. 2005. Trace-element composition of hydrothermal zircon and the alteration of Hadean zircon from the Jack Hills, Australia. *Geochimica et Cosmochimica Acta*, v. 69(3), pp. 637-648.

Hoskin, P.W.O. and Schaltegger, U. 2003. The composition of zircon and igneous and metamorphic petrogenesis, pp. 27-55. *In* Reviews in Mineralogy and Geochemistry: Zircon, v. 53.

Hudson, K. 1987. The occurrence of gallium in the Lake Zone. Unpublished M.Sc. thesis, Queen's University, Kingston.

Johnsen, O., Ferraris, G., Gault, R.A., Grice, J.D., Kampf, A.R. and Pekov, I.V. 2003. The nomenclature of eudialyte-group minerals. *The Canadian Mineralogist*, v. 41, pp. 785-794.

Kempe, U., Gotze, J., Dandar, S. and Habermann, D. 1999. Magmatic and metasomatic processes during formation of the Nb-Zr-REE deposits Khaldzan Buregte and Tsakhir (Mongolian Altai): Indications from a combined CL-SEM study. *Mineralogical Magazine*, v. 63(2), pp. 165-177.

Keppler, H. 1993. Influence of fluorine on the enrichment of high field strength trace elements in granitic rocks. *Contributions to Mineralogy and Petrology*, v. 114, pp. 479-488.

Kerrich, R. and King, R. 1993. Hydrothermal zircon and baddeleyite in Val d'Or Archean meothermal gold deposits: characteristics, compositions, and fluid-inclusion properties, with implications for timing of primary gold mineralization. *Canadian Journal of Earth Sciences*, v. 30, pp. 2334-2352.

Kogarko, L.N. 1974. Role of volatiles. *In* The Alkaline Rocks. London: John Wiley & Sons.

Kogarko, L.N. 1990. Ore-forming potential of alkaline magmas (*in* Alkaline Igneous rocks and carbonatites). *Lithos*, v. 26(1-2), pp. 167-175.

Kogarko, L.N., Williams, C.T. and Woolley, A.R. 2002. Chemical evolution and petrogenetic implications of loparite in the layered, agpaitic Lovozero complex, Kola Peninsula, Russia. *Mineralogy and Petrology*, v. 74, pp. 1-24.

Kovalenko, V.I., Tsaryava, G.M., Goreglyad, A.V., Yarmolyuk, V.V., Troitsky, V.A., Hervig, R.L. and Farmer, G.L. 1995. The peralkaline granite-related Khaldzan-Buregtey rare metal (Zr, Nb, REE) deposit, western Mongolia. *Economic Geology*, v. 90, pp. 530-547.

Larsen, L.M. and Sørensen, H. 1987. The Ilimaussaq intrusion; progressive crystallization and formation of layering in an agpaitic magma. *Geological Society of Special Publications*, v. 30, pp. 473-488.

Lichtervelde, M., Melcher, F. and Wirth, R. 2009. Magmatic vs. hydrothermal origins for zircon associated with tantalum mineralization in the Tanco pegmatite, Manitoba, Canada. *American Mineralogist*, v. 94, pp. 439-450.

Linnen, R.L. 1998. The solubility of Nb-Ta-Zr-Hf-W in granitic melts with Li and Li + F; constraints for mineralization in rare metal granites and pegmatites. *Economic Geology*, v. 93, pp. 1013-1025.

Linnen, R.L. and Keppler, H. 2002. Melt composition control of Zr/Hf fractionation in magmatic processes. *Geochimica et Cosmochimica Acta*, v. 66(18), pp. 3293-3301.

Lumpkin, G.R. 2001. Alpha-decay and aqueous durability of actinide host phases in natural systems. *Journal of Nuclear Materials*, v. 298, pp. 136-166.

Markl, G., Marks, M., Schwinn, G. and Sommer, H. 2001. Phase Equilibrium Constraints on Intensive Crystallization Parameters of the Ilimaussaq Complex, South Greenland. *Journal of Petrology*, v. 42(12), pp. 2231-2258.

Marks, M and Markl, G. 2001. Fractionation and Assimilation Processes in the Alkaline Augite Syenite Unit of the Ilimaussaq Intrusion, South Greenland, as Deduced from Phase Equilibria. *Journal of Petrology*, v. 42(10), pp. 1947-1969.

Marks, M., Schilling, J., Coulson, I.M., Wenzel, T. and Markl, G. 2008. The Alkaline-Peralkaline Tamazeght Complex, High Atlas Mountains, Morocco: Mineral Chemistry and Petrological Constraints for Derivation from a Compostionally Heterogeneous Mantle Source. *Journal of Petrology*, v. 49(6), pp. 1097-1131.

Marks, M., Vennemann, T., Siebel, W. and Markl, G. 2003. Quantification of magmatic and hydrothermal processes in peralkaline syenite-alkali granite complex based on textures, phase equilibria, and stable and radiogenic isotopes. *Journal of Petrology*, v. 44(7), pp. 1247-1280.

Marks, M., Vennemann, T., Siebel, W. and Markl, G. 2004. Nd-, O- and H-isotopic evidence for complex, closed-system fluid evolution of the peralkaline Ilimaussaq intrusion, South Greenland. *Geochimica and Cosmochimica Acta*, v. 68, pp. 3379-3395.

Marr, R.A., Baker, D.R. and Williams-Jones, A.E. 1998. Chemical controls on the solubility of Zr-bearing phases in simplified peralkaline melts and application to the Strange Lake intrusion, Québec-Labrador. *The Canadian Mineralogist*, v. 36, pp. 1001-1008.

Martin, R.F. 2006. A-type granites of crustal origin ultimately result from open-system fenitization-type reactions in an extensional environment. *Lithos, v. 91, pp. 125-136.*

McLemore, V.T. and Modreski, P.J. 1990. Mineralogy and geochemistry of altered rocks associated with Lemitar carbonatites, central New Mexico, U.S.A. *Lithos*, v. 26, pp. 99-113.

Migdisov, A.A. and Williams-Jones, A.E. 2002. A spectrophotometric study of neodymium(III) complexation in chloride solutions. *Geochimica et Cosmochimica Acta*, v. 66(24), pp. 4311-4323.

Migdisov, A.A. and Williams-Jones, A.E. 2007. An experimental study of the solubility and speciation of neodymium (III) fluoride in F-bearing aqueous solutions. *Geochimica et Cosmochimica Acta*, v. 71, pp. 3056-3069.

Migdisov, A.A., Williams-Jones, A.E. and Wagner, T. 2009. An experimental study of the solubility and speciation of the Rae Earth Elements (III) in fluoride- and chloride-bearing aqueous solutions at temperatures up to 300°C. *Geochimica et Cosmochimica Acta*, v. 73, pp. 7087-7109.

Miller, R.R. 1986. Geology of the Strange Lake Alkalic Complex and the associated Zr-Y-Be-REE mineralization. Newfoundland Department of Mines and Energy, Mineral Development Division Report 86-1, pp. 11-19.

Olivo, G.R. and Williams-Jones, A.E. 1999. Hydrothermal REE-rich eudialyte from the Pilanesberg Complex, South Africa. *The Canadian Mineralogist*, v. 37, pp. 653-663.

Pederson, J.C. and Lecouteur, P.C. 1991. The Thor Lake beryllium-rare metal deposits, Northwest Territories (*in* Mineral deposits of the Slave Province, Northwest Territories (field trip 13)). Open-File Report – Geological Survey of Canada, pp. 128-136.

Peiffert, C., Nguyen-Trung, C. and Cuney, M. 1996. Uranium in granitic magmas: Part 2. Experimental determination of uranium solubility and fluid-melt partition coefficients in the uranium oxide-halpogranite-H_2O-NaX (X = Cl, F) system at 720-770°C, 2 kbar. *Geochimica et Cosmochimica Acta*, v. 60, pp. 1515-1529.

Pettke, T. Audétat, A., Schaltegger, U. and Heinrich, C.A. 2005. Magmatic-to-hydrothermal crystallization in the W-Sn mineralized Mole Granite (NSW, Australia): Part II. Evolving zircon and thorite trace element chemistry. *Chemical Geology*, v. 220, pp. 191-213.

Pidgeon, R.T., O'Neil, J.R. and Silver, L.T. 1966. Uranium and lead isotopic stability in a metamict zircon under experimentally hydrothermal conditions. *Science*, v. 154, pp. 1538-1540.

Pinckston, D.R. 1989. Mineralogy of the Lake Zone, Thor Lake, N.W.T. M.Sc. thesis, University of Alberta, Edmonton.

Pinckston, D.R. and Smith, D.G.W. 1995. Mineralogy of the Lake Zone, Thor Lake rare-metals deposit, N.W.T., Canada. *Canadian Journal of Earth Sciences*, v. 32, pp. 516-532.

Pupin, J.P. 1980. Zircon and granite petrology. *Contributions to Mineralogy and Petrology*, v. 73, pp. 207-220.

Rae, D.A. and Chambers, A.D. 1988. Metasomatism in the North Qôroq centre, South Greenland: cathodoluminescence and mineral chemistry of alkali feldspars. *Trans. R. Soc. Edinburgh, Earth Sci*, v. 79, pp. 1-12.

Rubin, J.N., Henry, C.D. and Price, J.G. 1989. Hydrothermal zircons and zircon overgrowths, Sierra Blanca Peaks, Texas. *American Mineralogist*, v. 74, pp. 865-869.

Rubin, J.N., Henry, C.D. and Price, J.G. 1993. The mobility of zirconium and other "immobile" elements during hydrothermal alteration. *Chemical Geology*, v. 110, pp. 29-47.

Salvi, S., Fontan, F., Monchoux, P., Williams-Jones, A.E. and Moine, B. 2000. Hydrothermal mobilization of high field strength elements in alkaline igneous systems: evidence from the Tamazeght Complex (Morocco). *Economic Geology*, v. 95, pp. 559-576.

Salvi, S. and Williams-Jones, A.E. 1990. The role of hydrothermal processes in the granite-hosted Zr, Y, REE deposit at Strange Lake, Québec-Labrador: Evidence from fluid inclusions. *Geochimica et Cosmochimica Acta*, v. 54, pp. 2403-2418.

Salvi, S. and Williams-Jones, A.E. 1992. Reduced orthomagmatic C-O-H-N-NaCl fluids in the Strange Lake rare-metal granitic complex, Québec-Labrador, Canada. *European Journal of Mineralogy*, v. 4, pp. 1155-1174.

Salvi, S. and Williams-Jones, A.E. 1995. Zirconosilicate phase relations in the Strange Lake (Lac Brisson) pluton, Québec-Labrador, Canada. *American Mineralogist*, v. 80, pp. 1031-1040.

Salvi, S. and Williams-Jones, A.E. 1996. The role of hydrothermal processes in concentrating high-field strength elements in the Strange Lake peralkaline complex, northeastern Canada. *Geochimica et Cosmochimica Acta*, v. 60, pp. 1917-1932.

Salvi, S. and Williams-Jones, A.E. 2005. Alkaline granite-syenite deposits (*in* Rare-element geochemistry and mineral deposits). *Short Course Notes – Geological Association of Canada*, v. 17, pp. 315-341.

Schaltegger, U. 2007. Hydrothermal zircon. *Elements*, v. 3, pp. 51 and 79.

Schaltegger, U., Pettke, T., Audetat, A., Reusser, E. and Heinrich. C.A. 2005. Magmatic-to-hydrothermal crystallization in the W-Sn mineralized Mole Granite (NSW, Australia) Part I: Crystallization of zircon and REE-phosphates over three million years – a geochemical and U-Pb geochronological study. *Chemical Geology*, v. 220, pp. 215-235.

Schmitt, A.K., Trumbull, R.G., Dulski, P. and Emmermann, R. 2002. Zr-Nb-REE Mineralization in Peralkaline Granites from the Amis Complex, Brandberg (Namibia): Evidence for Magmatic Pre-enrichment from Melt Inclusions. *Economic Geology*, v. 97, pp. 399-413.

Sinclair, W.D., Jambor, J.L. and Birkett, T.C. 1992. Rare earths and the potential for rare earth deposits in Canada. *Exploration and Mining Geology*, v. 1, pp. 265-281.

Sinclair, W.D. and Richardson, D.G. 1994. Studies of rare-metal deposits in the Northwest Territories. Bulletin – Geological Survey of Canada, 495:99.

Sinha, A.K., Wayne, D.M. and Hewitt, D.A. 1992. The hydrothermal stability of zircon preliminary experimental and isotopic studies. *Geochimica et Cosmochimica Acta*, v. 56, pp. 3551-3560.

Smith, D.G.W., de St. Jorre, L., Reed, S.J.B. and Long, J.V.P. 1991. Zonally metamictized and other zircons from Thor Lake, Northwest Territories. *The Canadian Mineralogist*, v. 29, pp. 301-309.

Sørensen, H. 1997. The agpaitic rocks – an overview. *Mineralogical Magazine*, v. 61, pp. 485-498.

Sørensen, H., Bohse, H. and Bailey, J.C. 2006. The origin and mode of emplacement of lujavrites in the Ilimaussaq alkaline complex, South Greenland. *Lithos, v. 91*, pp. 286-300.

Taylor, R.P. and Pollard, P.J. 1996. Rare earth element mineralization in peralkaline systems; the T-zone-REE-Y-Be deposit, Thor Lake, Northwest Territories, Canada (*in* Rare earth minerals; chemistry, origin and ore deposits). *Mineralogical Society Series*, v. 7, pp.167-192.

Trueman, D.L., Pederson, J.C., de St. Jorre, L. and Smith, D.G.W. 1988. The Thor Lake rare-metal deposits, Northwest Territories: pp. 280-290, *in* Taylor, R.P. and Strong, D.F. (ed.), Recent Advances in the Geology of Granite-Related Mineral Deposits, *Canadian Institute of Mining and Metallurgy*, Special Volume 39.

Ussing, N.V. 1912. Geology of the country around Julianehaab, Greenland. *Meddr Grønland*, v. 38, p. 376.

Wallace, G.M., Whalen, J.B. and Martin, R.F. 1990. Agpaitic and miaskitic nepheline syenites of the McGerrigle Plutonic Complex, Gaspé, Québec: an unusual petrological association. *The Canadian Mineralogist*, v. 28, pp. 251-266.

Watson, B.E. 1979. Zircon saturation in felsic liquids: experimental results and applications to trace element geochemistry. *Contributions to Mineralogy and Petrology*, v. 70, pp. 407-419.

Wood, S.A. 1990. The aqueous geochemistry of the rare-earth elements and yttrium 2. Theoretical predictions of speciation in hydrothermal solutions to 350°C at saturation water vapor pressure. *Chemical Geology*, v. 88, pp. 99-125.

APPENDIX A

Back-scattered electron images of selected mineralized samples from the Nechalacho deposit

Mineral abbreviations are after Chace (1956) and Kretz (1983).

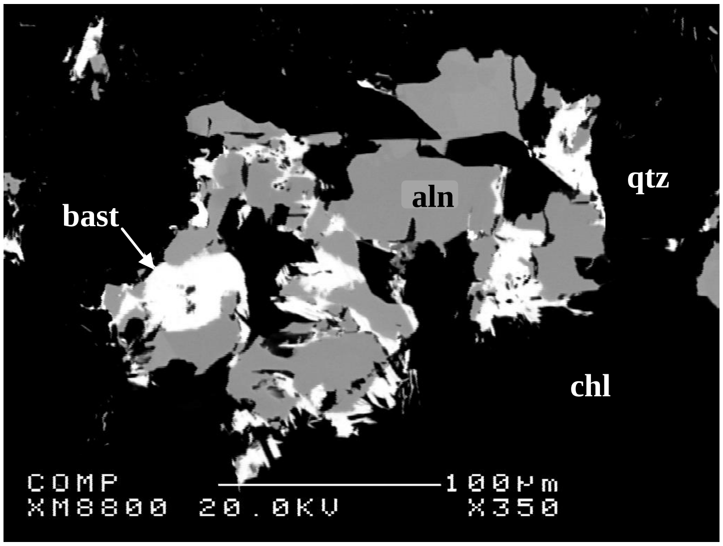

Figure 1

Sample L07-63: 117.9m

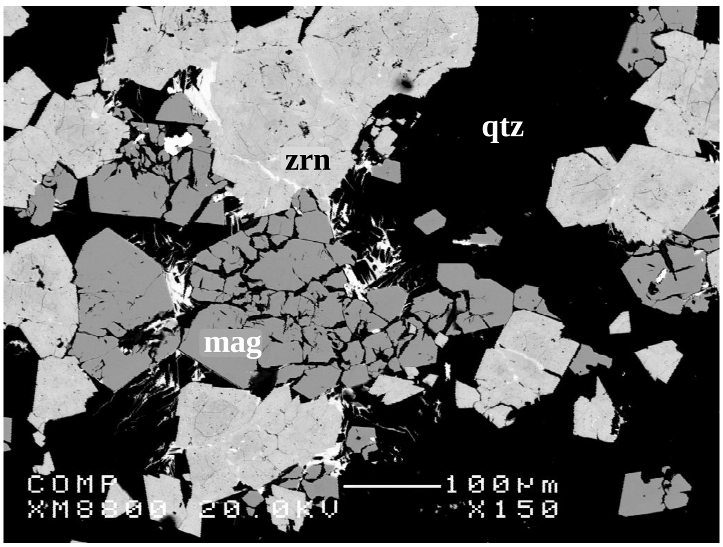

Figure 2

Sample L07-63: 117.9m

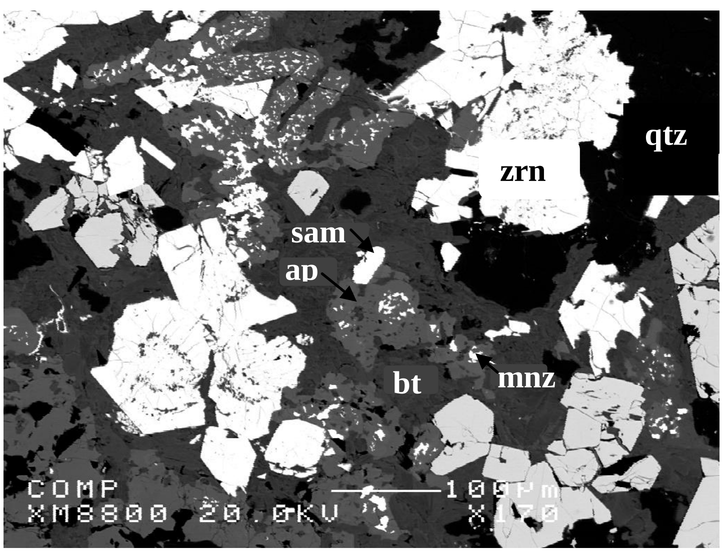

Figure 3

Sample L07-63: 117.9m

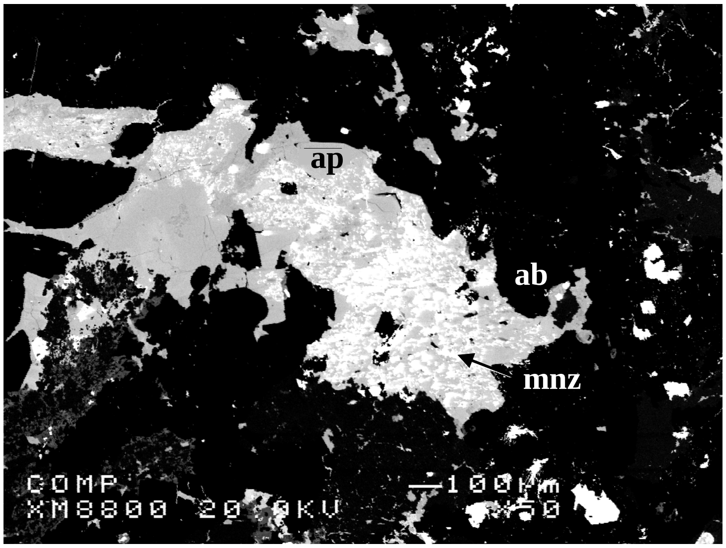

Figure 4

Sample L07-63: 96m

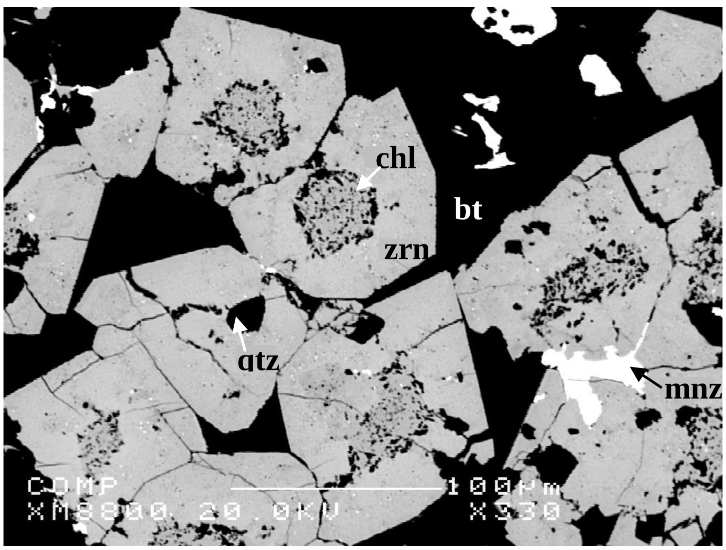

Figure 5

Sample L07-63: 131.1m

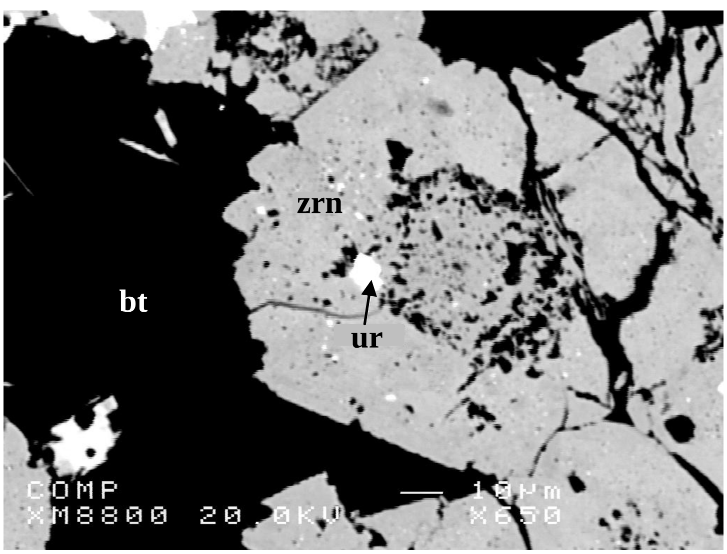

Figure 6

Sample L07-63: 131.1m

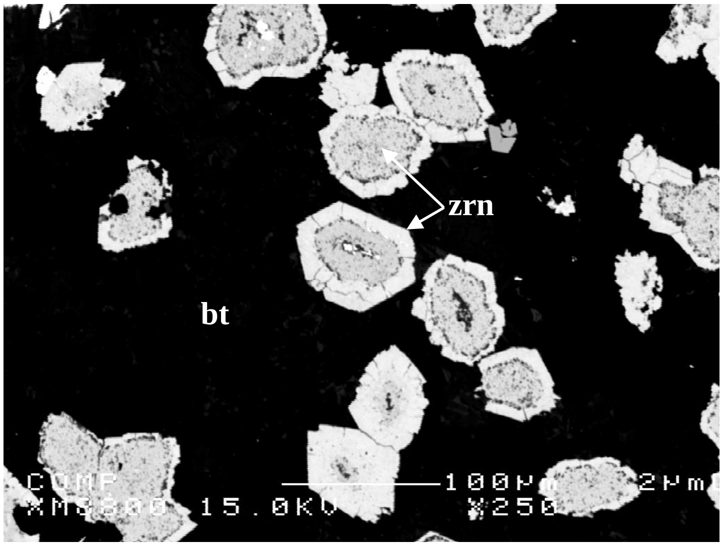

Figure 7

Sample L07-63: 171.2m

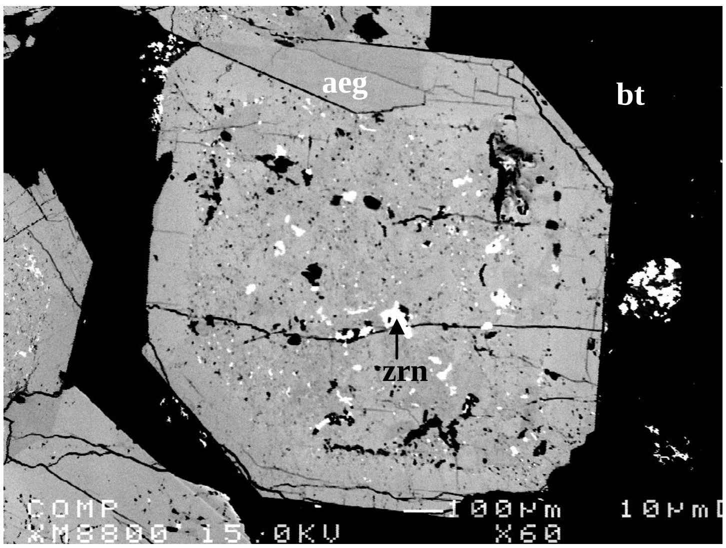

Figure 8

Sample 85/L6: 1039

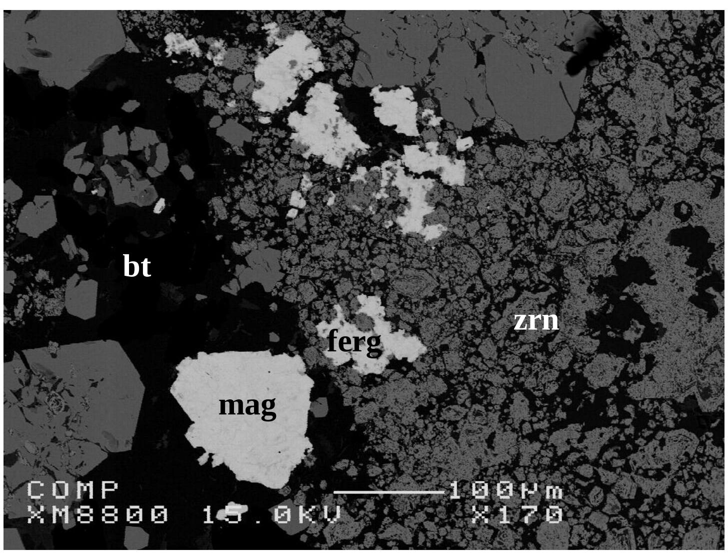

Figure 9

Sample L07-63: 131.1m

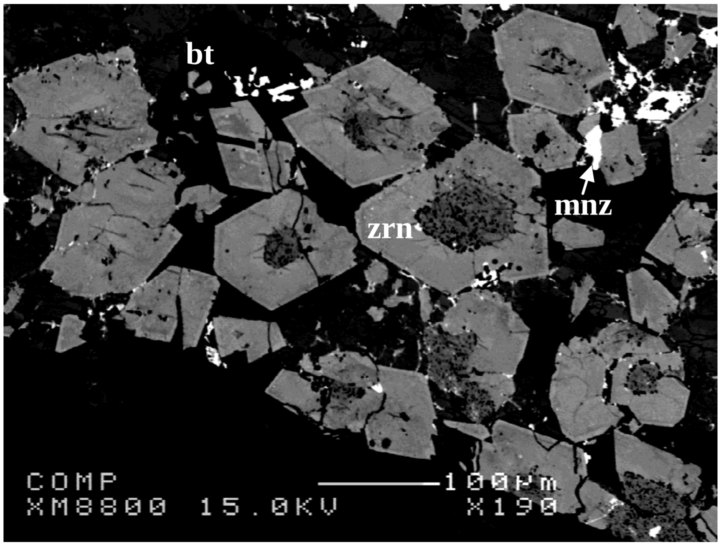

Figure 10

Sample L07-53: 77.25m

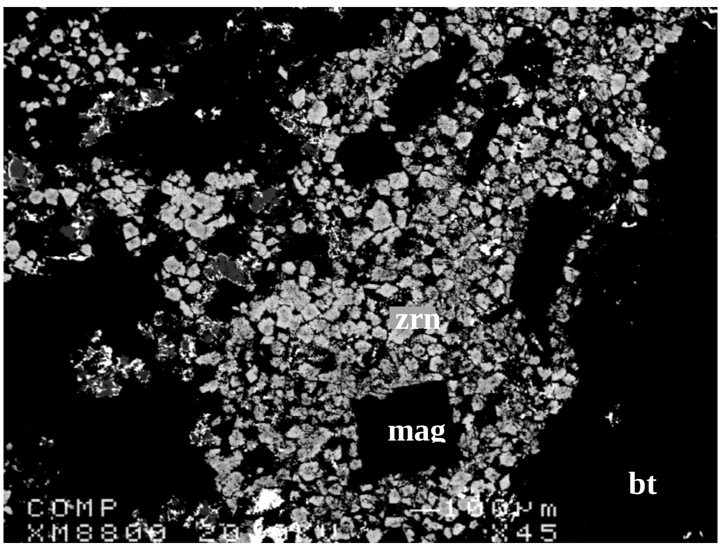

Figure 11

Sample L07-55: 100.1m

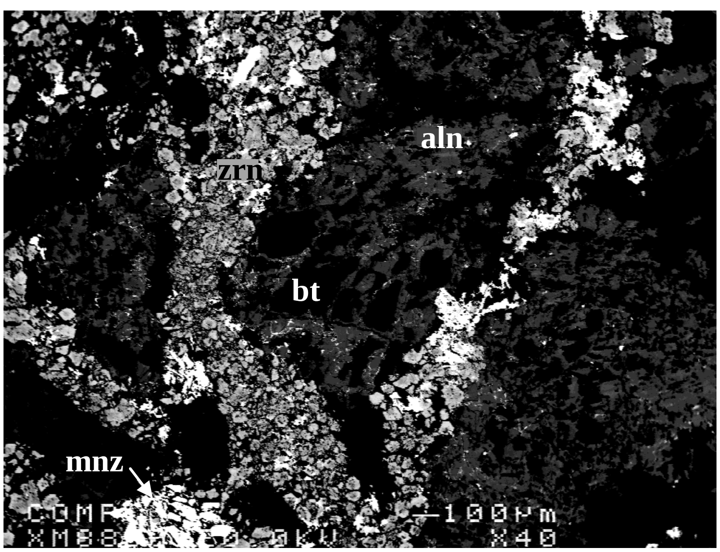

Figure 12

Sample L07-55: 100.1m

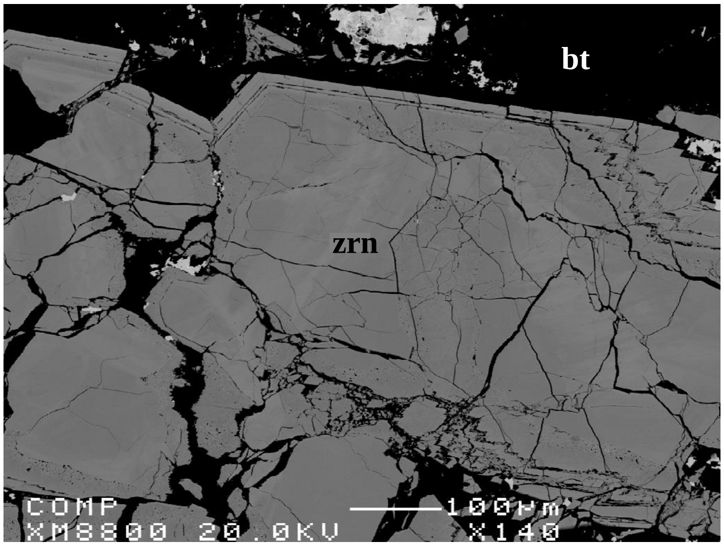

Figure 13

Sample L07-55: 105m

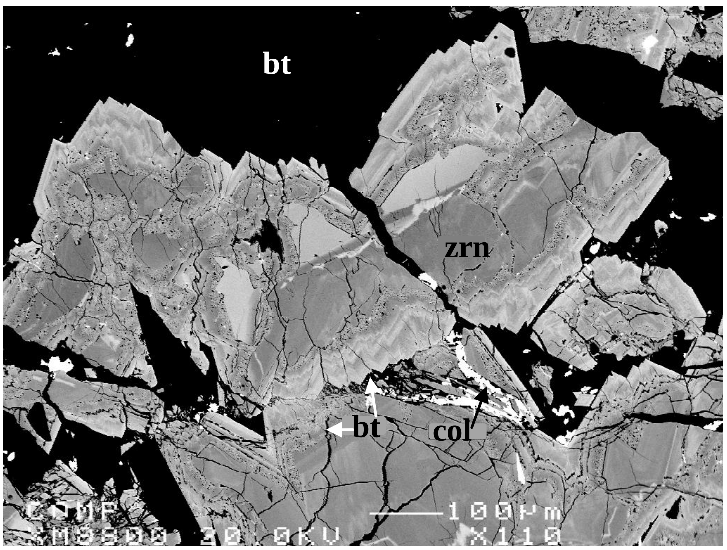

Figure 14

Sample L07-55: 105m

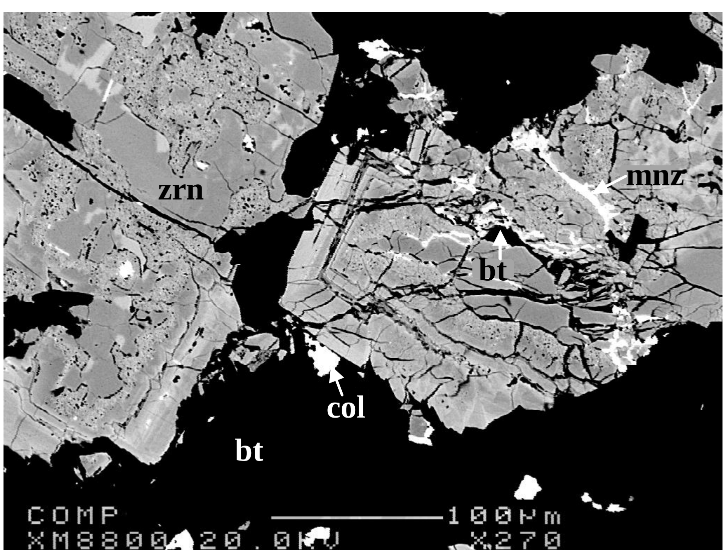

Figure 15

Sample L07-55: 105m

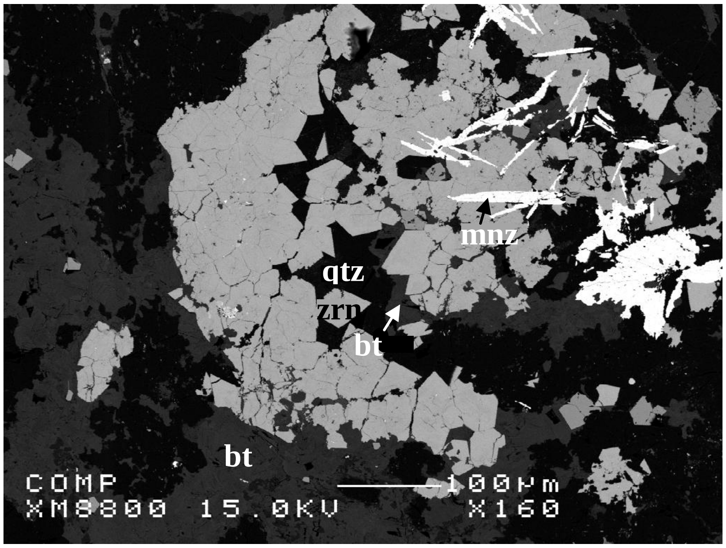

Figure 16

Sample L07-63: 44m

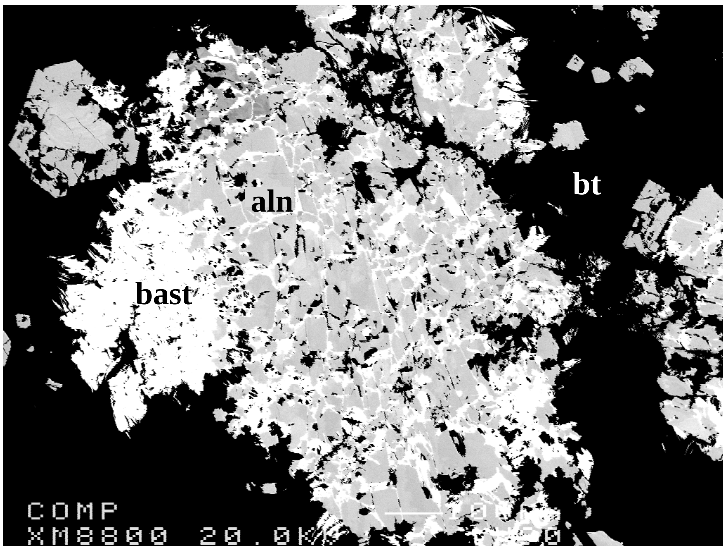

Figure 17

Sample L08-118: 50.7m

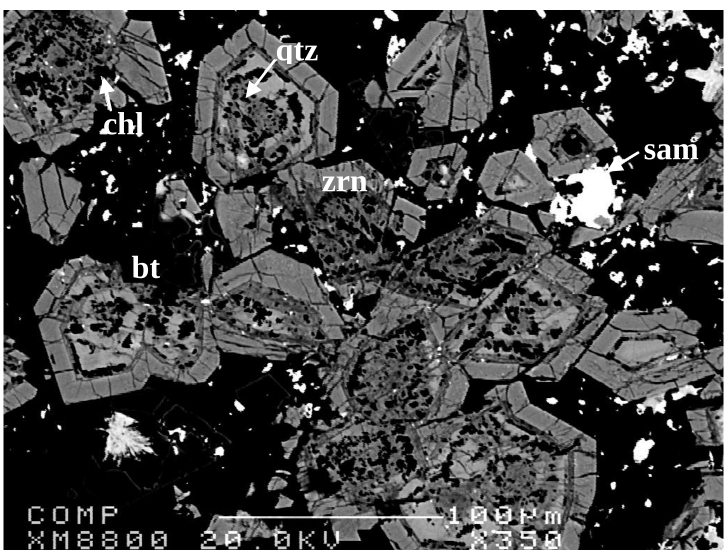

Figure 18

Sample L08-118: 50.7m

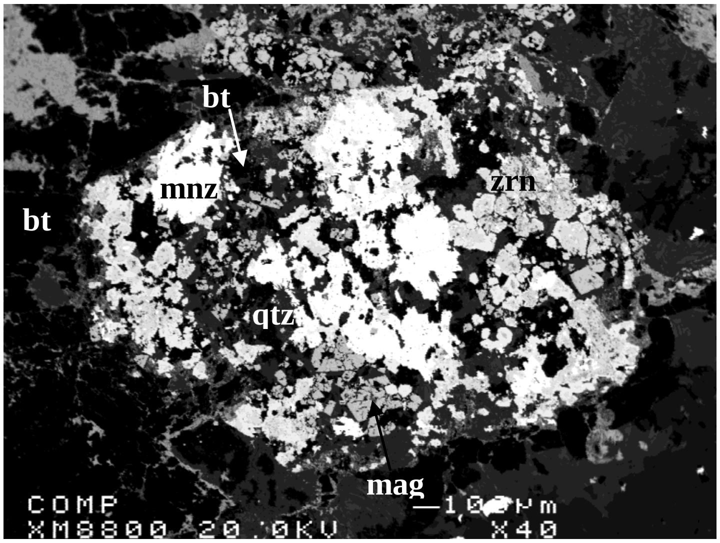

Figure 19

Sample L08-118: 130.7m

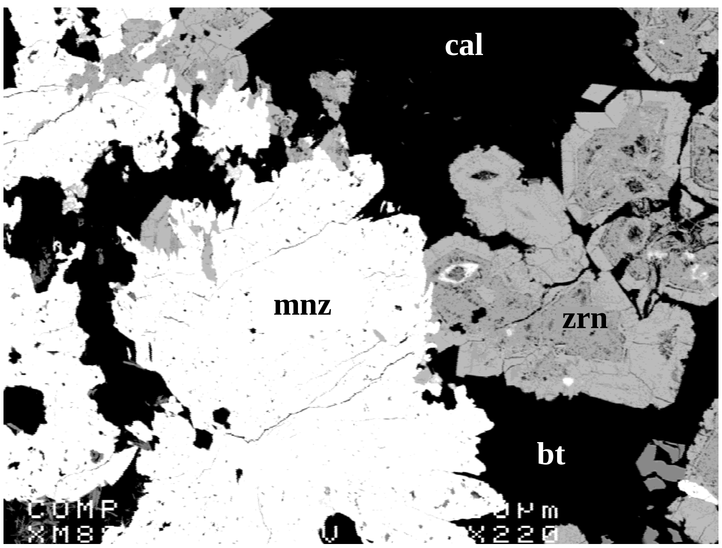

Figure 20

Sample L08-118: 130.7m

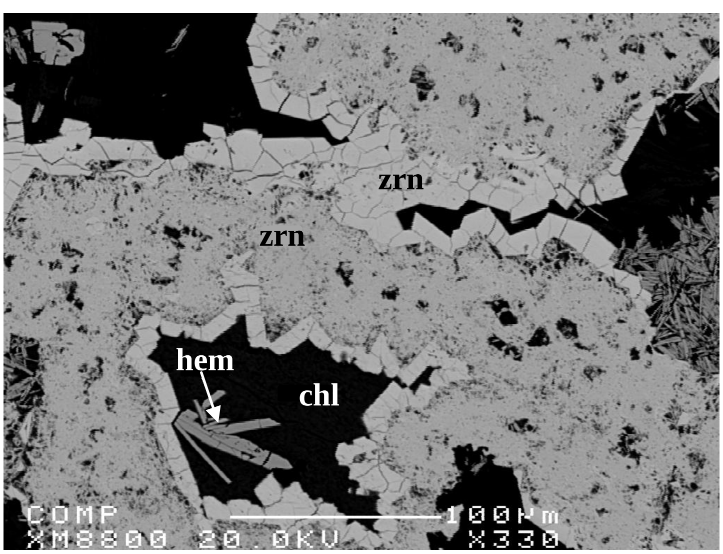

Figure 21

Sample L08-118: 130.7m

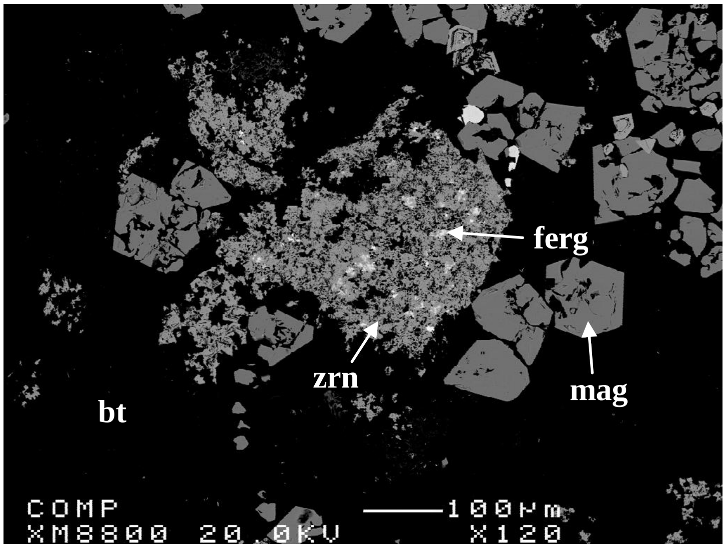

Figure 22

Sample L08-118: 155.5m

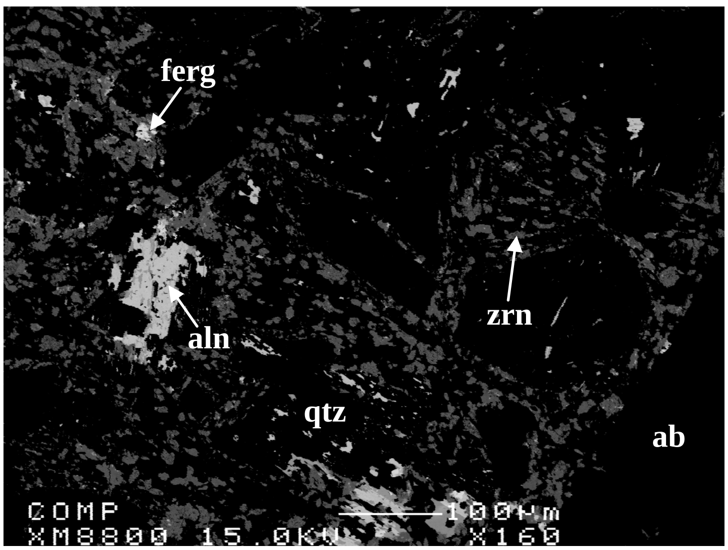

Figure 23

Sample L09-155: 176m

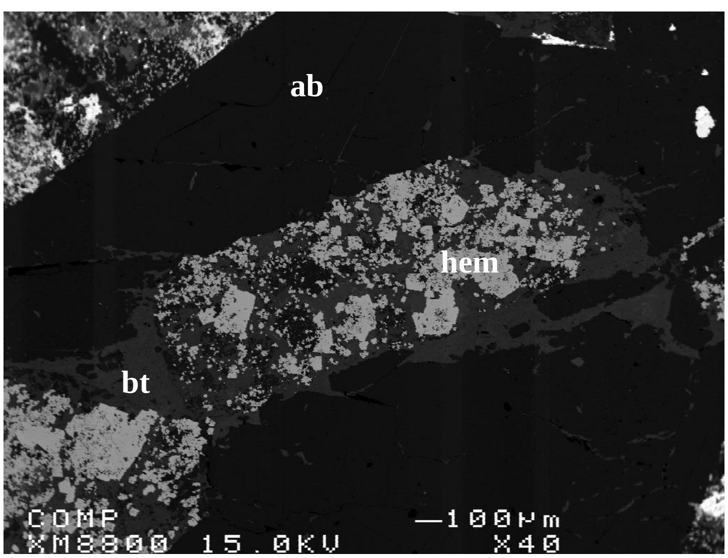

Figure 24

Sample L09-155: 176m

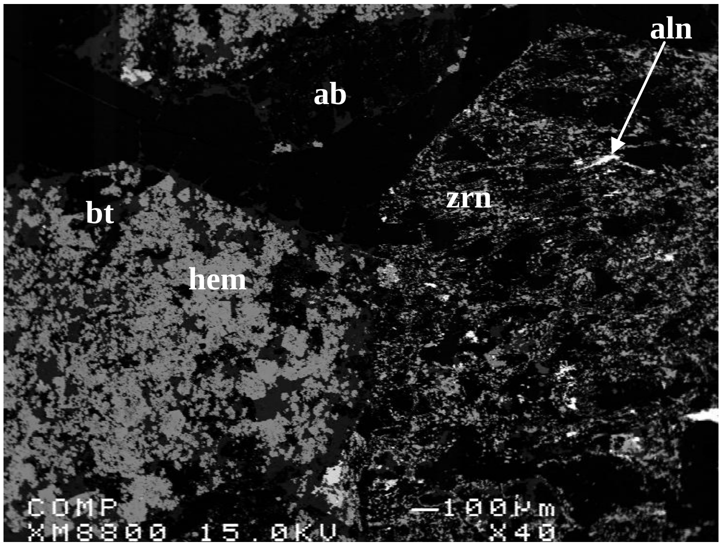

Figure 25

Sample L09-155: 176m

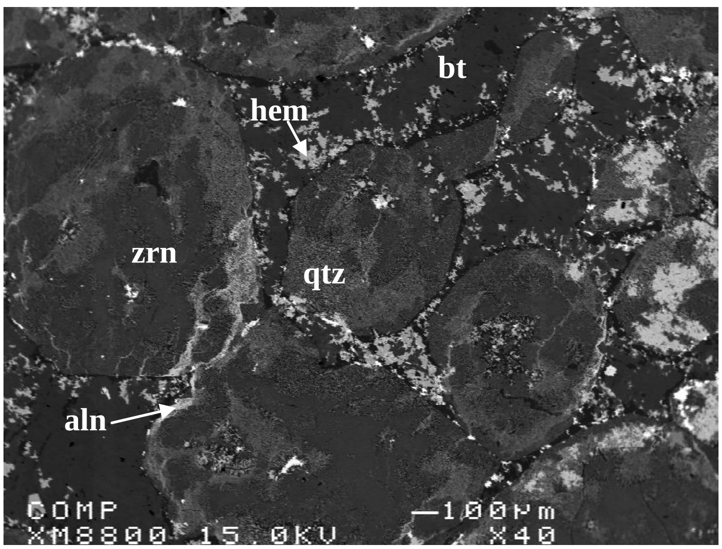

Figure 26

Sample L09-155: 176m

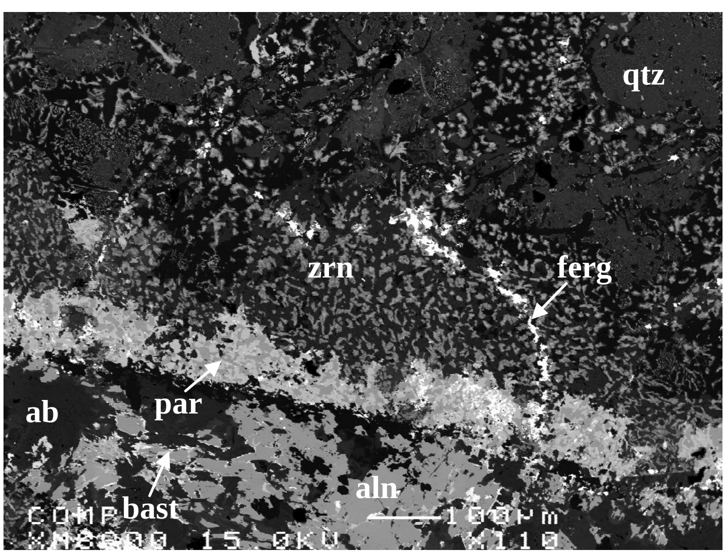

Figure 27

Sample L09-155: 176m

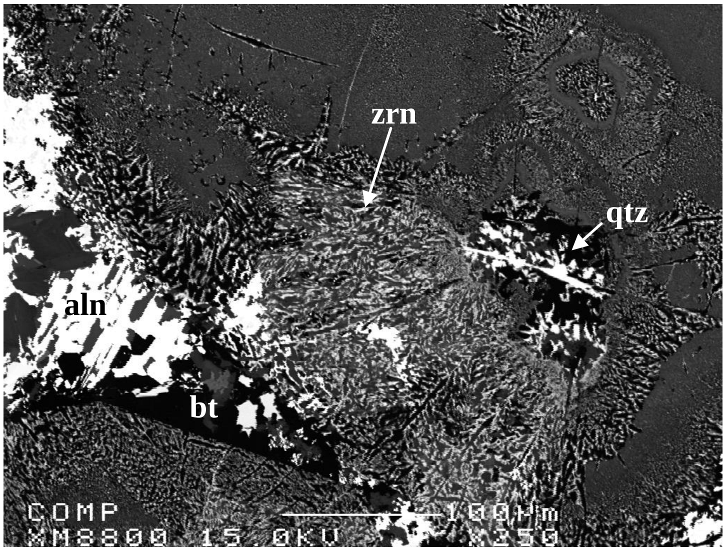

Figure 28

Sample L09-155: 188.25m

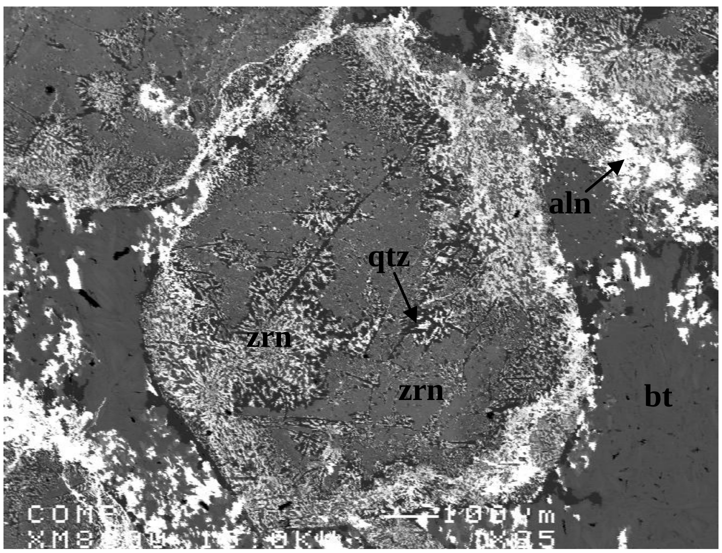

Figure 29

Sample L09-155: 188.25m

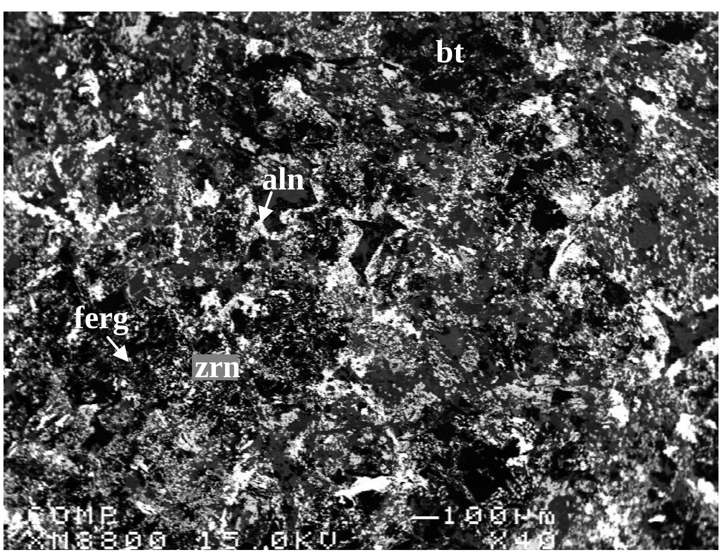

Figure 30

Sample L09-155: 189.6m

APPENDIX B

Back-scattered electron images and electron microprobe element maps of zircon in selected samples from the Nechalacho deposit

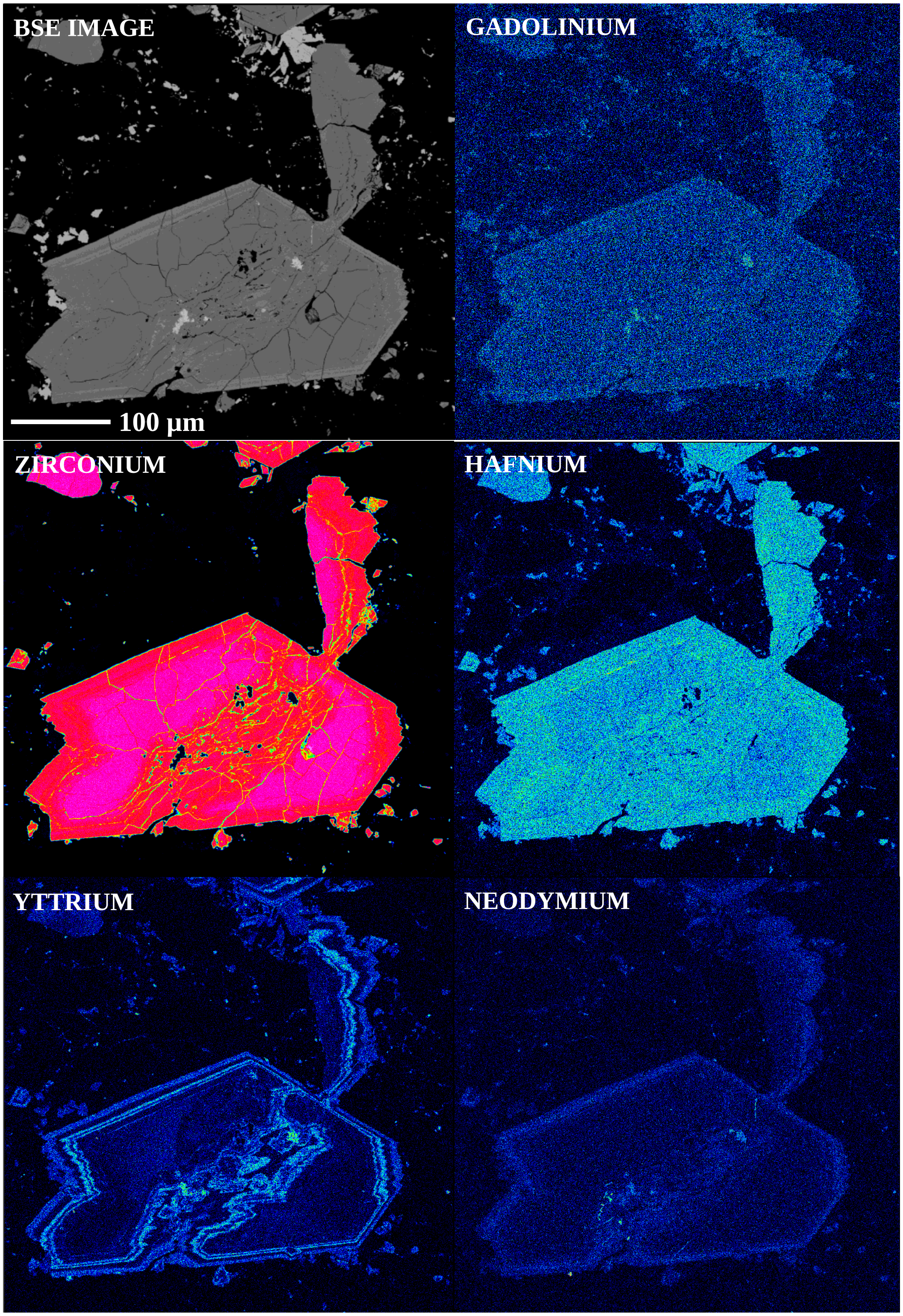

Figure 1. Electron microprobe element maps of a zircon crystal from sample L07-55: 105m, showing the distribution of gadolinium, zirconium, hafnium, yttrium and neodymium.

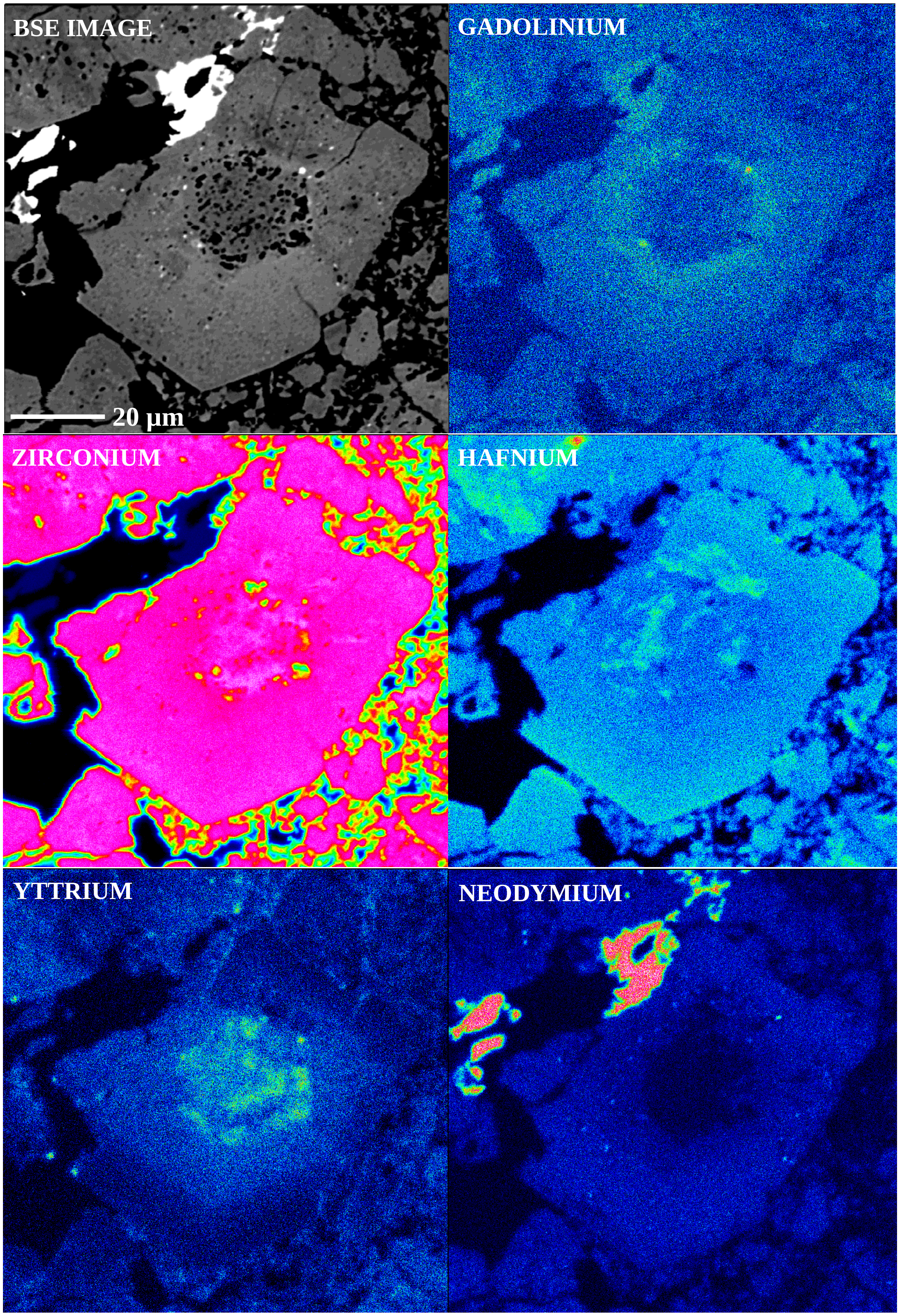

Figure 2. Electron microprobe element maps of a zircon crystal from sample L07-63: 131.1m, showing the distribution of gadolinium, zirconium, hafnium, yttrium and neodymium.

APPENDIX C

Electron microprobe analyses of zircon

No.	Sample	Ce_2O_3	Nd_2O_3	Sm_2O_3	Gd_2O_3	Dy_2O_3	Er_2O_3	Yb_2O_3	Y_2O_3	ZrO_2	HfO_2	SiO_2	Nb_2O_5	F	CaO	FeO	Al_2O_3	Total
1	L08-118: 130.7	0.06	0.16	0.13	0.44	0.55	0.34	0.16	3.64	56.64	0.99	29.06	0.93	0.12	0.28	1.99	0.15	96.21
2	L08-118: 130.7	0.14	0.44	0.31	0.58	0.55	0.24	0.10	2.70	59.19	1.24	28.15	1.82	0.93	0.15	0.69	0.19	97.63
3	L08-118: 130.7	0.06	b.d.	b.d.	0.33	0.50	0.35	0.24	3.54	57.98	1.39	29.54	0.46	0.18	0.23	0.72	0.12	96.51
4	L08-118: 130.7	0.11	0.43	0.32	0.65	0.67	0.25	0.14	3.23	58.83	1.07	28.50	2.53	0.90	0.12	0.85	0.17	98.97
5	L08-118: 130.7	0.05	b.d.	b.d.	0.38	0.46	0.25	0.16	2.96	57.71	1.08	29.25	1.64	0.53	0.31	1.02	0.22	96.50
6	L08-118: 130.7	b.d.	0.12	b.d.	0.38	0.48	0.34	0.25	3.88	56.07	0.98	29.06	0.43	b.d.	0.26	2.21	0.16	95.66
7	L08-118: 130.7	0.13	0.30	0.16	0.65	0.82	0.30	0.15	4.21	58.18	1.05	27.75	2.08	1.15	0.15	1.00	0.20	98.37
8	L08-118: 130.7	0.08	b.d.	b.d.	0.52	0.60	0.39	0.24	4.16	55.24	1.56	28.40	0.79	0.38	0.35	0.83	0.24	94.63
9	L08-118: 130.7	0.09	b.d.	0.19	0.74	0.96	0.36	0.23	5.05	57.27	1.00	27.75	1.66	1.14	0.11	0.36	0.18	97.36
10	L08-118: 130.7	b.d.	b.d.	b.d.	0.29	0.45	0.39	0.26	4.10	57.37	0.95	29.49	0.25	b.d.	0.23	0.81	0.20	95.72
11	L08-118: 130.7	0.05	0.17	0.12	0.77	0.98	0.40	0.23	5.35	56.31	1.01	27.78	1.47	1.05	0.13	0.57	0.11	96.90
12	L08-118: 130.7	0.07	b.d.	b.d.	0.40	0.55	0.49	0.31	4.83	55.09	0.98	28.34	0.37	0.15	0.32	0.66	0.18	93.98
13	L08-118: 130.7	0.06	b.d.	b.d.	1.01	1.74	0.74	0.29	7.24	54.90	0.90	27.41	1.09	1.23	0.09	0.17	0.06	97.37
14	L08-118: 130.7	b.d.	b.d.	b.d.	0.35	0.59	0.37	0.26	4.40	54.91	1.13	28.76	0.41	0.26	0.29	2.66	0.21	95.28
15	L08-118: 130.7	0.17	0.85	0.56	0.49	0.32	0.08	b.d.	0.89	59.01	1.19	28.69	2.78	0.75	0.20	0.72	0.16	97.16
16	L08-118: 130.7	0.05	b.d.	b.d.	0.40	0.64	0.49	0.31	5.51	55.04	1.01	28.97	0.28	0.25	0.34	0.63	0.20	95.27
17	L08-118: 130.7	0.22	1.01	0.75	0.69	0.30	b.d.	b.d.	0.40	60.14	0.98	28.04	3.13	0.80	0.18	0.55	0.14	97.40
18	L07-63: 171.2	b.d.	b.d.	b.d.	0.14	0.18	b.d.	0.14	1.40	57.79	1.04	30.73	0.15	b.d.	0.07	5.96	0.11	98.18
19	L07-63: 171.2	0.16	0.86	1.00	1.07	0.46	0.09	0.11	0.77	59.41	1.07	29.17	3.02	0.67	0.11	1.53	0.07	100.00
20	L07-63: 171.2	b.d.	b.d.	b.d.	0.18	0.22	0.15	0.17	1.60	59.89	1.00	30.97	0.01	b.d.	0.09	1.79	0.13	96.70
21	L07-63: 171.2	0.13	0.85	0.60	0.62	0.42	0.15	0.16	1.29	59.48	1.21	29.09	3.86	0.47	0.34	0.57	0.09	99.83
22	L07-63: 171.2	b.d.	b.d.	b.d.	0.07	0.16	0.10	0.14	1.33	60.23	1.11	31.22	b.d.	b.d.	0.10	3.50	0.15	98.68
23	L07-63: 171.2	b.d.	0.12	0.34	0.60	0.30	b.d.	0.13	0.94	54.46	1.11	31.14	1.69	b.d.	0.09	5.74	1.47	98.68
24	L07-63: 171.2	b.d.	b.d.	b.d.	b.d.	0.15	0.06	0.20	1.48	56.71	0.91	32.23	b.d.	0.13	b.d.	4.21	0.49	97.04
25	L07-63: 171.2	b.d.	b.d.	0.43	0.99	0.57	b.d.	0.12	1.54	53.39	0.95	32.31	2.02	0.26	0.06	6.06	0.92	100.28
26	L07-63: 171.2	b.d.	b.d.	b.d.	0.11	0.16	b.d.	0.11	1.11	57.24	1.04	30.72	b.d.	b.d.	0.05	4.77	0.78	96.47
27	L07-63: 171.2	0.13	0.69	0.57	0.65	0.38	0.14	0.14	1.29	57.27	1.23	31.05	3.70	0.39	0.15	0.56	0.11	98.82
28	L07-55: 100.1	0.26	0.74	0.66	0.83	0.34	0.06	b.d.	0.80	59.18	1.48	29.32	1.62	0.71	0.23	1.13	0.32	97.89
29	L07-55: 100.1	0.30	1.33	0.51	0.37	0.19	0.10	b.d.	0.59	60.52	1.19	29.40	2.36	0.66	0.10	0.32	0.08	98.51
30	L07-55: 100.1	0.05	b.d.	b.d.	0.13	b.d.	0.06	b.d.	0.69	62.84	0.99	31.39	0.13	0	0.12	0.90	0.06	98.02
31	L07-55: 100.1	0.29	1.21	0.45	0.33	0.23	0.08	0.09	0.70	61.17	1.04	29.41	3.57	0.36	0.09	0.74	0.06	100.24
32	L07-55: 100.1	0.58	0.59	0.41	0.48	0.21	0.08	b.d.	0.68	59.46	1.65	29.74	0.75	0.66	0.35	1.36	0.40	97.87
33	L07-55: 100.1	0.33	1.50	0.64	0.44	0.17	b.d.	b.d.	0.28	61.44	1.02	29.42	2.39	0.71	0.11	0.33	0.04	99.09
34	L07-55: 100.1	0.14	0.25	0.22	0.23	b.d.	b.d.	b.d.	b.d.	61.02	2.22	30.06	0.70	0.46	0.28	0.95	0.31	97.13
35	L07-55: 100.1	0.20	1.12	0.75	0.76	0.36	0.07	b.d.	0.64	60.33	0.99	29.40	3.22	0.72	0.07	0.55	0.06	99.54
36	L07-55: 100.1	0.24	0.64	0.44	0.42	0.12	0.06	b.d.	0.27	61.23	2.09	29.67	1.33	0.59	0.23	0.74	0.27	98.51
37	L07-55: 100.1	0.29	1.43	0.56	0.43	0.22	0.06	0.12	0.62	61.12	1.07	29.45	2.07	0.73	0.11	0.49	0.05	99.20

38	L07-55: 100.1	b.d.	b.d.	b.d.	0.13	0.14	b.d.	b.d.	0.90	62.46	0.75	31.40	b.d.	b.d.	0.07	1.53	0.21	98.37
39	L07-55: 100.1	0.22	1.30	0.70	0.64	0.25	0.07	b.d.	0.61	60.43	1.04	29.41	2.84	0.80	0.09	0.53	0.07	99.41
40	L07-55: 100.1	0.31	1.19	0.69	0.62	0.21	0.06	b.d.	0.55	59.89	1.15	29.51	1.93	0.40	0.21	1.93	0.20	99.36
41	L07-55: 100.1	0.18	0.71	0.38	0.38	0.13	0.09	0.15	0.77	59.95	1.67	29.66	1.73	0.38	0.17	1.59	0.14	98.52
42	L07-55: 100.1	0.31	0.81	0.46	0.43	0.18	b.d.	b.d.	0.38	59.27	1.83	29.86	1.23	0.47	0.23	1.63	0.33	97.61
43	L07-55: 100.1	0.14	0.80	0.36	0.33	0.26	0.22	0.37	1.52	59.44	1.16	29.59	2.98	0.81	0.06	0.63	0.08	99.04
44	L07-55: 100.1	0.25	0.60	0.53	0.58	0.36	0.07	b.d.	0.86	60.81	0.82	28.30	1.44	0.89	0.28	0.83	0.28	97.31
45	L07-55: 100.1	0.17	0.58	0.26	0.18	0.14	0.11	0.24	0.85	60.61	1.15	29.58	2.98	0.67	0.16	0.74	0.09	98.87
46	L07-55: 100.1	0.11	0.21	0.22	0.47	0.35	0.10	b.d.	1.29	60.58	1.65	28.92	0.68	0.92	0.32	1.08	0.37	97.39
47	L07-55: 100.1	0.35	1.47	0.64	0.34	0.11	0.11	0.08	0.36	60.43	0.95	29.41	2.42	0.49	0.12	0.26	0.09	97.92
48	L07-55: 100.1	0.15	0.21	0.19	0.43	0.28	0.07	b.d.	0.79	58.66	1.84	28.07	1.17	1.16	2.23	0.82	0.33	96.56
49	L07-55: 100.1	0.52	1.01	0.26	0.17	b.d.	0.09	0.13	0.53	61.36	1.22	28.45	2.07	1.00	0.22	0.58	0.09	97.95
50	L07-55: 100.1	0.04	b.d.	b.d.	0.15	0.21	0.11	b.d.	1.34	61.68	0.75	31.80	b.d.	b.d.	0.05	1.35	0.25	98.40
51	L07-55: 100.1	0.21	1.21	0.69	0.57	0.21	0.10	0.08	0.76	61.12	0.86	29.37	3.12	0.68	0.08	0.42	0.06	99.76
52	L07-55: 100.1	0.18	0.47	0.50	0.74	0.35	0.09	b.d.	0.81	60.06	1.67	28.55	1.75	0.63	0.22	0.61	0.17	97.11
53	L07-55: 100.1	0.31	1.32	0.48	0.31	0.14	0.06	0.08	0.42	60.84	1.15	29.62	2.54	0.33	0.13	0.53	0.10	98.71
54	L07-55: 100.1	0.30	1.30	0.66	0.51	0.23	0.06	0.09	0.61	61.62	0.92	29.31	2.64	0.74	0.10	0.37	0.06	99.81
55	L07-55: 100.1	0.46	1.06	0.23	0.19	0.17	0.08	0.08	0.53	60.43	1.18	28.41	3.09	0.98	0.23	0.64	0.11	98.07
56	L07-55: 100.1	0.14	0.23	0.23	0.43	0.26	0.07	b.d.	0.96	61.29	1.42	28.77	0.91	0.94	0.34	1.31	0.34	97.86
57	L07-55: 100.1	0.35	1.30	0.42	0.41	0.19	b.d.	b.d.	0.59	60.67	1.03	28.36	2.60	0.92	0.18	0.62	0.11	97.95
58	L07-55: 100.1	0.28	1.03	1.18	1.52	0.66	0.10	b.d.	1.34	59.36	0.90	28.39	1.68	1.17	0.08	0.58	0.12	98.45
59	L07-55: 100.1	0.32	1.30	0.44	0.35	0.14	0.06	0.08	0.47	61.52	1.16	29.06	1.97	0.68	0.16	0.56	0.09	98.50
60	L07-55: 100.1	0.22	0.79	1.05	1.62	0.75	0.11	b.d.	1.80	58.43	0.85	28.16	1.77	1.30	0.09	0.39	0.16	97.55
61	L07-55: 100.1	0.21	1.16	0.76	0.60	0.27	0.09	0.11	0.88	60.22	0.92	29.10	2.80	0.86	0.08	0.28	0.05	98.57
62	L07-55: 100.1	0.24	0.45	0.38	0.41	0.23	0.06	b.d.	0.42	60.76	1.94	29.01	1.12	0.62	0.32	0.68	0.23	97.10
63	L07-55: 100.1	0.24	1.33	0.80	0.62	0.21	0.09	b.d.	0.74	60.90	0.90	29.38	2.36	0.72	0.09	0.44	0.06	99.23
64	L07-55: 125.4	0.03	0.15	0.31	0.64	0.36	0.27	0.72	2.57	59.53	1.38	31.75	1.32	0.14	0.06	0.71	0.15	100.34
65	L07-55: 125.4	0.13	0.55	0.65	0.90	0.48	0.12	0.23	2.30	57.78	1.10	30.53	3.57	0.33	b.d.	1.10	0.19	100.34
66	L07-55: 125.4	b.d.	b.d.	b.d.	b.d.	0.06	0.12	0.36	1.05	60.03	1.34	31.33	b.d.	b.d.	0.04	3.39	0.05	98.03
67	L07-55: 125.4	b.d.	b.d.	b.d.	b.d.	b.d.	0.19	0.45	1.33	62.40	1.35	32.22	b.d.	b.d.	b.d.	1.03	0.06	99.41
68	L07-55: 125.4	0.05	b.d.	b.d.	0.13	0.18	0.24	0.60	2.11	61.08	1.26	31.92	b.d.	b.d.	0.04	1.30	0.03	99.23
69	L07-55: 125.4	b.d.	0.24	0.29	0.73	0.70	0.32	0.53	2.98	56.69	1.23	30.89	3.22	0.35	0.06	1.79	0.19	100.34
70	L07-55: 125.4	b.d.	b.d.	b.d.	b.d.	b.d.	0.07	0.38	0.91	58.14	1.20	32.17	0.23	b.d.	0.07	4.70	0.11	98.26
71	L07-55: 125.4	b.d.	b.d.	b.d.	b.d.	b.d.	0.07	0.35	0.83	57.33	1.32	31.71	0.08	b.d.	0.05	5.45	0.04	97.64
72	L07-55: 125.4	b.d.	b.d.	b.d.	0.12	b.d.	0.15	0.41	0.90	62.83	1.23	31.25	b.d.	b.d.	0.04	0.43	0.03	97.68
73	L07-55: 125.4	0.15	0.23	0.12	0.20	0.18	0.14	0.37	0.96	61.51	1.88	31.56	0.45	0.17	0.06	0.80	0.17	99.07
74	L08-118: 50.7	0.23	0.55	0.71	1.71	1.04	0.34	0.17	2.65	58.88	1.44	26.82	0.56	1.29	0.13	0.40	0.21	97.37
75	L08-118: 50.7	0.31	1.51	0.64	0.34	0.11	b.d.	b.d.	b.d.	61.75	0.73	28.88	2.58	0.79	0.15	0.27	0.08	98.28
76	L08-118: 50.7	0.19	0.48	0.70	1.54	0.84	0.24	0.16	2.32	57.72	1.42	27.05	0.63	0.94	0.36	1.10	0.28	96.51
77	L08-118: 50.7	0.19	1.31	0.98	0.56	0.16	b.d.	b.d.	b.d.	61.37	0.84	29.33	2.21	0.69	0.10	0.45	0.04	98.56

78	L08-118: 50.7	0.22	0.71	0.98	1.81	0.73	0.22	0.11	1.94	59.41	1.58	27.17	0.65	1.17	0.15	0.33	0.24	97.59
79	L08-118: 50.7	0.21	1.14	0.64	0.44	b.d.	b.d.	b.d.	0.02	61.25	0.69	29.42	3.46	0.80	0.15	0.45	0.12	98.98
80	L08-118: 50.7	0.12	0.26	0.21	0.84	0.86	0.35	0.23	3.10	54.41	1.24	27.00	0.69	0.68	0.29	1.52	0.39	92.82
81	L08-118: 50.7	0.29	1.50	0.70	0.45	b.d.	b.d.	b.d.	b.d.	60.92	0.71	29.29	3.10	0.58	0.15	0.41	0.07	98.43
82	L08-118: 50.7	0.20	0.70	0.87	1.44	0.57	0.34	0.35	2.34	58.61	1.54	27.19	0.77	1.06	0.13	0.27	0.16	96.82
83	L08-118: 50.7	0.25	1.29	0.73	0.39	b.d.	b.d.	b.d.	b.d.	61.72	0.78	29.40	2.95	0.54	0.12	0.30	0.07	98.85
84	L08-118: 50.7	0.21	0.83	1.06	1.52	0.54	0.19	0.22	1.91	58.73	1.43	27.82	1.16	1.12	0.12	0.46	0.20	97.74
85	L08-118: 50.7	0.30	1.45	0.71	0.38	b.d.	b.d.	b.d.	b.d.	60.83	0.75	29.01	2.89	0.82	0.14	0.48	0.09	98.11
86	L08-118: 50.7	0.18	0.47	0.62	1.69	1.00	0.32	0.15	2.70	58.43	1.50	26.49	1.16	1.22	0.20	0.50	0.25	96.94
87	L08-118: 50.7	0.18	1.18	1.07	0.81	0.23	0.09	b.d.	0.61	60.59	0.83	29.72	2.68	0.64	0.10	0.48	0.04	99.52
88	L08-118: 106.6	0.24	0.66	0.89	0.96	0.22	b.d.	b.d.	0.40	60.59	1.30	29.53	1.58	0.42	0.15	0.51	0.16	98.17
89	L08-118: 106.6	0.21	1.20	0.86	0.67	0.13	0.06	b.d.	0.48	60.95	0.87	29.17	3.48	0.39	0.09	0.55	0.08	99.47
90	L08-118: 106.6	0.84	0.42	b.d.	0.12	0.13	0.06	b.d.	0.57	62.39	0.84	30.41	2.01	0.70	0.15	0.61	b.d.	99.73
91	L08-118: 106.6	0.26	1.09	0.53	0.40	0.12	b.d.	b.d.	0.22	60.57	1.23	28.75	2.62	0.51	0.30	1.05	0.11	98.22
92	L08-118: 106.6	0.08	b.d.	b.d.	0.04	b.d.	b.d.	b.d.	b.d.	63.25	0.76	30.63	4.47	0.28	0.17	0.63	b.d.	100.49
93	L08-118: 106.6	0.25	1.04	0.62	0.48	0.20	0.09	0.12	0.65	60.97	1.13	28.93	2.46	0.47	0.18	0.47	0.18	98.56
94	L07-63: 54.2	0.13	0.53	0.94	1.50	0.66	0.16	b.d.	2.34	58.52	0.79	28.61	2.01	0.83	0.12	0.38	0.12	98.13
95	L07-63: 54.2	0.14	0.65	1.06	1.41	0.55	0.10	b.d.	1.99	58.35	0.74	28.20	1.97	0.85	0.11	0.19	0.12	96.94
96	L07-63: 54.2	0.16	0.52	0.82	1.52	0.71	0.15	b.d.	2.73	58.10	0.80	28.75	1.72	0.90	0.11	0.17	0.13	97.76
97	L07-63: 54.2	0.28	1.24	0.73	0.43	0.21	0.06	b.d.	0.61	60.44	1.15	27.90	2.02	0.90	0.26	0.27	0.12	96.90
98	L07-63: 54.2	0.14	0.35	0.82	1.64	0.81	0.15	b.d.	2.78	58.45	0.78	28.47	1.91	1.00	0.14	0.39	0.15	98.32
99	L07-63: 54.2	0.16	0.82	0.95	0.88	0.33	0.08	0.13	1.68	57.03	1.00	26.79	1.85	0.50	0.25	0.83	0.10	94.07
100	L07-63: 54.2	0.18	0.68	0.65	0.57	0.35	0.16	0.13	2.31	57.84	0.99	27.60	2.18	0.89	0.17	0.37	0.12	95.41
101	L07-63: 54.2	0.13	0.47	0.81	1.56	0.88	0.14	b.d.	3.18	58.14	0.76	27.34	1.67	0.86	0.06	0.21	0.12	96.83
102	L07-63: 54.2	0.21	0.88	0.97	0.82	0.32	b.d.	0.07	1.22	57.01	0.94	26.22	1.64	0.43	0.33	0.57	0.10	92.55
103	L07-63: 54.2	0.13	0.92	0.87	0.75	0.25	b.d.	b.d.	0.78	56.79	1.15	29.64	2.85	0.57	0.19	0.73	0.17	96.22
104	L07-63: 54.2	0.09	b.d.	b.d.	0.40	0.49	0.36	0.18	2.93	57.86	1.79	27.86	1.50	0.45	0.64	0.56	0.38	95.83
105	L07-63: 54.2	0.15	0.61	0.88	0.82	0.39	0.11	0.17	1.88	56.19	1.03	27.01	1.94	0.60	0.25	0.39	0.18	93.25
106	L07-63: 54.2	0.24	1.06	0.85	0.61	0.14	b.d.	b.d.	0.47	59.72	1.18	27.82	2.27	0.80	0.29	0.33	0.31	96.34
107	L07-63: 117.9	0.10	0.15	b.d.	b.d.	b.d.	b.d.	b.d.	b.d.	64.00	1.10	30.62	0	0.61	0.17	1.05	b.d.	97.78
108	L07-63: 117.9	0.46	1.02	0.27	0.25	b.d.	b.d.	0.14	0.40	62.20	1.24	28.09	3.06	0.63	0.22	0.38	0.10	98.93
109	L07-63: 117.9	0.17	0.44	0.44	0.92	0.53	0.15	0.14	1.51	60.42	0.89	28.34	1.54	0.99	0.15	0.43	0.18	97.33
110	L07-63: 117.9	0.39	1.11	0.41	0.33	0.12	0.07	0.09	0.50	61.13	1.08	28.81	3.01	0.79	0.24	0.23	0.11	98.68
111	L07-63: 117.9	0.34	0.54	0.16	0.13	b.d.	b.d.	b.d.	b.d.	52.72	1.43	10.14	1.29	0.69	0.16	0.39	0.09	68.00
112	L07-63: 117.9	0.42	0.86	0.21	0.12	b.d.	b.d.	0.22	0.57	61.08	1.23	28.77	2.90	0.69	0.20	0.38	0.08	98.14
113	L07-63: 117.9	0.09	0.00	b.d.	b.d.	b.d.	b.d.	b.d.	b.d.	63.71	1.51	29.95	0.00	0.58	0.26	0.68	0.03	96.82
114	L07-63: 117.9	0.53	0.93	0.20	0.13	b.d.	b.d.	0.15	0.23	61.92	1.33	28.50	2.52	0.50	0.22	0.24	0.07	98.03
115	L07-63: 117.9	0.33	0.67	0.26	0.18	b.d.	b.d.	b.d.	0.08	61.92	1.53	28.44	1.54	0.58	0.41	0.53	0.22	96.76
116	L07-63: 117.9	0.53	0.91	0.17	0.17	b.d.	b.d.	b.d.	0.09	61.68	1.30	28.72	3.23	0.40	0.27	0.34	0.08	98.52
117	L07-63: 131.1	0.05	b.d.	b.d.	0.29	0.28	0.11	0.11	2.03	60.89	0.72	30.39	0.35	0.14	0.33	0.40	0.08	96.44

118	L07-63: 131.1	0.26	1.09	0.86	0.69	0.22	b.d.	b.d.	0.44	60.95	0.96	28.75	3.18	0.33	0.20	0.41	0.11	98.79
119	L07-63: 131.1	0.26	1.27	0.76	0.59	0.16	b.d.	b.d.	0.14	61.37	1.03	28.74	2.84	0.35	0.22	0.19	0.09	98.40
120	L07-63: 131.1	0.35	0.99	0.25	0.17	b.d.	b.d.	b.d.	b.d.	62.46	1.27	28.23	3.32	0.40	0.28	0.45	0.12	98.51
121	L07-63: 131.1	0.15	0.72	0.65	0.69	0.21	b.d.	b.d.	0.80	60.57	0.91	29.00	3.09	0.41	0.23	0.35	0.07	97.95
122	L07-63: 131.1	0.24	0.79	0.39	0.33	0.12	b.d.	b.d.	0.34	62.00	1.06	29.30	2.57	0.34	0.16	0.58	0.08	98.53
123	L07-63: 131.1	0.16	0.20	0.26	0.42	0.24	0.08	b.d.	1.80	60.04	1.21	29.21	1.02	0.72	0.30	0.76	0.17	96.69
124	L07-63: 131.1	0.33	1.18	0.41	0.34	0.13	b.d.	b.d.	b.d.	62.66	1.14	28.43	3.02	0.42	0.19	0.34	0.06	98.91
125	L07-63: 131.1	0.17	0.39	0.33	0.48	0.14	b.d.	0.07	0.39	61.84	1.80	30.17	1.75	0.56	0.22	0.39	0.12	99.07
126	L07-63: 131.1	0.27	1.25	0.52	0.38	b.d.	b.d.	b.d.	b.d.	61.84	1.00	28.37	3.84	0.35	0.21	0.41	0.08	98.85
127	L07-63: 175.5	b.d.	0.02	b.d.	0.45	0.38	0.18	0.18	2.76	60.98	0.63	30.37	0.92	0.19	0.10	1.83	0.09	99.39
128	L07-63: 175.5	0.25	1.33	0.85	0.67	b.d.	b.d.	b.d.	0.34	60.48	1.08	29.28	3.84	0.55	0.36	0.29	0.09	99.67
129	L07-63: 175.5	b.d.	0.06	b.d.	0.36	0.37	0.12	0.13	2.87	59.16	0.68	29.13	0.18	b.d.	0.09	2.28	0.04	95.87
130	L07-63: 175.5	0.30	1.32	0.84	0.61	0.17	0.06	b.d.	0.26	61.24	1.12	27.69	2.57	0.70	0.17	0.15	0.06	97.26
131	L07-63: 175.5	0.07	0.16	0.42	0.61	0.31	0.10	b.d.	0.68	49.80	0.69	10.44	0.39	0.27	0.19	0.29	0.14	64.69
132	L07-63: 175.5	0.26	1.00	0.55	0.32	0.11	b.d.	b.d.	0.38	60.70	1.15	27.62	3.15	0.60	0.20	0.31	0.09	96.55
133	L07-63: 175.5	0.17	1.40	0.78	0.88	0.53	0.15	0.09	1.23	57.14	1.15	27.39	6.98	0.37	0.16	b.d.	0.06	98.96
134	L07-63: 175.5	0.60	1.20	0.20	0.17	b.d.	b.d.	b.d.	0.47	59.44	1.66	29.21	3.57	0.70	0.28	0.39	0.17	98.25
135	L07-63: 175.5	0.00	b.d.	b.d.	0.14	b.d.	b.d.	0.12	1.33	61.05	0.60	30.62	b.d.	0.12	0.11	3.10	0.17	97.94
136	L07-63: 175.5	0.43	1.31	0.32	0.17	b.d.	b.d.	b.d.	0.10	61.28	1.11	28.70	4.52	0.52	0.40	0.34	0.08	99.46
137	L08-118: 155.5	0.27	0.48	b.d.	0.15	b.d.	b.d.	b.d.	0.13	60.56	1.52	28.96	2.16	0.43	0.17	0.31	0.11	95.78
138	L08-118: 155.5	2.99	3.47	2.73	4.39	1.06	0.10	0.10	5.76	39.27	1.01	19.92	0.78	4.22	8.84	0.24	0.15	96.06
139	L08-118: 155.5	0.55	1.08	0.23	0.26	0.11	b.d.	b.d.	0.20	60.62	1.16	29.08	3.17	0.66	0.16	0.32	0.19	98.11
140	L08-118: 155.5	12.15	6.45	1.33	1.06	0.15	b.d.	b.d.	0.87	34.07	0.65	18.16	b.d.	5.41	9.53	2.91	b.d.	98.23
141	L08-118: 155.5	0.37	0.67	0.17	0.18	0.13	b.d.	b.d.	0.21	61.87	1.42	30.49	2.36	0.30	0.11	0.32	0.15	99.08
142	L08-118: 155.5	0.87	1.37	0.36	0.28	0.16	b.d.	b.d.	0.37	59.38	1.41	29.48	2.96	0.54	0.17	0.28	0.30	98.57
143	L08-118: 155.5	0.07	0.17	0.20	1.11	1.31	0.29	0.07	3.92	57.66	1.11	27.71	0.89	0.32	0.11	1.67	0.11	97.39
144	L08-118: 155.5	0.32	1.17	0.37	0.31	b.d.	b.d.	b.d.	0.10	61.78	1.02	29.13	2.93	0.60	0.17	0.37	0.07	98.67
145	L08-118: 157.2	0.08	0.28	0.25	1.14	1.23	0.12	b.d.	3.13	55.80	1.06	26.65	0.87	0.98	0.10	6.79	0.16	98.68
146	L08-118: 157.2	0.33	1.13	0.25	0.18	b.d.	b.d.	b.d.	b.d.	61.36	1.10	28.73	2.89	0.56	0.15	0.23	0.07	97.22
147	L08-118: 157.2	b.d.	b.d.	b.d.	0.36	0.26	0.11	b.d.	1.89	56.84	1.09	30.55	0.32	0.18	0.44	1.22	0.48	94.64
148	L08-118: 157.2	0.41	1.42	0.31	0.11	b.d.	b.d.	b.d.	b.d.	61.33	1.11	29.50	3.19	0.19	0.22	0.25	0.06	98.67
149	L08-118: 157.2	0.29	1.27	0.32	0.23	b.d.	b.d.	b.d.	0.07	61.46	1.08	29.17	3.13	0.61	0.12	0.32	0.07	98.28
150	L08-118: 157.2	0.10	0.27	0.27	1.10	1.29	0.32	0.08	4.51	58.35	1.20	25.96	0.53	1.17	0.10	b.d.	0.16	95.56
151	L08-118: 157.2	0.23	1.13	0.28	0.23	b.d.	b.d.	b.d.	0.28	60.72	1.10	29.50	3.39	0.51	0.11	0.25	0.09	98.25
152	L08-118: 157.2	0.19	0.93	0.34	0.28	b.d.	b.d.	b.d.	0.63	60.96	0.99	29.60	3.19	0.55	0.10	0.49	0.06	98.60
153	L08-118: 157.2	0.03	b.d.	b.d.	0.18	0.12	b.d.	b.d.	1.29	54.41	1.07	28.01	0.12	b.d.	0.08	15.97	0.05	101.83
154	L08-118: 157.2	0.30	1.10	0.42	0.21	b.d.	b.d.	b.d.	0.56	61.65	1.15	29.74	2.02	0.59	0.11	0.34	0.06	98.69
155	L08-118: 157.2	b.d.	0.03	b.d.	0.30	0.42	0.18	b.d.	2.52	58.86	1.10	30.32	0.47	0.14	0.22	0.56	0.08	95.92
156	L08-118: 157.2	0.20	0.96	0.40	0.27	b.d.	b.d.	b.d.	0.67	60.97	1.10	29.31	3.26	0.41	0.11	0.32	0.07	98.32
157	L08-118: 157.2	b.d.	b.d.	b.d.	0.22	0.24	0.15	b.d.	2.41	60.31	1.14	30.49	0.19	b.d.	0.13	1.41	0.08	97.81

158	L08-118: 157.2	0.28	1.28	0.43	0.30	0.19	b.d.	b.d.	0.20	61.74	1.05	28.84	3.04	0.52	0.15	0.52	0.06	98.84
159	L08-118: 157.2	0.07	0.23	0.20	1.06	1.34	0.46	0.17	5.46	58.54	1.17	25.60	0.34	1.15	0.11	b.d.	0.12	96.10
160	L08-118: 157.2	0.30	1.21	0.39	0.25	b.d.	b.d.	b.d.	b.d.	60.77	1.09	28.84	2.94	0.48	0.14	0.30	0.08	97.06
161	L07-55: 105	b.d.	b.d.	b.d.	0.00	b.d.	0.08	0.11	0.10	66.07	1.28	32.54	b.d.	b.d.	b.d.	b.d.	b.d.	100.36
162	L07-55: 105	0.44	1.33	0.30	0.20	0.13	0.06	b.d.	0.19	61.61	1.29	29.34	1.93	0.82	0.17	0.51	0.09	98.54
163	L07-55: 105	b.d.	b.d.	b.d.	b.d.	b.d.	b.d.	b.d.	b.d.	66.21	1.15	32.15	b.d.	b.d.	0.04	0.12	b.d.	100.02
164	L07-55: 105	0.35	1.13	0.29	0.22	0.16	0.08	b.d.	0.24	62.16	1.30	29.23	2.13	0.68	0.22	0.51	0.15	99.03
165	L07-55: 105	b.d.	b.d.	b.d.	b.d.	b.d.	b.d.	b.d.	b.d.	61.15	1.83	28.86	0.35	0.24	0.82	0.86	0.19	94.56
166	L07-55: 105	0.10	0.48	0.33	0.66	0.67	0.21	b.d.	1.97	59.77	1.26	29.12	1.50	0.67	0.13	0.29	0.23	97.98
167	L07-55: 105	b.d.	b.d.	b.d.	b.d.	b.d.	b.d.	b.d.	b.d.	63.57	1.78	29.03	0.71	0.28	0.49	0.83	0.35	97.14
168	L07-55: 105	0.36	0.88	0.15	b.d.	b.d.	b.d.	b.d.	b.d.	60.58	1.28	28.88	1.95	0.66	0.41	0.70	0.36	96.61
169	L07-55: 105	0.17	b.d.	b.d.	b.d.	b.d.	b.d.	b.d.	b.d.	63.71	1.59	28.61	2.06	0.20	0.60	1.06	0.14	98.37
170	L07-55: 105	0.14	0.59	0.36	0.58	0.76	0.20	b.d.	1.78	59.76	1.27	29.02	1.39	0.63	0.11	0.54	0.16	97.61
171	L07-55: 105	b.d.	b.d.	b.d.	b.d.	b.d.	0.09	0.11	0.12	66.40	1.71	32.52	b.d.	b.d.	b.d.	b.d.	b.d.	101.23
172	L07-55: 105	0.40	1.00	0.22	0.15	b.d.	b.d.	b.d.	b.d.	60.81	1.34	28.74	1.71	0.72	0.35	0.51	0.28	96.84
173	L07-55: 105	b.d.	b.d.	b.d.	b.d.	b.d.	b.d.	b.d.	b.d.	66.19	1.58	32.58	b.d.	b.d.	b.d.	b.d.	b.d.	100.54
174	L07-55: 105	0.32	1.06	0.35	0.20	0.18	b.d.	b.d.	0.18	60.97	1.25	28.66	1.65	0.64	0.34	0.60	0.21	97.07
175	L07-63: 34.3	0.07	b.d.	b.d.	b.d.	b.d.	b.d.	b.d.	0.16	61.00	0.76	30.32	b.d.	0.25	0.28	1.22	0.06	94.44
176	L07-63: 34.3	0.43	1.27	0.71	0.42	0.15	0.10	b.d.	0.40	59.99	0.94	28.49	b.d.	0.30	0.11	0.22	0.14	93.85
177	L07-63: 34.3	0.32	1.52	0.52	0.34	0.15	0.06	0.08	0.32	59.75	1.08	28.45	b.d.	0.19	0.13	0.34	0.10	93.55
178	L07-63: 34.3	0.47	0.51	0.11	b.d.	b.d.	b.d.	0.15	b.d.	60.18	0.81	30.12	b.d.	0.17	0.25	0.56	0.19	93.79
179	L07-63: 34.3	0.27	1.27	0.50	0.42	b.d.	0.14	b.d.	0.41	59.92	1.19	28.74	b.d.	0.13	0.13	0.32	0.11	94.24
180	L07-63: 34.3	0.44	0.75	0.17	b.d.	b.d.	b.d.	b.d.	0.07	60.12	1.35	28.69	b.d.	0.12	0.25	0.82	0.21	93.49
181	L07-63: 34.3	0.08	1.37	0.87	0.62	b.d.	0.09	0.10	0.42	58.79	0.99	28.36	b.d.	0.42	0.09	0.13	0.09	92.63
182	L07-63: 34.3	0.30	0.86	0.36	0.25	b.d.	b.d.	0.10	0.26	59.46	0.99	28.62	b.d.	0.23	0.32	0.71	0.30	92.83
183	L07-63: 34.3	0.18	1.19	0.67	0.52	b.d.	0.29	b.d.	0.41	59.50	1.25	28.22	b.d.	0.23	0.12	0.35	0.11	93.58
184	L07-63: 34.3	0.34	1.25	0.54	0.40	b.d.	b.d.	b.d.	0.45	60.07	1.24	28.59	b.d.	0.26	0.12	0.26	0.10	94.10
185	L07-63: 34.3	0.21	0.19	0.11	b.d.	b.d.	b.d.	b.d.	b.d.	59.99	1.24	28.98	b.d.	0.33	0.37	0.66	0.26	92.64
186	L07-63: 34.3	0.39	1.45	0.34	0.36	b.d.	b.d.	b.d.	0.33	60.11	1.25	28.58	b.d.	0.21	0.13	0.27	0.09	93.80
187	L07-63: 34.3	0.19	1.47	0.48	0.36	b.d.	0.06	0.08	0.38	59.78	1.11	28.94	b.d.	0.20	0.10	0.35	0.10	93.86
188	L07-53: 77.25	b.d.	b.d.	b.d.	0.29	0.34	b.d.	0.22	2.44	55.85	1.75	28.87	b.d.	0.47	0.28	2.39	0.61	93.66
189	L07-53: 77.25	0.22	1.43	0.39	0.48	b.d.	0.19	b.d.	0.18	60.54	0.86	27.99	b.d.	0.23	0.14	0.34	0.10	93.35
190	L07-53: 77.25	b.d.	1.25	0.53	b.d.	b.d.	0.11	0.11	0.24	59.78	0.73	27.82	b.d.	0.21	0.13	0.12	0.09	91.39
191	L07-53: 77.25	0.18	0.12	b.d.	0.28	0.42	b.d.	b.d.	3.13	56.85	0.49	28.50	b.d.	0.26	0.51	1.12	0.18	92.18
192	L07-53: 77.25	0.32	1.21	0.52	0.41	b.d.	b.d.	b.d.	0.14	60.62	0.84	28.27	b.d.	0.14	0.13	0.23	0.08	93.13
193	L07-53: 77.25	0.24	0.78	0.38	0.29	0.38	b.d.	b.d.	0.11	60.54	0.95	28.46	b.d.	0.15	0.11	0.41	0.07	93.29
194	L07-53: 77.25	0.13	b.d.	b.d.	0.29	0.12	b.d.	b.d.	2.04	56.57	1.90	29.07	b.d.	0.30	0.40	1.03	0.27	92.53
195	L07-53: 77.25	0.21	1.37	0.63	0.22	b.d.	b.d.	b.d.	0.13	59.98	1.02	28.14	b.d.	0.13	0.16	0.38	0.07	92.72
196	L07-53: 77.25	0.22	1.45	0.32	0.41	b.d.	b.d.	b.d.	0.28	59.71	1.13	28.20	b.d.	b.d.	0.17	0.26	0.07	92.79

197	L07-53: 77.25	0.34	1.45	0.52	0.33	b.d.	b.d.	b.d.	0.26	59.21	0.73	28.12	b.d.	0.18	0.13	0.33	0.08	91.99
198	L07-53: 77.25	b.d.	b.d.	0.15	b.d.	b.d.	0.16	b.d.	1.16	60.83	0.64	30.37	b.d.	b.d.	0.12	0.51	0.06	94.48
199	L07-53: 77.25	0.21	1.37	0.57	0.55	b.d.	b.d.	b.d.	0.34	59.49	0.94	28.46	b.d.	0.25	0.24	0.49	0.08	93.41
200	L07-53: 77.25	0.43	1.01	0.14	b.d.	b.d.	0.26	b.d.	b.d.	59.30	1.34	27.83	b.d.	0.19	0.41	0.94	0.15	92.32
201	L07-53: 77.25	0.34	1.14	0.53	0.62	0.16	0.15	b.d.	0.65	59.88	0.69	26.84	b.d.	0.33	0.18	0.30	0.07	92.10
202	L07-53: 77.25	0.11	1.49	0.40	0.24	0.12	b.d.	b.d.	0.10	58.56	1.39	29.01	b.d.	0.15	0.11	0.48	0.10	92.42
203	L07-53: 77.25	0.25	1.11	0.41	0.34	0.29	b.d.	b.d.	0.12	59.24	1.20	28.84	b.d.	b.d.	0.09	0.52	0.07	92.81
204	L07-53: 146.7	0.10	b.d.	b.d.	b.d.	b.d.	0.26	0.14	0.69	41.89	0.83	30.73	b.d.	b.d.	0.19	12.85	3.37	91.26
205	L07-53: 146.7	0.16	0.20	b.d.	b.d.	0.31	b.d.	b.d.	0.98	60.07	1.03	30.45	b.d.	b.d.	0.05	1.13	0.30	94.77
206	L07-53: 146.7	b.d.	b.d.	b.d.	b.d.	0.26	0.21	0.18	1.02	60.58	1.25	31.68	b.d.	b.d.	0.04	1.40	0.33	97.13
207	L07-53: 146.7	b.d.	b.d.	0.13	b.d.	b.d.	0.28	0.13	0.94	53.92	1.21	31.30	b.d.	b.d.	0.09	5.73	1.33	95.21
208	L07-53: 146.7	b.d.	b.d.	b.d.	b.d.	b.d.	0.09	0.17	1.13	59.67	1.17	31.08	b.d.	b.d.	0.06	1.70	0.44	95.86
209	L07-53: 146.7	b.d.	b.d.	b.d.	b.d.	b.d.	0.08	b.d.	1.04	59.38	1.27	31.28	b.d.	b.d.	0.05	2.55	0.40	96.40
210	L07-53: 146.7	b.d.	b.d.	b.d.	b.d.	0.12	0.17	0.11	0.87	51.20	1.14	30.16	b.d.	b.d.	0.18	7.45	2.04	93.55
211	L07-53: 146.7	b.d.	b.d.	b.d.	b.d.	b.d.	0.21	0.22	1.08	57.61	1.31	30.43	b.d.	b.d.	0.27	3.66	0.73	95.78
212	L07-53: 146.7	b.d.	b.d.	b.d.	0.16	0.13	0.16	0.30	1.32	61.99	1.35	30.74	b.d.	b.d.	0.16	0.41	0.04	96.91
213	L07-53: 146.7	0.11	b.d.	b.d.	0.13	b.d.	b.d.v	0.18	1.13	60.12	1.62	30.62	b.d.	b.d.	0.06	1.65	0.39	96.17
214	L07-53: 146.7	b.d.	b.d.	b.d.	b.d.	b.d.	0.15	0.09	1.08	58.30	1.38	30.50	b.d.	b.d.	0.11	3.24	0.79	96.03
215	L07-53: 146.7	0.06	b.d.	b.d.	0.21	0.25	0.14	0.07	1.02	52.78	1.00	30.78	b.d.	b.d.	0.09	6.96	1.39	95.01
216	L07-63: 40.3	0.61	1.70	0.59	0.18	b.d.	0.25	b.d.	0.05	60.91	1.20	28.91	b.d.	0.21	0.12	0.25	0.08	95.40
217	L07-63: 40.3	0.34	1.52	0.46	0.22	b.d.	0.36	b.d.	0.07	59.87	1.05	28.99	b.d.	0.20	0.16	0.29	0.18	94.23
218	L07-63: 40.3	0.30	1.40	0.29	0.18	b.d.	b.d.	b.d.	b.d.	60.69	0.87	28.45	b.d.	0.11	0.22	0.42	0.14	93.26
219	L07-63: 40.3	0.62	1.84	0.36	b.d.	b.d.	0.09	b.d.	b.d.	60.69	1.02	28.41	b.d.	0.26	0.19	0.22	0.07	94.40
220	L07-63: 40.3	0.39	0.57	0.42	0.25	b.d.	0.27	b.d.	b.d.	60.21	1.82	29.31	b.d.	0.37	0.28	0.67	0.38	95.28
221	L07-63: 40.3	0.34	1.75	0.55	0.34	b.d.	b.d.	0.08	b.d.	60.12	0.78	29.16	b.d.	0.29	0.11	0.54	0.11	94.90
222	L07-63: 40.3	0.34	1.53	0.68	0.28	0.19	0.22	b.d.	b.d.	59.27	0.81	28.41	b.d.	0.28	0.15	0.73	0.13	93.29
223	L09-155: 189.6	b.d.	b.d.	b.d.	0.08	b.d.	0.15	0.20	0.77	34.04	0.86	61.35	0.07	b.d.	0.04	0.27	0.05	98.20
224	L09-155: 189.6	0.08	0.15	b.d.	0.23	0.24	0.27	0.35	1.59	58.94	1.62	30.70	1.30	b.d.	0.09	0.77	0.31	97.00
225	L09-155: 189.6	0.23	b.d.	b.d.	0.29	0.48	0.34	0.25	2.50	38.04	0.94	51.96	1.82	b.d.	0.23	0.75	0.62	98.90
226	L09-155: 189.6	0.08	b.d.	b.d.	0.10	0.15	0.21	0.27	1.31	40.62	0.96	53.44	0.21	b.d.	b.d.	0.27	0.12	98.02
227	L09-155: 189.6	0.13	0.27	0.11	0.42	0.52	0.43	0.43	2.63	55.28	1.38	32.88	3.18	b.d.	0.09	0.89	0.13	99.03
228	L09-155: 189.6	0.06	0.21	0.11	0.32	0.34	0.35	0.39	2.08	58.73	1.52	31.03	2.10	b.d.	0.07	0.40	0.15	98.11
229	L09-155: 189.6	0.07	b.d.	b.d.	0.18	0.15	0.18	0.28	1.34	55.77	1.40	31.88	0.53	0.21	0.20	1.93	1.21	95.85
230	L09-155: 189.6	0.10	b.d.	b.d.	0.19	0.14	0.23	0.33	1.48	53.07	1.32	32.03	0.87	0.44	0.06	2.20	1.53	94.35
231	L09-155: 189.6	0.06	0.12	b.d.	0.21	0.25	0.29	0.36	1.68	58.71	1.47	29.93	1.16	0.06	0.43	0.52	0.42	95.97
232	L09-155: 189.6	b.d.	b.d.	b.d.	0.11	b.d.	0.20	0.34	1.21	55.85	1.40	32.31	b.d.	0.35	0.10	1.19	0.96	94.41
233	L09-155: 189.6	0.05	0.14	b.d.	0.24	0.25	0.27	0.38	1.93	55.81	1.40	35.19	1.40	b.d.	0.05	1.03	0.23	98.57
234	L09-155: 189.6	0.24	0.21	b.d.	0.25	0.24	0.22	0.24	1.68	55.71	1.40	33.48	1.94	b.d.	0.08	2.03	0.32	98.54
235	L09-155: 189.6	0.37	0.32	0.11	0.27	0.21	0.15	0.10	1.27	55.16	1.48	34.64	2.55	b.d.	0.22	0.15	0.20	97.56
236	L09-155: 176	b.d.	b.d.	0.15	0.49	0.51	0.08	0.22	2.02	42.94	1.03	36.96	4.03	b.d.	0.14	11.82	0.05	100.71

237	L09-155: 176	b.d.	b.d.	b.d.	0.16	0.18	0.15	0.34	1.36	53.92	1.20	38.67	0.75	b.d.	0.08	1.35	0.17	98.65
238	L09-155: 176	b.d.	b.d.	b.d.	0.10	b.d.	0.14	0.24	1.12	57.02	1.33	31.94	0.15	b.d.	0.05	3.94	0.34	96.76
239	L09-155: 176	b.d.	b.d.	b.d.	0.15	0.15	0.17	0.21	1.34	58.21	1.51	31.30	0.71	b.d.	0.05	4.05	0.14	98.21
240	L09-155: 176	b.d.	b.d.	b.d.	b.d.	b.d.	0.13	0.24	1.12	57.68	1.34	30.21	0.12	b.d.	0.47	3.97	0.50	96.11
241	L09-155: 176	b.d.	b.d.	b.d.	0.10	b.d.	0.13	0.21	1.10	56.64	1.34	31.75	0.07	b.d.	0.04	4.25	0.80	96.78
242	L09-155: 176	b.d.	b.d.	b.d.	0.18	0.29	0.22	0.22	1.50	60.05	1.48	30.76	0.68	b.d.	0.07	b.d.	0.03	95.82
243	L09-155: 176	b.d.	b.d.	b.d.	0.22	0.23	0.22	0.22	1.39	59.63	1.44	29.75	0.96	b.d.	0.04	0.19	0.05	94.54
244	L09-155: 176	b.d.	b.d.	b.d.	0.15	0.19	0.21	0.22	1.30	58.51	1.45	31.60	0.46	b.d.	0.06	1.28	0.21	95.76
245	L09-155: 176	b.d.	b.d.	b.d.	b.d.	b.d.	0.07	0.25	0.95	52.69	1.19	34.54	0.09	b.d.	b.d.	6.84	0.51	97.49
246	L09-155: 176	b.d.	b.d.	b.d.	b.d.	b.d.	b.d.	0.21	0.71	36.64	0.82	54.01	b.d.	b.d.	b.d.	4.05	0.42	97.19
247	L09-155: 176	b.d.	b.d.	b.d.	0.20	0.15	0.19	0.22	1.23	50.05	1.19	41.16	1.09	b.d.	0.05	0.25	0.06	96.22
248	L09-155: 176	b.d.	b.d.	b.d.	0.11	0.14	0.19	0.22	1.29	60.27	1.46	32.17	0.08	b.d.	b.d.	b.d.	b.d.	96.30
249	L09-155: 183.5	0.06	b.d.	b.d.	b.d.	b.d.	0.07	0.20	0.71	46.04	1.03	47.81	b.d.	b.d.	0.06	2.72	0.63	99.66
250	L09-155: 183.5	0.05	b.d.	b.d.	b.d.	b.d.	0.08	0.20	0.77	53.05	1.26	35.69	0.10	b.d.	0.05	3.87	1.03	96.73
251	L09-155: 183.5	0.05	b.d.	b.d.	b.d.	b.d.	0.06	0.10	0.50	22.32	0.54	68.46	0.39	b.d.	b.d.	2.40	0.67	95.73
252	L09-155: 183.5	0.06	b.d.	b.d.	0.12	0.12	0.14	0.27	1.41	48.54	1.08	37.77	0.20	b.d.	0.07	4.42	1.50	95.90
253	L09-155: 183.5	0.05	b.d.	b.d.	b.d.	0.12	0.07	0.21	1.16	39.79	1.07	37.66	0.25	b.d.	0.05	7.32	2.65	90.79
254	L09-155: 183.5	0.05	b.d.	b.d.	0.10	b.d.	0.15	0.21	1.22	43.61	1.01	48.81	0.23	b.d.	0.05	2.66	0.67	99.04
255	L09-155: 183.5	b.d.	b.d.	b.d.	b.d.	b.d.	0.13	0.27	1.22	52.39	1.36	30.94	0.08	b.d.	0.23	5.89	1.93	94.96
256	L09-155: 183.5	0.06	b.d.	b.d.	b.d.	b.d.	0.12	0.19	0.65	45.16	0.98	45.70	0.09	b.d.	0.05	1.69	0.49	95.40
257	L09-155: 183.5	0.11	b.d.	b.d.	b.d.	b.d.	0.12	0.20	0.71	47.80	1.10	45.68	0.24	b.d.	0.06	2.04	0.59	99.02
258	L09-155: 183.5	0.07	b.d.	b.d.	b.d.	b.d.	0.11	0.22	0.81	53.53	1.25	35.86	0.16	b.d.	0.05	2.98	0.69	96.14
259	L09-155: 183.5	0.05	b.d.	b.d.	b.d.	b.d.	0.08	0.21	0.81	51.94	1.23	38.49	0.07	b.d.	0.04	3.04	0.74	96.92
260	L09-155: 183.5	0.16	b.d.	b.d.	0.10	0.16	0.14	0.23	0.91	56.49	1.44	33.14	0.56	b.d.	0.10	2.62	0.58	96.86
261	L09-155: 183.5	0.08	b.d.	b.d.	b.d.	b.d.	0.11	0.25	0.96	57.39	1.46	30.61	0.68	b.d.	0.08	3.51	0.79	96.28
262	L09-155: 183.5	b.d.	b.d.	b.d.	b.d.	0.11	0.08	0.23	0.90	52.17	1.25	31.40	0.18	b.d.	0.09	6.84	1.75	95.21
263	L09-155: 183.5	b.d.	b.d.	b.d.	b.d.	b.d.	0.16	0.17	0.81	51.81	1.23	41.60	0.09	b.d.	b.d.	0.79	0.18	97.16
264	L09-155: 183.5	0.09	b.d.	b.d.	b.d.	b.d.	0.12	0.25	0.89	58.22	1.35	30.98	0.26	b.d.	0.08	2.74	0.75	96.23
265	L09-155: 183.5	0.05	b.d.	b.d.	b.d.	0.11	0.16	0.24	0.98	59.13	1.39	31.10	0.10	b.d.	0.05	2.51	0.62	96.64
266	L09-155: 189.6	0.15	b.d.	0.18	0.51	0.66	0.43	0.41	2.77	54.08	1.42	30.12	4.04	b.d.	0.09	3.02	0.25	98.67
267	L09-155: 189.6	b.d.	b.d.	b.d.	b.d.	0.14	0.25	0.37	1.50	60.13	1.46	32.49	0.17	b.d.	0.04	0.18	0.05	97.27

Notes: b.d. = below detection limits, which are as follows for oxides (wt. %): Ce, 0.04; Nd, 0.11; Sm, 0.09; Gd, 0.09; Dy, 0.11; Er, 0.05; Yb, 0.06; Y, 0.05; Zr, 0.11; Hf, 0.10; Si, 0.03; Nb, 0.06; F, 0.11; Ca, 0.03; Fe, 0.12; Al, 0.02.

APPENDIX D

Electron microprobe analyses of fergusonite-(Y)

No.	Sample	Ce_2O_3	Pr_2O_3	Nd_2O_3	Sm_2O_3	Eu_2O_3	Gd_2O_3	Dy_2O_3	Er_2O_3	Yb_2O_3	Y_2O_3	Nb_2O_5	HfO_2	CaO	FeO	ThO_2	Ta_2O_5	Total
1	L07-53: 146.7	0.13	0.34	2.00	2.30	0.92	7.13	6.17	1.66	0.75	22.73	43.47	b.d.	0.43	0.57	0.18	3.62	92.07
2	L07-53: 146.7	0.48	0.30	2.30	1.69	1.54	7.13	8.14	1.56	0.22	24.55	48.61	0.23	0.07	0.44	b.d.	1.13	97.18
3	L07-53: 146.7	0.54	0.17	2.20	2.49	1.36	7.06	5.93	2.14	0.66	23.64	44.55	b.d.	0.22	0.40	0.15	3.53	93.51
4	L07-53: 146.7	0.45	b.d.	1.89	2.33	1.32	7.44	6.42	2.42	0.59	23.93	45.90	b.d.	0.21	0.27	0.22	2.81	94.49
5	L07-53: 146.7	0.34	b.d.	2.16	2.56	0.97	7.30	5.94	2.18	0.80	23.40	45.18	b.d.	0.18	0.33	0.24	3.52	93.60
6	L07-53: 146.7	0.54	0.34	2.29	2.21	0.50	6.84	6.16	1.19	0.73	23.58	44.09	b.d.	0.26	0.86	0.27	3.47	92.86
7	L07-55: 100.1	0.34	b.d.	1.54	1.66	0.58	8.20	7.36	2.33	0.48	24.39	47.62	0.33	0.20	b.d.	0.60	1.07	97.31
8	L07-55: 100.1	0.58	0.39	3.25	2.44	0.70	6.92	6.33	2.61	0.68	24.72	47.89	0.32	0.07	b.d.	0.14	1.65	99.10
9	L07-55: 100.1	0.16	b.d.	0.86	1.57	0.33	7.17	6.17	2.77	1.08	26.76	47.47	0.38	0.12	b.d.	0.65	2.59	98.54
10	L07-55: 100.1	0.21	b.d.	1.27	1.89	0.40	7.42	6.17	2.61	0.95	25.47	46.66	0.39	0.13	b.d.	0.85	2.17	97.24
11	L07-55: 100.1	0.48	0.36	3.78	3.77	1.13	8.64	6.16	1.96	0.41	21.76	47.44	0.22	0.19	b.d.	0.13	1.33	97.94
12	L07-55: 100.1	0.50	0.23	2.75	2.94	0.83	8.25	5.70	2.05	0.62	25.07	47.56	0.33	0.18	b.d.	0.16	1.87	99.20
13	L09-155: 189.6	1.23	0.60	4.31	3.63	0.97	7.77	5.54	1.55	0.34	23.01	46.92	0.33	0.25	b.d.	b.d.	1.41	98.29
14	L09-155: 189.6	0.32	b.d.	2.14	4.43	1.11	8.80	5.17	1.85	0.51	22.88	46.11	0.35	0.30	b.d.	b.d.	2.94	97.23
15	L09-155: 189.6	0.52	0.37	3.81	3.95	1.04	8.29	5.66	1.83	0.41	22.28	47.35	0.28	0.16	0.13	b.d.	1.72	98.08
16	L09-155: 189.6	0.55	0.22	3.54	4.10	0.98	6.08	3.56	1.16	0.38	27.06	47.45	0.22	0.39	0.44	0.38	1.59	99.77
17	L09-155: 189.6	0.23	b.d.	1.90	3.40	0.73	6.08	3.60	1.19	0.56	28.96	47.74	0.26	0.43	0.39	0.80	2.62	100.64
18	L09-155: 189.6	0.37	0.28	2.71	2.90	0.68	5.63	3.99	1.19	0.41	28.00	46.98	b.d.	0.58	2.06	0.91	2.07	100.41
19	L09-155: 189.6	0.14	b.d.	1.00	2.93	0.81	5.85	3.88	1.63	0.89	29.71	47.44	0.24	0.41	0.21	0.36	2.89	100.19
20	L09-155: 189.6	0.39	0.28	2.46	3.13	0.82	5.84	4.17	1.17	0.35	28.17	46.07	b.d.	0.36	1.50	0.18	2.42	99.16
21	L09-155: 189.6	0.28	b.d.	2.33	3.14	0.81	5.61	3.47	1.23	0.50	29.51	46.25	0.20	0.33	0.61	b.d.	2.81	98.86
22	L09-155: 189.6	0.52	0.41	4.65	5.42	1.22	7.89	5.45	1.99	0.96	20.82	46.18	b.d.	0.27	0.15	0.33	1.37	100.05
23	L09-155: 189.6	0.47	0.39	3.99	4.50	1.01	8.76	5.20	2.27	1.17	22.11	45.27	0.23	0.31	0.16	0.52	1.77	100.22
24	L09-155: 189.6	0.51	0.26	3.00	4.01	1.02	6.46	4.66	2.27	1.55	23.14	46.30	0.31	0.54	0.29	1.31	1.66	99.34
25	L09-155: 189.6	0.85	0.45	4.52	4.56	1.09	6.34	4.82	2.13	1.35	22.12	46.25	0.25	0.40	b.d.	1.03	1.63	99.94
26	L07-63: 171.2	0.53	0.48	2.57	2.35	0.64	5.61	6.44	2.81	1.23	25.78	45.77	0.32	0.29	0.28	0.15	3.01	100.49
27	L07-63: 171.2	0.53	0.22	2.75	3.26	0.94	6.50	6.35	2.75	1.17	24.86	45.17	0.30	0.12	0.15	0.19	2.92	100.61
28	L07-63: 171.2	0.54	0.19	2.72	3.02	0.88	6.42	6.52	2.79	1.18	24.44	44.93	0.24	0.15	0.25	0.25	3.50	100.30
29	L07-63: 171.2	0.68	0.40	3.99	3.81	0.95	6.50	6.03	2.45	1.02	22.54	44.14	0.28	0.35	0.32	0.28	3.43	99.35
30	L07-63: 171.2	0.74	0.36	3.70	3.76	0.89	6.52	6.12	2.62	1.16	24.04	45.11	0.29	0.20	0.24	0.27	2.38	100.59
31	L07-63: 171.2	1.01	0.58	4.74	3.62	0.85	6.12	6.49	2.50	0.90	22.78	44.12	0.25	0.17	0.46	b.d.	2.68	99.58

32	L07-63: 171.2	0.43	b.d.	1.78	1.36	0.55	5.23	7.01	2.33	0.69	25.69	45.21	0.26	0.27	2.48	0.77	2.71	99.57
33	L07-63: 171.2	0.41	b.d.	1.44	1.39	0.46	4.94	6.91	2.41	0.82	27.13	47.35	0.35	0.22	1.81	1.19	0.98	100.14
34	L07-63: 171.2	0.17	b.d.	0.91	0.92	0.42	4.65	8.31	2.78	0.96	25.24	45.75	0.34	0.27	1.44	1.54	2.46	99.14
35	L07-63: 171.2	1.01	0.22	2.39	1.80	0.58	5.29	6.58	2.01	0.69	23.51	44.14	0.33	0.49	2.06	1.04	4.16	98.94
36	L07-63: 171.2	0.19	b.d.	1.03	0.90	0.37	4.15	6.71	2.39	0.83	24.47	40.78	0.24	0.96	2.32	2.26	5.97	95.99

Notes: b.d. = below detection limits, which are as follows for oxides (wt. %): Ce, 0.05; Pr, 0.20; Nd, 0.25; Sm, 0.10; Eu, 0.17; Gd, 0.20; Dy, 0.24; Er, 0.11; Yb, 0.11; Y, 0.10; Nb, 0.10; Hf, 0.17; Ca, 0.03; Fe, 0.13; Th, 0.13; Ta, 0.16.

APPENDIX E

Electron microprobe analyses of ferrocolumbite

No.	Sample	Sm_2O_3	Er_2O_3	Y_2O_3	Nb_2O_5	Ta_2O_5	MgO	ThO_2	UO_2	FeO	MnO	TiO_2	CaO	SnO_2	Total
1	L07-63: 171.2	b.d.	b.d.	0.39	68.90	6.60	0.24	b.d.	b.d.	19.94	2.02	1.52	b.d.	0.18	99.92
2	L07-63: 171.2	b.d.	b.d.	0.27	69.92	7.95	0.20	b.d.	b.d.	17.93	4.25	0.16	b.d.	b.d.	100.78
3	L07-63: 171.2	b.d.	b.d.	0.43	67.16	6.67	0.18	b.d.	b.d.	19.96	1.72	2.42	0.08	0.38	99.21
4	L07-63: 171.2	b.d.	b.d.	0.69	68.15	6.90	0.27	b.d.	b.d.	17.39	3.98	1.07	0.06	0.24	98.89
5	L07-63: 171.2	b.d.	b.d.	0.54	68.25	7.29	0.20	b.d.	b.d.	19.47	2.44	1.43	0.21	0.26	100.16
6	L07-53: 146.7	b.d.	0.14	0.19	72.62	1.33	0.17	b.d.	b.d.	19.55	1.74	3.07	0.05	0.26	99.51
7	L07-53: 146.7	b.d.	0.13	0.17	72.98	1.51	0.17	b.d.	b.d.	19.41	2.19	2.11	0.06	0.16	99.11
8	L07-53: 146.7	b.d.	0.13	0.22	73.94	0.92	0.15	b.d.	0.09	17.97	3.81	2.09	0.11	0.13	99.81
9	L07-53: 146.7	b.d.	0.12	0.44	72.23	0.74	0.15	b.d.	0.17	19.14	3.00	2.89	0.13	0.24	99.51
10	L07-53: 146.7	0.52	b.d.	0.14	73.83	0.85	0.36	0.15	0.27	19.52	1.86	2.37	0.06	0.19	100.56
11	L07-53: 146.7	b.d.	0.19	0.15	74.57	0.71	0.22	0.05	0.07	18.35	3.45	1.80	b.d.	0.15	99.78
12	L07-53: 146.7	b.d.	b.d.	b.d.	65.10	9.32	0.30	b.d.	b.d.	19.51	1.32	2.63	b.d.	b.d.	98.66

Notes: b.d. = below detection limits, which are as follows for oxides (wt. %): Sm, 0.09; Er, 0.09; Y, 0.07; Nb, 0.11; Ta, 0.14; Mg, 0.02; Th, 0.05; U, 0.04; Fe, 0.11; Mn, 0.14; Ti, 0.07; Ca, 0.02; Sn, 0.05.

APPENDIX F

Electron microprobe analyses of monazite-(Ce)

No.	Sample	La_2O_3	Ce_2O_3	Pr_2O_3	Nd_2O_3	Sm_2O_3	Eu_2O_3	Gd_2O_3	Dy_2O_3	Y_2O_3	P_2O_5	F	CaO	FeO	ThO_2	Total
1	L07-63: 34.3	12.59	32.40	4.18	16.17	2.24	b.d.	0.63	b.d.	0.15	30.12	0.47	0.07	b.d.	0.37	99.57
2	L07-63: 34.3	11.02	27.16	4.13	17.66	3.63	b.d.	1.57	b.d.	0.11	30.29	0.51	0.09	0.19	3.20	100.61
3	L07-63: 34.3	11.25	28.23	4.19	17.95	3.40	b.d.	1.32	0.31	0.14	30.22	0.52	0.12	0.15	2.30	100.66
4	L07-63: 34.3	13.12	34.93	4.23	14.73	1.41	b.d.	0.60	b.d.	0.07	30.23	0.52	b.d.	b.d.	b.d.	99.82
5	L07-63: 34.3	13.55	34.55	4.05	14.29	1.64	b.d.	0.57	b.d.	0.18	30.61	0.48	0.17	b.d.	b.d.	100.34
6	L07-63: 34.3	13.57	33.26	4.35	14.99	1.82	b.d.	0.95	b.d.	0.46	30.66	0.51	0.09	b.d.	b.d.	100.80
7	L07-63: 34.3	13.12	32.03	4.16	15.60	2.10	b.d.	1.43	b.d.	0.20	30.23	0.56	0.07	0.25	0.13	100.08
8	L07-63: 34.3	13.89	32.79	4.33	15.08	1.87	b.d.	1.44	b.d.	0.29	30.22	0.52	0.11	b.d.	b.d.	100.57
9	L07-63: 34.3	14.88	34.65	4.43	14.16	0.91	b.d.	0.30	b.d.	0.06	30.29	0.52	b.d.	b.d.	b.d.	100.31
10	L07-53: 77.25	12.24	32.87	4.25	17.31	1.19	b.d.	b.d.	b.d.	0.06	30.14	0.41	0.06	b.d.	1.14	100.26
11	L07-53: 77.25	12.49	32.22	4.73	18.06	1.30	b.d.	b.d.	b.d.	0.00	30.12	0.46	0.07	b.d.	0.75	100.78
12	L07-53: 77.25	15.99	31.90	3.70	12.82	1.43	b.d.	0.99	0.29	0.85	30.38	0.63	0.77	b.d.	0.17	99.83
13	L07-53: 77.25	13.48	33.03	4.21	15.54	1.92	b.d.	0.84	b.d.	0.00	30.30	0.52	0.11	b.d.	0.73	100.81
14	L07-63: 40.3	13.09	35.29	4.31	14.54	0.95	b.d.	b.d.	b.d.	0.00	30.15	0.46	0.07	b.d.	0.89	100.14
15	L07-63: 40.3	12.90	33.36	4.59	15.87	1.81	b.d.	0.86	b.d.	0.30	30.44	0.42	0.17	b.d.	b.d.	100.82
16	L07-63: 40.3	14.57	34.69	4.08	13.82	1.04	b.d.	0.43	b.d.	0.14	30.33	0.55	0.29	0.39	b.d.	100.59
17	L07-63: 40.3	14.31	34.63	4.48	14.13	0.97	b.d.	0.41	b.d.	0.11	30.27	0.54	0.25	b.d.	0.15	100.41
18	L07-63: 40.3	14.04	33.48	4.31	17.09	1.49	0.20	0.25	b.d.	0.07	29.10	0.56	0.14	0.14	0.00	100.66
19	L07-63: 40.3	13.79	34.91	4.60	15.48	1.32	0.14	0.28	b.d.	0.06	29.64	0.53	0.08	0.15	0.00	100.76
20	L07-63: 40.3	14.31	33.39	4.31	15.69	1.64	0.21	0.67	b.d.	0.31	29.41	0.51	0.21	0.04	0.00	100.57
21	L07-63: 40.3	13.85	33.02	4.18	15.56	1.67	0.22	0.72	0.13	0.45	29.88	0.52	0.19	0.10	0.00	100.28
22	L07-63: 40.3	14.53	33.09	4.17	15.74	1.55	0.27	0.55	0.11	0.27	29.70	0.53	0.19	0.12	0.00	100.59
23	L07-63: 40.3	13.29	32.03	3.94	13.47	1.96	0.33	1.23	b.d.	0.18	29.47	0.48	0.41	0.32	3.30	100.29
24	L07-63: 40.3	11.16	30.25	4.01	15.29	2.48	0.36	2.06	0.58	0.89	29.22	0.48	0.56	1.00	1.66	99.79
25	L07-63: 40.3	15.87	32.90	3.91	13.15	1.09	0.15	0.81	0.16	0.42	28.22	0.46	0.10	0.26	2.78	100.08
26	L07-63: 34.3	13.69	31.25	3.84	13.80	1.75	0.29	1.35	0.29	0.61	28.87	0.36	0.54	0.44	2.57	99.50
27	L07-63: 34.3	13.74	32.51	4.00	14.21	1.67	0.29	1.29	0.28	0.39	29.53	0.46	0.16	b.d.	1.61	99.96
28	L07-63: 34.3	15.33	34.53	4.02	13.57	1.27	0.22	0.74	b.d.	0.10	29.28	0.41	0.11	0.05	0.93	100.44
29	L07-63: 34.3	14.87	34.32	4.16	13.68	1.24	0.21	0.67	0.11	0.15	29.46	0.49	0.12	0.08	0.95	100.28
30	L07-63: 34.3	15.48	33.60	4.09	14.06	1.59	0.24	0.84	b.d.	0.19	29.64	0.54	0.24	0.06	0.45	100.85
31	L07-63: 34.3	15.68	33.96	4.02	13.42	1.39	0.25	0.73	b.d.	0.15	28.89	0.52	0.36	0.06	0.87	100.15

32	L07-53: 77.25	14.25	33.51	4.18	14.21	1.81	0.23	0.92	b.d.	0.15	29.28	0.56	0.17	0.19	1.25	100.52
33	L07-53: 77.25	14.35	30.80	4.02	16.92	2.96	0.39	1.75	0.14	0.10	28.68	0.48	0.08	b.d.	0.30	100.78
34	L07-53: 77.25	15.85	32.69	3.91	13.82	2.06	0.33	1.29	b.d.	0.17	28.56	0.49	0.34	0.12	0.72	100.24
35	L07-53: 77.25	16.22	34.27	3.90	13.34	1.51	0.22	0.82	0.13	0.12	29.11	0.48	0.45	b.d.	0.11	100.47
36	L07-53: 77.25	15.02	33.87	4.13	14.39	1.65	0.28	0.87	b.d.	0.06	29.77	0.48	0.28	0.03	0.11	100.77
37	L07-53: 77.25	15.56	34.10	4.19	14.05	1.62	0.17	0.82	b.d.	0.11	28.23	0.52	0.37	b.d.	0.09	99.65
38	L07-55: 100.1	15.72	27.77	3.30	11.42	1.20	0.28	1.38	0.57	2.57	30.34	0.33	0.57	0.04	4.57	99.91
39	L07-55: 100.1	15.69	28.54	3.26	11.50	1.27	0.30	1.25	0.53	2.15	30.36	0.41	0.30	0.07	4.53	99.99
40	L07-55: 100.1	15.73	27.93	3.33	11.39	1.26	0.27	1.41	0.58	2.53	30.46	0.40	0.31	b.d.	4.59	100.00
41	L07-55: 100.1	16.65	28.25	3.39	11.48	1.26	0.28	1.36	0.61	2.27	30.21	0.37	0.35	b.d.	4.43	100.75
42	L07-55: 100.1	16.57	28.43	3.24	11.24	1.26	0.28	1.30	0.61	2.29	29.96	0.33	0.35	b.d.	4.57	100.29
43	L07-55: 100.1	15.60	28.42	3.36	12.06	1.40	0.28	1.47	0.65	2.54	30.34	0.47	0.43	b.d.	3.51	100.32
44	L07-55: 100.1	16.27	28.38	3.23	11.59	1.25	0.29	1.38	0.55	2.48	29.42	0.42	0.25	b.d.	4.59	99.92
45	L07-55: 100.1	16.29	28.27	3.37	11.60	1.30	0.28	1.39	0.63	2.42	29.93	0.41	0.27	b.d.	4.47	100.43
46	L07-55: 100.1	15.70	28.95	3.48	12.74	1.46	0.31	1.36	0.52	1.60	30.40	0.40	0.18	b.d.	3.53	100.48
47	L07-55: 100.1	16.56	28.31	3.42	11.45	1.24	0.23	1.28	0.64	2.24	30.12	0.36	0.31	b.d.	4.61	100.60

Notes: b.d. = below detection limits, which are as follows for oxides (wt. %): La, 0.10; Ce, 0.10; Pr, 0.11; Nd, 0.11; Sm, 0.08; Eu, 0.03; Gd, 0.09; Dy, 0.11; Y, 0.03; P, 0.08; F, 0.16; Ca, 0.02; Fe, 0.04; Th, 0.05.

APPENDIX G

Electron microprobe analyses of allanite-(Ce)

No.	Sample	La_2O_3	Ce_2O_3	Pr_2O_3	Nd_2O_3	Sm_2O_3	Eu_2O_3	Gd_2O_3	Y_2O_3	SiO_2	FeO	Al_2O_3	CaO	MgO	MnO	Total
1	L07-63: 34.3	6.95	11.93	1.43	4.86	0.56	0.13	0.41	0.12	31.16	15.39	14.81	8.66	0.55	0.40	97.35
2	L07-63: 34.3	7.06	12.08	1.48	5.06	0.53	0.16	0.52	0.18	31.22	14.45	14.39	8.88	0.63	0.51	97.14
3	L07-63: 34.3	7.62	12.64	1.31	3.64	0.27	0.13	0.21	0.27	31.94	15.08	11.61	8.46	0.57	0.33	94.54
4	L07-63: 34.3	5.93	11.03	1.34	4.25	0.41	b.d.	0.44	0.53	31.45	10.81	16.03	8.92	0.57	0.52	93.03
5	L07-63: 34.3	7.21	12.73	1.35	3.89	0.29	b.d.	0.21	0.20	32.15	12.91	15.19	8.25	0.64	0.44	96.01
6	L07-55: 100.1	7.09	12.73	1.54	4.81	0.48	b.d.	0.42	0.17	32.26	12.71	17.85	9.39	0.48	0.43	100.58
7	L07-55: 100.1	6.48	10.63	1.16	4.17	0.46	0.14	0.52	0.34	32.79	10.93	20.87	10.25	0.53	0.50	99.81
8	L07-55: 100.1	7.39	11.59	1.43	4.46	0.44	b.d.	0.39	0.09	32.17	14.02	16.45	9.68	0.38	0.47	99.07
9	L07-55: 100.1	5.81	10.19	1.18	4.03	0.39	0.12	0.38	0.44	32.98	11.30	20.26	10.94	0.62	0.33	99.01
10	L07-55: 100.1	7.67	12.49	1.43	4.50	0.53	0.16	0.35	0.09	31.15	15.75	13.64	9.00	0.33	0.32	97.41
11	L07-55: 100.1	6.76	11.76	1.36	4.62	0.48	0.13	0.42	0.21	31.87	11.78	19.23	9.08	0.94	0.39	99.19
12	L07-55: 100.1	7.15	12.93	1.32	4.09	0.43	b.d.	0.27	0.17	32.04	12.52	15.98	8.29	0.52	0.98	97.10
13	L07-55: 100.1	6.28	11.48	1.42	4.34	0.46	b.d.	0.40	0.10	33.09	12.00	16.44	8.48	0.43	0.91	96.53
14	L07-55: 100.1	6.91	13.14	1.60	4.79	0.30	0.27	0.16	0.13	31.19	14.76	16.16	8.10	0.29	0.83	98.63
15	L07-55: 100.1	6.58	13.52	1.58	4.59	0.25	0.24	0.15	0.18	31.36	14.75	16.07	8.82	0.22	0.52	98.81
16	L07-55: 100.1	6.64	13.05	1.74	5.24	0.42	0.32	0.27	0.17	31.24	14.89	16.00	8.74	0.10	0.38	99.19
17	L07-55: 100.1	6.01	13.89	1.79	5.21	0.35	0.23	0.24	0.20	31.48	14.14	16.67	8.33	0.16	0.65	99.33
18	L07-55: 100.1	5.77	13.33	1.82	5.75	0.49	0.29	0.23	0.20	31.27	14.81	16.01	8.45	0.09	0.56	99.07
19	L07-55: 100.1	6.41	14.19	1.59	4.30	0.14	0.20	b.d.	b.d.	31.45	14.05	16.88	8.64	0.14	0.68	98.70
20	L07-55: 100.1	5.60	15.42	1.81	3.86	b.d.	0.21	b.d.	0.04	31.63	14.45	16.22	8.66	0.20	0.43	98.60
21	L07-55: 100.1	5.81	15.22	1.79	4.16	b.d.	0.21	b.d.	b.d.	31.16	15.17	15.52	8.45	0.10	0.59	98.26
22	L07-53: 146.7	8.04	13.30	1.36	3.41	b.d.	0.15	b.d.	b.d.	31.41	15.07	15.72	9.32	0.29	0.47	98.63
23	L07-53: 146.7	7.84	12.99	1.29	4.16	0.11	0.23	0.15	b.d.	31.27	15.60	15.26	8.81	0.16	0.67	98.52
24	L07-53: 146.7	4.49	10.78	1.27	4.71	0.50	0.16	0.24	b.d.	32.96	12.12	19.50	11.01	0.30	0.88	98.95
25	L07-53: 146.7	4.72	12.14	1.52	5.28	0.45	0.30	0.19	0.04	32.12	12.95	18.10	9.87	0.33	0.98	99.00
26	L07-53: 146.7	5.52	11.34	1.29	4.30	0.38	0.16	0.18	b.d.	31.85	13.72	17.38	10.18	0.44	1.08	97.90
27	L07-53: 146.7	5.49	11.64	1.37	4.30	0.35	0.14	0.23	b.d.	32.12	13.04	17.88	9.91	0.50	1.20	98.20
28	L08-118: 50.7	4.78	12.20	1.58	5.14	0.50	0.20	0.24	0.04	31.91	13.53	17.52	9.75	0.31	1.08	98.78
29	L08-118: 50.7	7.50	13.48	1.48	4.59	0.28	0.20	0.14	0.05	31.22	15.86	14.70	8.60	0.22	0.51	98.83
30	L08-118: 50.7	6.52	13.73	1.51	4.42	0.39	0.25	0.24	0.16	31.42	15.31	15.27	8.45	0.30	0.57	98.54

31	L08-118: 50.7	6.81	13.49	1.55	4.75	0.31	0.23	0.22	0.07	31.04	14.37	16.63	8.40	0.27	0.59	98.71
32	L08-118: 50.7	7.40	13.38	1.55	4.26	0.28	0.22	0.16	0.05	31.45	15.05	15.96	8.14	0.38	0.89	99.16
33	L08-118: 50.7	7.14	13.86	1.48	4.46	0.15	0.20	0.12	0.05	31.33	15.23	15.01	8.50	0.29	0.54	98.35

Notes: b.d. = below detection limits, which are as follows for oxides (wt. %): La, 0.27; Ce, 0.07; Pr, 0.17; Nd, 0.21; Sm, 0.08; Eu, 0.11; Gd, 0.09; Y, 0.03; Si, 0.03; Fe, 0.04; Al, 0.02; Ca, 0.02; Mg, 0.02; Mn, 0.04.

APPENDIX H

Electron microprobe analyses of bastnäsite-(Ce)

No.	Sample	La_2O_3	Ce_2O_3	Pr_2O_3	Nd_2O_3	Sm_2O_3	Eu_2O_3	Gd_2O_3	Dy_2O_3	Y_2O_3	F	CaO	FeO	CO_2	Total
1	L07-63: 34.3	16.81	37.25	4.34	14.65	1.14	0.33	0.31	0.16	0.11	6.79	0.15	b.d.	20.73	100.00
2	L07-63: 34.3	15.93	41.38	4.72	13.53	0.80	b.d.	0.25	b.d.	0.08	5.40	0.29	b.d.	19.59	100.00
3	L07-63: 34.3	17.03	38.39	4.39	13.37	0.80	b.d.	0.42	b.d.	0.15	7.87	0.08	b.d.	20.58	100.00
4	L07-63: 34.3	16.65	38.67	4.53	13.65	0.69	b.d.	0.28	b.d.	0.11	9.90	b.d.	b.d.	19.43	100.00
5	L07-63: 34.3	19.20	38.37	4.08	12.42	0.69	0.29	0.33	b.d.	0.09	6.47	0.20	b.d.	20.44	100.00
6	L07-63: 34.3	18.50	36.07	4.49	14.43	0.88	b.d.	0.29	b.d.	0.13	10.09	0.25	b.d.	18.78	100.00
7	L07-63: 34.3	16.00	35.26	2.31	9.07	1.66	0.59	0.75	b.d.	0.29	6.82	b.d.	b.d.	30.08	100.00
8	L07-63: 40.3	16.15	35.71	4.42	15.93	1.41	0.34	0.73	b.d.	0.35	8.76	0.12	b.d.	19.67	100.00
9	L07-63: 40.3	16.09	34.62	4.54	15.52	1.21	0.24	0.49	b.d.	0.25	9.84	0.95	0.37	19.86	100.00
10	L07-63: 40.3	16.79	36.03	4.09	15.41	1.21	0.29	0.39	b.d.	0.27	9.27	b.d.	b.d.	19.91	100.00
11	L07-63: 40.3	22.91	33.82	3.56	12.96	0.69	b.d.	0.31	b.d.	0.05	10.80	b.d.	b.d.	19.15	100.00
12	L07-63: 40.3	18.18	34.82	3.99	13.29	1.19	0.26	1.00	0.24	0.74	10.00	0.21	b.d.	20.31	100.00
13	L07-63: 40.3	19.79	35.76	4.10	12.72	0.97	b.d.	0.64	b.d.	0.16	9.44	b.d.	b.d.	20.23	100.00
14	L07-63: 40.3	18.56	36.14	3.99	13.72	0.90	b.d.	0.57	b.d.	0.16	6.46	0.27	b.d.	21.67	100.00
15	L07-63: 40.3	18.60	36.42	3.97	12.64	0.94	0.32	0.47	b.d.	0.17	9.03	0.55	b.d.	20.64	100.00
16	L07-63: 40.3	15.73	34.15	3.98	16.34	1.80	0.59	1.35	0.12	0.32	6.72	0.16	b.d.	21.35	100.00
17	L07-63: 40.3	15.33	34.48	4.14	17.24	1.60	0.54	1.35	0.17	0.24	6.56	b.d.	b.d.	20.98	100.00
18	L07-63: 40.3	15.05	34.51	4.50	16.57	1.87	0.63	1.37	0.11	0.31	6.80	b.d.	b.d.	21.00	100.00
19	L07-53: 77.25	15.02	34.09	4.56	16.97	1.73	0.56	1.42	0.11	0.24	6.55	0.18	b.d.	21.25	100.00
20	L07-53: 77.25	15.53	33.73	4.41	16.86	2.02	0.57	1.76	0.15	0.32	6.27	b.d.	b.d.	20.87	100.00
21	L07-53: 77.25	15.39	33.01	4.28	16.90	1.96	0.48	1.46	0.25	0.60	6.67	0.08	b.d.	21.62	100.00
22	L07-53: 77.25	15.79	33.82	4.43	17.40	1.91	0.49	1.45	0.24	0.57	6.92	b.d.	b.d.	19.80	100.00
23	L07-53: 77.25	15.68	33.73	4.19	16.79	1.85	0.59	1.61	0.35	0.82	6.75	b.d.	b.d.	20.37	100.00
24	L07-63: 34.3	14.40	33.68	4.32	17.99	1.96	0.49	1.58	0.30	0.65	6.48	b.d.	0.20	20.53	100.00
25	L07-63: 34.3	15.34	33.28	4.62	17.03	1.87	0.47	1.60	0.32	0.80	6.44	0.09	b.d.	20.71	100.00
26	L07-63: 34.3	13.09	30.78	4.70	22.93	2.13	0.60	0.48	b.d.	0.09	8.60	0.10	0.30	19.70	100.00

Notes: b.d. = below detection limits, which are as follows for oxides (wt. %): La, 0.15; Ce, 0.14; Pr, 0.19; Nd, 0.38; Sm, 0.07; Eu, 0.22; Gd, 0.21; Dy, 0.09; Y, 0.03; F, 0.04; Ca, 0.07; Fe, 0.17.

APPENDIX I

Electron microprobe analyses of eudialyte from sample 85-L6: 349.

No.	Na_2O	F	ZrO_2	Ce_2O_3	SiO_2	Y_2O_3	Pr_2O_3	K_2O	La_2O_3	Nd_2O_3	CaO	Dy_2O_3	MnO	Gd_2O_3	HfO_2	Nb_2O_5	Sm_2O_3	Yb_2O_3	Er_2O_3	Total
1	9.77	0.11	11.25	1.79	48.18	1.49	0.18	0.35	1.09	0.85	9.48	0.30	6.25	0.39	0.28	2.91	0.20	0.09	0.13	95.28
2	10.75	0.27	10.62	1.88	46.72	2.33	0.21	0.42	1.18	0.65	8.95	0.36	6.41	0.41	0.29	3.77	0.14	0.17	0.20	95.76
3	11.28	0.17	10.73	1.95	46.14	2.36	0.23	0.47	1.24	0.64	8.99	0.42	6.63	0.42	0.37	3.86	b.d.	0.12	0.20	96.33
4	11.17	0.17	10.73	2.13	45.62	2.02	0.20	0.45	1.35	0.86	8.95	0.34	6.55	0.35	0.29	3.92	0.12	0.11	0.19	95.85
5	10.77	0.26	10.77	1.86	46.82	2.69	0.18	0.48	1.18	0.58	8.83	0.44	6.28	0.50	0.34	3.98	0.14	0.16	0.26	96.48
6	11.06	0.22	10.68	2.07	46.50	2.43	0.23	0.48	1.34	0.70	8.97	0.37	6.59	0.42	0.31	3.93	0.11	0.16	0.23	96.71
7	11.34	0.22	10.70	0.90	46.90	1.59	0.26	0.47	1.66	1.16	9.36	0.27	6.77	0.39	0.36	3.97	0.24	0.08	0.15	96.77
8	11.14	0.27	10.80	1.13	47.09	1.72	0.27	0.46	1.51	1.30	9.18	0.29	6.58	0.43	0.38	3.82	0.28	0.07	0.13	96.84
9	10.51	0.23	10.63	1.00	47.28	1.54	0.29	0.46	1.64	1.04	9.25	0.24	6.78	0.42	0.27	3.87	0.25	0.07	0.13	95.89
10	11.38	0.17	10.43	2.36	45.31	1.86	0.22	0.46	1.63	0.70	9.06	0.28	6.75	0.37	0.28	3.84	0.11	0.06	0.18	95.45
11	10.98	0.13	10.65	2.39	46.23	1.83	0.15	0.43	1.68	0.67	9.18	0.40	6.68	0.33	0.41	3.77	0.11	0.08	0.16	96.29
12	11.03	0.25	10.68	1.81	46.81	2.97	0.16	0.46	1.21	0.55	8.97	0.50	6.12	0.45	0.24	3.99	0.12	0.14	0.28	96.67
13	10.98	0.24	10.38	2.21	46.49	1.96	0.15	0.49	1.41	0.76	9.33	0.34	6.23	0.36	0.34	3.93	0.14	0.11	0.18	96.00
14	10.42	0.25	10.82	1.91	46.45	2.57	0.18	0.47	1.23	0.59	9.38	0.45	6.25	0.34	0.25	4.09	0.11	0.14	0.25	96.07
15	11.15	0.24	10.86	2.40	45.74	1.25	0.29	0.51	1.44	0.89	9.51	0.22	6.40	0.32	0.26	4.00	0.20	0.07	0.14	95.94
16	10.95	0.25	10.96	1.85	46.87	2.38	0.17	0.49	1.23	0.67	9.41	0.42	6.17	0.40	0.22	4.04	0.17	0.16	0.21	96.93
17	11.23	0.20	10.79	1.92	46.18	2.26	0.17	0.51	1.22	0.68	9.39	0.39	6.29	0.36	0.32	3.92	0.13	0.13	0.23	96.31
18	11.31	0.27	10.79	1.81	46.27	2.95	0.17	0.46	1.12	0.56	8.93	0.56	6.13	0.47	0.31	4.00	0.18	0.16	0.26	96.61
19	10.97	0.21	10.77	1.94	46.65	2.83	0.17	0.46	1.27	0.70	9.10	0.49	6.24	0.42	0.31	3.83	0.10	0.16	0.27	96.80
20	11.31	0.23	10.73	2.00	45.92	2.20	0.21	0.47	1.33	0.68	9.17	0.37	6.39	0.43	0.31	3.95	0.15	0.13	0.21	96.11
21	11.26	0.17	10.60	1.82	45.85	2.53	0.17	0.49	1.23	0.56	9.05	0.38	6.36	0.43	0.34	3.96	0.12	0.14	0.25	95.79

Notes: b.d. = below detection limits, which are as follows for oxides (wt. %): Na, 0.03; F, 0.11; Zr, 0.11; Ce, 0.04; Si, 0.03; Y, 0.05; Pr, 0.05; K, 0.03; La, 0.15; Nd, 0.11; Ca, 0.03; Dy, 0.11; Mn, 0.03; Gd, 0.09; Hf, 0.10; Nb, 0.06; Sm, 0.09; Yb, 0.06; Er, 0.05.

APPENDIX J

Bulk rock analyses of 1 - 2 m long intervals of drill core from L07-55 (data provided by Avalon Rare Metals Inc.). Y, REE, Nb, Zr and Hf oxides reported in ppm and Si, Al, Fe, Mg, Ca, Na and K oxides reported in wt. %.

depth_from	Y_2O_3	La_2O_3	Ce_2O_3	Pr_2O_3	Nd_2O_3	Sm_2O_3	Gd_2O_3	Dy_2O_3	Yb_2O_3	Nb_2O_5	ZrO_2	HfO_2	SiO_2	Al_2O_3	Fe_2O_3	MgO	CaO	Na_2O	K_2O	Total
15.3	523	3969	9623	1123	4244	610	345	135	24	1163	11733	229	54.93	10.98	8.91	3.57	4.11	0.34	5.47	96.50
17.0	1056	5766	15047	1658	6486	978	480	226	60	3588	40892	647	48.94	9.59	6.52	3.52	6.11	0.08	5.12	92.33
19.0	1060	6990	18090	2012	7644	1093	536	236	62	3401	40218	649	48.64	9.01	6.54	3.33	6.50	0.07	5.08	91.90
21.0	1585	13189	33317	3547	11660	2095	1183	478	93	5336	31839	585	37.75	7.18	13.25	4.60	7.53	0.04	2.92	89.33
23.0	1353	10883	25324	2581	9589	1343	790	443	67	4108	18024	399	55.55	7.70	12.12	3.37	2.52	0.05	2.74	92.47
25.0	2669	15245	37828	3971	11660	2129	1432	884	105	7235	23757	527	50.95	7.84	13.50	3.59	2.83	0.03	1.64	88.84
27.0	1114	7549	18292	1948	7215	1029	570	311	66	4644	29923	540	48.61	10.36	15.94	5.26	1.94	0.04	3.47	92.65
28.0	605	4436	10137	1163	4103	552	392	150	36	2024	15550	310	51.98	12.77	10.50	3.60	2.70	0.19	7.85	95.85
28.0	523	4414	10024	1066	3805	499	239	139	32	1680	12231	276	52.54	12.99	9.88	3.40	2.85	0.19	8.17	96.56
30.0	705	5120	12175	1244	4537	643	333	191	54	1922	15188	370	54.96	11.44	8.91	3.21	3.05	0.17	7.18	95.64
32.0	639	5600	12423	1243	4452	643	355	192	38	3377	11059	262	55.54	10.90	10.86	4.02	2.45	0.14	5.68	96.21
34.0	606	4707	10271	1070	3793	517	284	168	34	2596	10024	252	56.81	11.42	9.10	3.77	2.41	0.16	6.80	96.48
36.0	655	6881	14856	1439	4961	620	360	207	35	4000	5286	145	54.73	10.53	10.74	4.47	2.45	0.15	6.00	96.02
37.0	1589	21256	44990	4313	11660	1820	1020	566	68	3887	8740	218	49.57	8.97	12.34	4.24	3.76	0.15	2.91	89.46
39.0	1127	10449	22446	2270	8075	1105	678	379	44	3653	6140	147	53.28	7.79	13.80	5.37	3.33	0.06	2.40	94.09
41.0	2393	11952	26461	2621	9696	1501	1145	726	98	7092	28062	503	37.78	3.70	25.51	4.16	7.29	0.03	0.94	90.23
43.0	2452	29897	58550	6143	11660	3425	2151	951	76	3542	8138	191	41.65	3.20	20.88	4.84	4.15	0.02	1.38	85.23
45.0	790	3477	6907	785	2944	436	313	207	27	7709	5336	115	52.05	8.91	19.86	5.70	1.67	0.81	4.33	96.94
47.0	210	1043	2171	256	924	120	65	44	11	2458	5557	113	61.00	14.74	8.50	3.06	0.28	1.84	7.27	98.55
49.0	346	1023	2128	254	925	122	73	64	31	1742	7490	169	59.16	11.98	11.50	4.03	0.85	0.16	7.15	98.32
51.0	254	532	1116	135	499	66	35	40	29	1643	13167	279	61.91	9.79	11.89	4.47	0.99	0.11	5.53	98.07
53.0	327	854	1693	204	711	93	49	47	37	1002	12343	293	50.80	4.76	10.91	6.03	8.54	0.07	2.63	97.96
55.0	393	2527	4558	596	2031	240	94	73	38	1172	22182	432	54.92	4.36	17.06	8.34	3.06	0.12	2.71	96.47
57.0	170	858	1733	209	730	97	47	36	5	1250	2005	43	50.57	5.02	21.84	7.38	3.92	0.12	2.37	99.04
58.8	121	895	1800	219	755	91	34	29	3	839	1056	19	50.27	14.62	9.22	3.98	3.49	0.26	10.90	99.26
61.0	87	1477	2727	317	1042	115	35	27	3	336	551	9	57.94	16.03	3.55	1.60	2.14	0.38	13.34	99.12
63.0	82	1769	2855	349	1124	124	45	25	3	172	631	9	59.20	16.68	2.81	1.21	1.54	0.41	14.10	99.15
65.0	94	1069	1947	225	731	78	21	17	2	331	866	12	57.55	15.59	4.96	2.00	2.19	0.33	12.42	99.30
67.0	147	611	1255	149	502	60	28	26	6	706	2104	36	54.16	15.55	5.55	2.41	3.54	1.90	9.92	99.25

69.0	115	552	1139	139	470	54	23	20	4	446	874	16	52.91	15.39	8.58	3.15	3.48	1.50	9.11	99.43
71.0	942	1391	2714	330	1138	177	136	168	44	2169	13397	236	51.97	14.19	8.74	3.27	3.99	3.37	5.28	97.69
71.0	1576	2014	3701	529	1862	292	295	284	77	2506	19916	321	50.52	13.62	9.45	3.54	3.77	3.20	4.91	96.49
73.7	92	388	671	75	244	35	22	14	3	198	1344	36	49.63	24.20	7.24	4.15	0.10	2.28	8.34	99.52
76.0	71	103	203	23	85	15	12	10	3	85	1324	37	50.61	24.70	6.05	3.77	0.14	2.76	7.61	99.66
78.0	54	215	418	50	177	26	12	9	2	325	446	14	51.96	21.98	7.21	4.81	0.10	3.14	7.48	99.72
80.3	1224	14937	31281	3020	9271	1058	392	326	43	6809	4038	130	32.70	4.37	21.28	10.52	7.98	0.06	2.35	92.57
80.9	103	1614	2661	293	901	86	29	27	3	562	1039	15	64.97	17.23	3.97	1.21	0.51	9.23	0.54	99.26
83.0	26	397	733	84	271	28	7	6	1	230	551	13	64.64	18.99	2.91	0.81	0.14	9.63	1.58	99.75
84.7	41	466	1015	128	449	55	16	10	2	413	664	16	51.06	23.74	6.40	3.95	0.15	2.18	8.31	99.57
86.3	25	205	412	51	181	24	9	5	1	135	282	5	62.70	20.90	2.19	1.42	0.03	8.34	2.88	99.78
87.9	101	605	1235	152	529	79	40	21	7	783	3941	64	53.35	22.50	6.09	3.87	0.18	4.63	5.59	99.10
90.0	55	160	312	38	130	19	11	9	2	286	875	23	52.72	22.20	7.72	4.00	0.08	4.04	6.34	99.72
92.0	45	285	574	68	227	28	10	8	2	547	699	14	55.25	21.33	6.26	3.84	0.05	5.10	5.47	99.68
94.4	662	1801	3675	468	1639	233	107	81	76	7556	58385	940	47.82	5.49	20.77	6.57	2.84	0.31	3.41	92.48
96.0	811	3036	5771	830	3048	514	289	132	42	4951	37296	591	49.38	9.01	20.43	7.13	0.56	0.70	4.94	94.14
98.0	337	1417	2701	322	1074	142	76	70	20	3838	30156	541	55.31	8.93	17.40	5.26	1.03	1.88	2.19	95.88
100.0	752	4829	12014	1316	4582	681	364	243	44	10277	67550	1430	44.36	4.87	23.75	7.44	1.45	0.05	3.28	88.91
102.0	483	3621	6019	766	2510	305	160	138	21	3426	18651	441	49.07	7.13	21.33	5.46	3.16	1.41	3.15	96.30
104.0	1023	2213	4189	607	2211	399	267	187	73	7563	56962	1012	43.05	11.67	17.83	2.85	3.51	4.94	2.02	92.48
105.4	230	1378	2449	275	900	115	71	63	16	3351	8364	149	62.83	18.13	4.77	0.56	0.37	10.07	0.57	98.30
107.0	674	3451	6251	745	2374	261	164	175	54	5230	29948	481	38.69	10.48	14.82	4.77	7.15	2.82	3.97	95.09
109.3	919	3268	5729	696	2215	249	154	197	96	6176	46600	695	47.18	8.58	16.45	6.37	3.41	1.65	3.18	93.27
110.4	203	1831	3230	361	1140	114	44	54	14	1614	6723	122	63.67	16.95	4.32	1.27	0.79	8.67	0.91	98.48
112.0	555	3092	5364	649	2035	189	65	115	47	4054	19906	352	50.01	13.90	9.68	4.32	3.52	5.88	2.21	96.23
114.0	452	2630	4317	534	1748	188	65	95	36	2995	22319	412	50.55	13.40	10.77	4.22	3.17	5.83	2.22	96.34
116.0	611	2527	4652	617	2190	304	154	115	49	3732	28041	496	55.37	14.79	8.05	3.21	1.71	6.93	1.67	95.67
116.0	640	2779	5327	729	2561	338	242	133	55	3798	29600	552	54.49	13.69	8.28	3.51	2.22	6.62	1.61	95.21
118.0	1859	4462	11565	1363	5260	970	618	357	132	8444	48493	855	46.60	9.94	16.93	5.79	1.71	1.59	3.67	91.53
120.0	4691	4054	9934	1261	4912	997	892	973	320	7476	59843	1063	39.02	7.11	25.74	6.62	2.08	0.22	3.52	89.99
122.0	2497	2813	5798	822	3258	640	523	490	202	4732	33856	613	37.75	11.68	23.87	9.08	1.14	1.08	5.69	94.33
124.0	3199	3063	6455	904	3510	774	695	623	344	6677	46254	848	45.98	9.18	16.14	6.25	4.07	1.46	4.44	92.56
126.0	2464	2473	4868	681	2594	539	474	464	272	4460	33820	637	42.90	8.87	17.21	6.60	5.65	1.12	5.21	94.37
128.0	3571	3005	6340	893	3483	775	726	725	359	6113	42039	792	40.59	10.47	14.17	5.23	5.65	2.28	5.04	92.94
130.0	3074	2735	5539	791	3112	696	649	611	289	6505	40614	774	42.36	11.81	13.93	5.01	4.77	3.04	5.13	93.48
132.0	3324	2523	4999	716	2796	627	598	698	272	6055	31954	611	47.57	11.97	11.64	4.35	3.96	2.84	5.66	94.31
134.0	5033	4355	11759	1429	5823	1275	1139	1197	459	6611	60329	1200	36.74	8.69	22.50	5.74	4.30	0.68	5.58	89.69

136.0	5435	4348	11222	1361	5388	1194	1139	1271	506	9035	63756	1260	41.75	10.56	17.37	3.68	3.10	1.82	5.81	89.25
138.0	2603	2328	4683	673	2705	613	593	590	230	4708	37700	764	49.24	13.00	10.72	2.55	3.49	3.87	5.53	94.16
140.0	2357	2348	4791	698	2817	664	695	640	149	6820	37662	789	43.71	12.23	7.88	5.29	5.78	3.42	5.56	94.09
142.0	918	1314	2805	370	1452	313	291	252	63	2414	12613	355	51.41	16.61	6.52	3.67	2.51	3.23	8.45	97.70
144.0	88	229	489	62	237	47	37	23	6	375	1945	52	51.97	21.53	5.91	4.51	0.17	1.09	11.22	99.45
146.0	148	341	740	94	361	67	48	37	12	570	3168	84	52.07	15.58	9.41	5.23	1.96	3.13	8.00	99.31